

STRESSES AND DEFLECTIONS OF UNSWEPT AND  
SWEPT THIN-WALLED BEAMS

Thesis by  
Howard Henry Dixon

In Partial Fulfillment of the Requirements

For the Degree of  
Doctor of Philosophy

California Institute of Technology

Pasadena, California

1951

## ACKNOWLEDGMENT

It is a pleasure to acknowledge the interest and assistance offered by members of the Aeronautics Staff of the California Institute of Technology. I am particularly indebted to Dr. Yuan-cheng Fung, my research advisor, whose clear insight greatly aided the progress of this research, and to Professor Ernest E. Sechler, for whose personal encouragement I am grateful. I should like to express my appreciation to Dr. Max L. Williams for our discussions on the problems of swept wings.

I wish to acknowledge the cooperation of the staff of the N. A. C. A. in providing detailed data on the results of their experimental investigation on a swept box beam.

I desire to express my gratitude to my parents, to the Douglas Aircraft Company Scholarship Board and the Guggenheim Aeronautical Laboratory for the financial assistance that made it possible for me to pursue graduate studies.

I was ably aided in the rather extensive calculations by Mrs. Dorothy Eaton and Mrs. Mary-Evelyn Bryden. The final form of the illustrations and figures were competently done by Mr. Bryan Lambert, Mr. Ralph Perrault, and Miss Gerry Ellis. The tedious task of typing the manuscript was excellently performed by Mrs. Virginia Boughton.

## SUMMARY

A method is presented for the determination of the stresses and deflections of unswept and swept, thin-walled beams of uniform closed cross section. The cross section, loading distribution and boundary conditions are assumed to be arbitrary. The method is based on the differential equation governing the behavior of orthogonal elastic shells. The differential equation is transformed into a difference equation and the solution obtained by the relaxation technique. A comparison of the theoretical solution and experimental data for a swept back wing with a carry through bay under symmetrical bending showed good agreement.

A tapered wing may be treated by approximating the variation by a series of spanwise steps.

As the difference equations are a system of simultaneous algebraic equations, they may be solved by automatic calculating equipment or by electric analogue computers as well as by the relaxation technique.

## TABLE OF CONTENTS

PART	PAGE
I. Introduction	1
II. Formulation of the Differential Equations Governing the Orthogonal Shell Problem	4
III. Transformation of the Differential Equations into Difference Equations	13
IV. Relaxation Procedure for the Solution of the Difference Equations	25
V. General Procedure for the Determination of Stresses and Deflections of Thin-Walled Beams	30
5.1 Orthogonal Beams	30
a. Simply Supported Beam	31
b. Cantilever Beam with an Orthogonal Support	31
5.2 Cantilever Beam with a Rigid Oblique Support	32
5.3 Beam on Multiple Supports Representing a Swept Back Wing with a Carry Through Bay	34
VI. Comparison of the Finite Difference Method and the Analytical Solutions for a Cantilever Beam with a Rigid Orthogonal Support	42
VII. Comparison of the Theoretical Solutions and Experimental Data for a Swept Back Wing with a Carry Through Bay Under Symmetrical Bending	47



## TABLE OF NOTATION

$a_{SH}$	= area of sheet element resisting normal stress - sq. in.
$a_{ST}$	= area of stiffener element - sq. in.
$a_j$	= $a_{SH} + a_{ST}$ = equivalent area of elements resisting normal stress - sq. in.
$A_w$	= area of monocoque cross section - sq. in.
$A_H$	= horizontal shear resistant area - sq. in.
$A_V$	= vertical shear resistant area - sq. in.
$c$	= normal chord of the outer panel - in.
$E$	= Young's modulus - psi.
$E'$	= $E/(1 - \mu^2)$ - psi.
$G$	= shearing modulus of elasticity - psi.
$H$	= horizontal section shear - lb.
$h$	= height of beam cross section - in.
$I_c$	= central moment of inertia - in. <sup>4</sup>
$r$	= radius from origin of principal shear axis to a tangent through the wall element - in.
$s$	= tangential coordinate
$t$	= wall thickness of monocoque section - in.
$T$	= section torque - in. lb.
$u$	= horizontal displacement - in.
$v$	= vertical displacement - in.
$V$	= vertical section shear - lb.
$w$	= axial displacement - in.

## TABLE OF NOTATION (Continued)

$\left. \begin{array}{l} x \\ y \\ z \end{array} \right\}$	=	rectangular coordinates
$\alpha$	=	angle between tangent to a wall element and the x axis - deg.
$\gamma$	=	shearing strain - radians
$\epsilon$	=	normal strain - in./in.
$\mu$	=	Poisson's ratio
$\varphi$	=	angle of twist (rotation) of the cross section - radians
$\psi$	=	angle of sweep back - deg.
$\lambda$	=	angle of resolution of normal stress in the outer panel sheet element - deg.
$\beta$	=	included angle between outer panel sheet element and inner longitudinal axis - deg.
$\xi$	=	tangential displacement - in.
$\sigma$	=	normal stress - psi.
$\tau$	=	shearing stress - psi.

### SUBSCRIPTS

i	=	inner panel of swept back wing with a carry through bay
o	=	outer panel of swept back wing with a carry through bay
j, n	=	quantities on the shell surface defined by their values at the stiffeners
$k, R$	=	quantities on the shell surface defined by their values over the sheet
$s$	=	tangential coordinate
$Z$	=	rectangular (axial) coordinate

## I. INTRODUCTION

Since early in 1947, the structures group at GALCIT has been investigating theoretically and experimentally the effect of sweep upon the stress and deflection distribution in aircraft wings. In 1950, Dr. E. E. Sechler and the author undertook the task of reviewing the existing structural analysis methods, experimental data, and aeroelastic effects for swept wings with solid, thick-walled and thin-walled sections. This review indicated that no satisfactory solution is available for the stresses and deflections in a thin-walled, swept wing structure. The theoretical determination of the stresses that exist in such a swept wing under static load requires the analysis of a swept, redundant, cantilever structure of variable cross section with an elastic support. The available theoretical methods of treatment of this problem are the energy methods, the method of consistent deformations, and methods in which loads are arbitrarily assigned to various elements of the structure.

The energy methods are available to be used in those cases where equilibrium conditions are not sufficient in themselves to specify the stress distribution, and use is made of the fact that the actual distribution corresponds to a minimum of the energy. The energy methods may use either Castigliano's theorem, or a least (virtual) work analysis. Castigliano's theorem proceeds from the expression for the elastic energy  $U$  stored in the structure by the application to the points 1, 2, . . . i of the forces  $P_i$ , torques  $T_i$ , and bending moments  $M_i$ , and gives equations for the

displacements  $\lambda_i$  in the direction of the loads  $P_i$ , the angles of twist  $\alpha_i$  in the direction of the torques  $T_i$ , and the angles of rotation  $\theta_i$  in the direction of the moments  $M_i$ . The equations are:

$$\lambda_i = \frac{\partial U}{\partial P_i} \qquad \alpha_i = \frac{\partial U}{\partial T_i} \qquad \theta_i = \frac{\partial U}{\partial M_i}$$

The least work analysis applies the method of minimum complementary energy and minimum potential energy. The principle of minimum complementary energy is a variational condition on the stresses, and the principle of minimum potential energy is a variational condition on the displacements. The former expresses a condition which defines the correct state of stress that satisfies the equilibrium conditions and the boundary conditions on the stresses; whereas the latter determines the correct deformation configuration consistent with the boundary conditions on the deflections.

The principle of the method of consistent deformations assumes that the elements of the structure are considered as free bodies in equilibrium under the action of forces and moments. At the joints, the elements have the same translational and rotational displacements, or in other words, the deformations are consistent. If there are many elements, the method inherently requires the solution of a large number of simultaneous equations. The concept of an elastic axis is not used in the method. The effects of warping of the cross section and shear lag may be considered.

The methods in which loads are arbitrarily assigned to various elements of the structure usually use the elastic axis concept, and consider that one group of elements resists the bending loads, and another group of elements

resists the torsion loads.

However, the knowledge of the structural behavior of swept wings with thin-walled cross sections is not complete. There are no known existing accurate solutions of the problem, and the approximate methods show only fair agreement with experimental data. Therefore, there is a need for a theoretical approach that will be as accurate as possible, and at the same time provide a procedure to obtain an engineering solution.

As a result, a theoretical solution has been developed in which the problem is formulated in terms of the differential equation from the theory of orthogonal elastic shells. The assumption of the preservation of the normal cross section is relaxed in the neighborhood of the oblique support, in order to account for the boundary conditions and the effect of root ribs. The solution of the differential equation is obtained by means of finite difference methods. Although automatic calculating equipment and electric analogue computers may be used to solve the difference equations, the relaxation method is used due to its flexibility for investigational purposes, and its effectiveness as an engineering procedure.

## II. FORMULATION OF THE DIFFERENTIAL EQUATION GOVERNING THE ORTHOGONAL SHELL PROBLEM

Contributions to the formulation of the orthogonal shell problem have been made by a large number of authors. An excellent review of these contributions, and additional extensions have been made by Bescoter (Reference 1). The following formulation is taken from Bescoter's work, and modified where necessary to permit the eventual use of numerical calculation.

In this formulation, the following assumptions are made:

- (1) The physical beam is replaced by a similar theoretical beam having ribs, flanges, stiffeners, and sheets.
- (2) The cross sections of the beam are uniform, and contain closely spaced internal rigid diaphragms which stabilize the shell and preserve the cross-sectional shape. The diaphragms are infinitely stiff in their own planes but are completely free to warp out of their planes.
- (3) The flanges and stiffeners are straight and transmit only axial loads.
- (4) The sheet is sufficiently thin so that the stresses are uniformly distributed over the thickness of the wall. The sheet transmits axial and shear loads but does not transmit bending loads.
- (5) There are no cut outs.
- (6) Hooke's Law is assumed.

In the derivation of the differential equation, it is assumed that the beam has a thin-walled, unstiffened cross section, consisting of a single cell without sharp corners or discontinuities in thickness.

The beam and coordinate system are shown in Figure 1, with a point on the beam identified by the coordinate  $z$  along axis of the beam, and the coordinate  $s$  measured around the peripheral center line of the beam. The idealized differential element of the shell is shown in Figure 2. The element has variable thickness in the  $s$  direction and constant thickness in the  $z$  direction.

Assuming that Hooke's law is applicable, and neglecting the normal forces due to the diaphragms, the stress strain relationships are

$$\sigma_z - \mu \sigma_s = E \epsilon_z \quad \sigma_s - \mu \sigma_z = E \epsilon_s \quad \tau_{sz} = G \gamma_{sz} \quad (1)$$

where

$E$  = Young's modulus

$G$  = shearing modulus of elasticity

$\epsilon_s, \epsilon_z$  = normal strain along the tangential and axial coordinate respectively

$\sigma_s, \sigma_z$  = normal stress along the tangential and axial coordinate respectively

$\mu$  = Poisson's ratio

$\tau_{sz}$  = shearing stress in the  $sz$  plane

$\gamma_{sz}$  = shearing strain in the  $sz$  plane

Due to the assumption of stiff diaphragms,  $\epsilon_s = 0$ . Therefore,

$$\sigma_z = \frac{E}{1-\mu^2} \epsilon_z = E' \epsilon_z \quad (2)$$

where

$$E' = \frac{E}{1-\mu^2}$$

The stress  $\sigma_s$  and strain  $\epsilon_s$  do not appear in Part II henceforth, and the subscripts of the remaining stresses and strains will be dropped with the following change of notation:

$$\sigma = \sigma_z \quad \epsilon = \epsilon_z \quad \tau = \tau_{sz} \quad \gamma = \gamma_{sz}$$

The strains at a point may be expressed in terms of the axial displacement  $w$  and tangential displacement  $\xi$  by

$$\epsilon = \frac{\partial w}{\partial z} \quad \gamma = \frac{\partial w}{\partial s} + \frac{\partial \xi}{\partial z} \quad (3)$$

The stresses may be expressed in terms of the displacements by

$$\sigma = E' \frac{\partial w}{\partial z} \quad (4)$$

$$\tau = G \left( \frac{\partial w}{\partial s} + \frac{\partial \xi}{\partial z} \right)$$

where  $s, z$  = tangential and axial coordinate respectively

$\xi, w$  = tangential and axial displacement respectively.

The forces acting on the differential element are shown in Figure 2.

The stress components acting in the circumferential direction on the faces of an element of the thin wall are balanced by the forces from the diaphragms acting on the inner surface of the wall. Hence only the equation of equilibrium of the element in the axial direction need be considered. The equation is

$$\frac{\partial \sigma}{\partial z} \left( t + \frac{1}{2} \frac{dt}{ds} ds \right) ds dz + \frac{\partial (\tau t)}{\partial s} ds dz = 0$$

where  $t$  = wall thickness of monocoque section.



Assuming the changes in thickness are small, then

$$t \frac{\partial \sigma}{\partial z} + \frac{\partial (Tt)}{\partial s} = 0 \quad (5)$$

In order to obtain an equation for axial displacements, the strain compatibility equation is formed by substituting Equations (4) into Equation (5), giving

$$t \frac{\partial}{\partial z} (E' \frac{\partial W}{\partial z}) + \frac{\partial}{\partial s} \left[ t G \left( \frac{\partial W}{\partial s} + \frac{\partial \delta}{\partial z} \right) \right] = 0$$

or

$$\frac{E't}{G} \frac{\partial^2 W}{\partial z^2} + \frac{\partial}{\partial s} \left( t \frac{\partial W}{\partial s} \right) + \frac{\partial}{\partial s} \left( t \frac{\partial \delta}{\partial z} \right) = 0$$

It is convenient to use the principal shear axes as the coordinate axes of the cross section. The location of these axes may be computed by the formulas given by Duberg (Reference 2). At any given point of the wall, draw a tangent to the centerline as shown in Figure 3(a). The radius from the origin of the principal shear axes to the tangent is  $r$ , while the angle made by the tangent with the positive direction of the  $x$  axis is  $\alpha$ . The location of the principal shear axes is defined in terms of  $r$  and  $\alpha$  by the condition that the following line integrals vanish around the cell,

$$\begin{aligned} \oint t r \cos \alpha \, ds &= 0 \\ \oint t r \sin \alpha \, ds &= 0 \\ \oint t \cos \alpha \sin \alpha \, ds &= 0 \end{aligned} \quad (7)$$

The section properties associated with the principal shear axes are defined by:

$$\begin{aligned}
 I_c &= \oint t r^2 ds \\
 A_H &= \oint t \cos^2 \alpha ds \\
 A_V &= \oint t \sin^2 \alpha ds
 \end{aligned} \tag{8}$$

where

$I_c$  = central moment of inertia (corresponds to polar moment of inertia)

$A_H$  = horizontal shear resistant area

$A_V$  = vertical shear resistant area

$A_w$  = area of monocoque cross section

$$= \oint t ds = A_H + A_V$$

The tangential displacement  $\xi$  may be eliminated from Equation (6) by further use of the assumption of rigid bulkheads. The horizontal displacement  $u$  and vertical displacement  $v$  are parallel to the principal shear axes and regarded as the translations of the origin of the shear axis. The contributions that each of these displacements make to the tangential displacement are illustrated in Figure 3.

If the displacements of the rigid body are small, the rotational and translational contributions may be superimposed to give

$$\xi = r\varphi + u \cos \alpha + v \sin \alpha$$

and

$$\frac{\partial \xi}{\partial z} = r \frac{d\varphi}{dz} + \cos \alpha \frac{du}{dz} + \sin \alpha \frac{dv}{dz} \tag{9}$$

where  $\varphi$  = angle of twist (rotation) of the cross section.

The section torque and external shears are related to the internal shearing stresses by the following equations,

$$T = \oint t \tau r ds$$

$$H = \oint t \tau \cos \alpha ds$$

$$V = \oint t \tau \sin \alpha ds$$

where

H = horizontal section shear

T = section torque

V = vertical section shear

If Equation (4) is substituted into Equation (10), then

$$T = G \oint t r \frac{\partial w}{\partial s} ds + G \oint t r \frac{\partial \xi}{\partial z} ds \quad (11)$$

$$H = G \oint t \cos \alpha \frac{\partial w}{\partial s} ds + G \oint t \cos \alpha \frac{\partial \xi}{\partial z} ds$$

$$V = G \oint t \sin \alpha \frac{\partial w}{\partial s} ds + G \oint t \sin \alpha \frac{\partial \xi}{\partial z} ds$$

Substituting Equation (9), and omitting the integrals which vanish by Equations (7), then

$$T = G \oint t r \frac{\partial w}{\partial s} ds + G \frac{d\varphi}{dz} \oint t r^2 ds$$

$$H = G \oint t \cos \alpha \frac{\partial w}{\partial s} ds + G \frac{du}{dz} \oint t \cos^2 \alpha ds$$

$$V = G \oint t \sin \alpha \frac{\partial w}{\partial s} ds + G \frac{dv}{dz} \oint t \sin^2 \alpha ds \quad (12)$$

Introduction of principal shear axes permits the above equations to be solved for the derivatives of  $\varphi$ ,  $u$  and  $v$  independently, rather than as a simultaneous system. Inserting the section constants given in Equation (8) into Equation (12), and solving for the displacement gives

$$\frac{d\phi}{dz} = \frac{T}{GI_c} - \frac{1}{I_c} \oint tr \frac{\partial w}{\partial s} ds$$

$$\frac{du}{dz} = \frac{H}{GA_H} - \frac{1}{A_H} \oint t \cos \alpha \frac{\partial w}{\partial s} ds$$

$$\frac{dv}{dz} = \frac{V}{GA_V} - \frac{1}{A_V} \oint t \sin \alpha \frac{\partial w}{\partial s} ds$$

The assumption that the cross section is a single cell without sharp corners implies that the functions  $t(s)$  and  $r(s)$ , are continuous. Thus, as it will be seen that  $\frac{\partial w}{\partial s}$  is continuous, integration by parts transforms the equations into the following form:

$$\frac{d\phi}{dz} = \frac{T}{GI_c} + \frac{1}{I_c} \oint w \frac{d(tr)}{ds} ds$$

$$\frac{du}{dz} = \frac{H}{GA_H} + \frac{1}{A_H} \oint w \frac{d(t \cos \alpha)}{ds} ds \quad (13)$$

$$\frac{dv}{dz} = \frac{V}{GA_V} + \frac{1}{A_V} \oint w \frac{d(t \sin \alpha)}{ds} ds$$

An expression for  $\xi$  which will permit its elimination from Equation (6) may be obtained from Equation (9) by substituting in Equation (13) to give:

$$\begin{aligned} \frac{d\xi}{dz} = & \frac{Tr}{GI_c} + \frac{H \cos \alpha}{GA_H} + \frac{V \sin \alpha}{GA_V} + \frac{r}{I_c} \oint w \frac{d(tr)}{ds} ds \\ & + \frac{\cos \alpha}{A_H} \oint w \frac{d(t \cos \alpha)}{ds} ds + \frac{\sin \alpha}{A_V} \oint w \frac{d(t \sin \alpha)}{ds} ds \end{aligned} \quad (14)$$

This equation may be substituted into Equation (4) to give:

$$\begin{aligned} \tau = G \left[ \frac{\partial w}{\partial s} + \frac{Tr}{GI_c} + \frac{H \cos \alpha}{GA_H} + \frac{V \sin \alpha}{GA_V} + \right. \\ \left. + \frac{r}{I_c} \oint w \frac{d(tr)}{ds} ds + \frac{\cos \alpha}{A_H} \oint w \frac{d(t \cos \alpha)}{ds} ds \right. \\ \left. + \frac{\sin \alpha}{A_V} \oint w \frac{d(t \sin \alpha)}{ds} ds \right] \end{aligned} \quad (15)$$

Equation (14) may be substituted into Equation (6) to obtain the following expression governing the displacements:

$$\begin{aligned} & \frac{E't}{G} \frac{\partial^2 W}{\partial z^2} + \frac{\partial}{\partial s} \left( t \frac{\partial W}{\partial s} \right) + \frac{\partial}{\partial s} \left[ t \left( \frac{Tr}{GI_c} + \frac{H \cos \alpha}{GA_H} + \frac{V \sin \alpha}{GA_V} + \right. \right. \\ & \left. \left. \frac{r}{I_c} \oint W \frac{d(tr)}{ds} ds + \frac{\cos \alpha}{A_H} \oint W \frac{d(t \cos \alpha)}{ds} ds + \right. \right. \\ & \left. \left. \frac{\sin \alpha}{A_V} \oint W \frac{d(t \sin \alpha)}{ds} ds \right) \right] = 0 \end{aligned}$$

Simplifying,

$$\begin{aligned} & \frac{E't}{G} \frac{\partial^2 W}{\partial z^2} + \frac{\partial}{\partial s} \left( t \frac{\partial W}{\partial s} \right) = - \left[ \frac{T}{GI_c} \frac{d(tr)}{ds} + \frac{H}{GA_H} \frac{d(t \cos \alpha)}{ds} \right. \\ & \left. + \frac{V}{GA_V} \frac{d(t \sin \alpha)}{ds} + \frac{1}{I_c} \frac{d(tr)}{ds} \oint W \frac{d(tr)}{ds} ds \right. \\ & \left. + \frac{1}{A_H} \frac{d(t \cos \alpha)}{ds} \oint W \frac{d(t \cos \alpha)}{ds} ds + \frac{1}{A_V} \frac{d(t \sin \alpha)}{ds} \oint W \frac{d(t \sin \alpha)}{ds} ds \right] \end{aligned} \quad (16)$$

A similar expression may be developed for the axial stress.

Equation (16) may be simplified if the cross section of the beam and the corresponding boundary conditions are symmetrical about one or both principal shear axes. In this event, all or part of the actions of torsion, horizontal bending, and vertical bending become separated, and permit the solution of a simple system of independent equations. The development of like expressions is given in Reference 1.

In the case of a cross section and boundary conditions which are symmetrical about both principal shear axes, the equation becomes

$$\frac{E't}{G} \frac{\partial^2 W}{\partial z^2} + \frac{\partial}{\partial s} \left( t \frac{\partial W}{\partial s} \right) = 0 \quad (\text{axial forces})$$

$$\text{or, } \frac{E't}{G} \frac{\partial^2 W}{\partial z^2} + \frac{\partial}{\partial s} \left( t \frac{\partial W}{\partial s} \right) = - \frac{1}{I_c} \frac{d(tr)}{ds} \left[ \frac{T}{G} + \oint W \frac{d(tr)}{ds} ds \right] \quad (17)$$

$$\text{or, } = - \frac{1}{A_H} \frac{d(t \cos \alpha)}{ds} \left[ \frac{H}{G} + \oint W \frac{d(t \cos \alpha)}{ds} ds \right]$$

$$\text{or, } = - \frac{1}{A_V} \frac{d(t \sin \alpha)}{ds} \left[ \frac{V}{G} + \oint W \frac{d(t \sin \alpha)}{ds} ds \right]$$

In the case of a cross section and boundary conditions which are symmetrical about the x axis, the equation becomes

$$\frac{E't}{G} \frac{\partial^2 W}{\partial z^2} + \frac{\partial}{\partial s} \left( t \frac{\partial W}{\partial s} \right) = - \frac{1}{A_H} \frac{d(t \cos \alpha)}{ds} \left[ \frac{H}{G} + \oint W \frac{d(t \cos \alpha)}{ds} ds \right] \quad (18)$$

$$\text{or, } = - \frac{1}{I_c} \frac{d(tr)}{ds} \left[ \frac{T}{G} + \oint W \frac{d(tr)}{ds} ds \right] \\ - \frac{1}{A_V} \frac{d(t \sin \alpha)}{ds} \left[ \frac{V}{G} + \oint W \frac{d(t \sin \alpha)}{ds} ds \right]$$

In the case of a cross section and boundary conditions which are symmetrical about the y axis, the equation becomes:

$$\frac{E't}{G} \frac{\partial^2 W}{\partial z^2} + \frac{\partial}{\partial s} \left( t \frac{\partial W}{\partial s} \right) = - \frac{1}{A_V} \frac{d(t \sin \alpha)}{ds} \left[ \frac{V}{G} + \oint W \frac{d(t \sin \alpha)}{ds} ds \right]$$

$$\text{or, } \quad (19)$$

$$= - \frac{1}{I_c} \frac{d(tr)}{ds} \left[ \frac{T}{G} + \oint W \frac{d(tr)}{ds} ds \right] \\ - \frac{1}{A_H} \frac{d(t \cos \alpha)}{ds} \left[ \frac{H}{G} + \oint W \frac{d(t \cos \alpha)}{ds} ds \right]$$

### III. TRANSFORMATION OF THE DIFFERENTIAL EQUATIONS INTO DIFFERENCE EQUATIONS

The solution of linear differential equations with known boundary conditions may be obtained by finite difference methods. The differential equation governing the unknown function is transformed into a difference equation and the solution of the difference equation is obtained at a finite number of points within the boundary. As the set of points at which the desired function is sought may be made arbitrarily dense, the solution of the difference equation approaches the solution of the differential equation to any desired degree of accuracy. The difference problem may be solved by Southwell's relaxation method (Reference 3), which is defined as "a systematic sequence of localized changes of the wanted function that steadily brings the 'residuals' toward their desired value."

The difference equation is obtained from the differential equation by expressing the differentials and integrals in terms of finite differences. The finite differences may be obtained by the procedures given in Reference (4).

Suppose a function  $f(u)$  is given for the values  $a_0, a_1, \dots, a_n$  of its argument  $u$ . It is required to find the value of the function or its derivatives at some point  $x(u)$  in which the intervals of the argument are not constant. This problem may be solved by the application of Newton's formula for unequal values of the argument. (Ref. Chapter II, Reference (4).) In order to derive this formula, consider what are called differences

of tabular values. The quantity

$$f(a_1, a_0) = \frac{f(a_1) - f(a_0)}{a_1 - a_0}$$

is called a divided difference of first order. In the same manner, divided differences of second and third order are respectively:

$$f(a_2, a_1, a_0) = \frac{f(a_2, a_1) - f(a_1, a_0)}{a_2 - a_0}$$

$$f(a_3, a_2, a_1, a_0) = \frac{f(a_3, a_2, a_1) - f(a_2, a_1, a_0)}{a_3 - a_0}$$

The divided differences of higher orders are formed in the same way.

Let  $f(u)$  be a function whose divided differences of (say) order 4 vanish; and suppose that its values for the arguments  $a_0, a_1, a_2, a_3$  are known. The value of the function for any other argument  $x(u)$  may be obtained in the following way: since the divided differences of order 4 vanish, it follows that the differences of order 3 are constant, or

$$f(u, a_0, a_1, a_2) = f(a_0, a_1, a_2, a_3)$$

By definition of the divided difference of order 3,

$$f(u, a_0, a_1) = f(a_0, a_1, a_2) + (u - a_2)f(u, a_0, a_1, a_2)$$

Again, by definition

$$\begin{aligned} f(u, a_0) &= f(a_0, a_1) + (u - a_1)f(u, a_0, a_1) \\ &= f(a_0, a_1) + (u - a_1) [f(a_0, a_1, a_2) + (u - a_2)f(u, a_0, a_1, a_2)] \end{aligned}$$

Also, by definition

$$f(u) = f(a_0) + (u - a_0)f(u, a_0)$$



whence

$$f(u) = f(a_0) + (u - a_0) f(a_0, a_1) + (u - a_0)(u - a_1) f(a_0, a_1, a_2) \\ + (u - a_0)(u - a_1)(u - a_2) f(a_0, a_1, a_2, a_3)$$

Now let  $(u - a_n) = \alpha_n$ , and by induction

$$f(u) = f(a_0) + \alpha_0 f(a_0, a_1) + \alpha_0 \alpha_1 f(a_0, a_1, a_2) + \dots + \\ + \alpha_0 \alpha_1 \dots \alpha_{n-1} f(a_0, a_1, \dots, a_n) + \text{Remainder} \quad (20)$$

where Remainder =  $\alpha_0 \alpha_1 \dots \alpha_n f(u, a_0, \dots, a_n)$

The derivatives of a function in terms of its divided differences may be expressed by differentiating both sides of Newton's Equation (20), so that

$$f'(u) = f(a_0, a_1) + (\alpha_0 + \alpha_1) f(a_0, a_1, a_2) \\ + (\alpha_0 \alpha_1 + \alpha_0 \alpha_2 + \alpha_1 \alpha_2) f(a_0, a_1, a_2, a_3) + \dots \quad (21)$$

$$\frac{1}{2} f''(u) = f(a_0, a_1, a_2) + (\alpha_0 + \alpha_1 + \alpha_2) f(a_0, a_1, a_2, a_3) + \dots$$

and so on.

In order to obtain any desired accuracy, the Newton Equation (20) for the expansion of a function in terms of its divided differences should include such orders of differences that the remainder term is less than some pre-assigned amount. However, accuracy may also be obtained by a reduction of the length of the intervals. In the following, the divided differences of third and higher orders will be neglected, and the accuracy

of the solution obtained by progressive reduction of the intervals.

There are a number of methods of numerically evaluating a definite integral. Among the most common are the Newton-Cotes formulae, of which the simplest case is

$$\int_a^{a+w} f(u) du = \frac{1}{2} w [f(a) + f(a+w)] \quad (22)$$

which is known as the trapezoidal rule. It is exact when  $f(u)$  is a function whose first differences are constant over the interval  $(a, a+w)$ . When  $f(u)$  is a function whose first differences are not constant, the difference between the two sides of the above equation may be written

$$\frac{1}{12} w^3 f''(a + \theta w)$$

where  $0 < \theta < 1$

To apply the finite differences procedure to the analysis of a swept wing, it is necessary to form the differences of the value of the dependent variable for unequal intervals of the independent variable. Consider the particular case of the differential Equation (16) for elastic shells.

Assume that the solution of the equation is desired in the domain  $D$  of the  $s, z$  plane bounded by a closed curve  $\Gamma$  as shown in Figure 4. Superimpose on the Domain  $D$  an arbitrary orthogonal mesh of lines parallel to the  $s$  and  $z$  coordinate axes. The lines parallel to the  $z$  and  $s$  axes are identified by the nomenclature  $j - 1, j, j + 1$ , and  $n - 1, n, n + 1$ , etc. respectively, and the regions of the domain between the lines parallel to the  $z$  and  $s$  axes are identified by  $k, k + 1$  and  $R, R + 1$

etc. respectively. The intervals between the lines parallel to the  $s$  axis are constant and are equal to  $l$ . The intervals between the lines parallel to the  $z$  axis are not constant and are equal to  $L_K$ ,  $L_{K+1}$ , etc. This identifies the mesh nodes and intervals in the neighborhood of a point  $(j(s), n(z))$ .

In order to transform the differential equation into a difference equation based on the mesh network illustrated in Figure 4, express the terms in Equation (16) as a function of the differences at a point  $(j, n)$  as follows. The second derivative of a function is given by Equation (21) to be

$$\frac{1}{2!} f''(u) = f(a_0, a_1, a_2) + \dots$$

$$f''(u) = \frac{2}{a_0 - a_2} \left[ \frac{f(a_0) - f(a_1)}{a_0 - a_1} - \frac{f(a_1) - f(a_2)}{a_1 - a_2} \right] + \dots$$

Recalling that third order differences are neglected, and that the intervals in the directions parallel to the  $z$  and  $s$  coordinates are equal and unequal respectively, then the equation becomes

$$\begin{aligned} \frac{E't}{G} \frac{\partial^2 W}{\partial z^2} &= \frac{E't}{G} \left\{ -\frac{2}{2l} \left[ \frac{w_{n-1} - w_n}{-l} - \frac{w_n - w_{n+1}}{-l} \right]_j \right\} \\ &= \frac{E't}{G} \frac{1}{l^2} (w_{n+1} + w_{n-1} - 2w_n)_j \end{aligned}$$

and

$$\begin{aligned} \frac{\partial}{\partial s} \left( t \frac{\partial W}{\partial s} \right) &= \frac{2}{-(L_K + L_{K+1})_j} \left\{ \left( \frac{t_K}{-L_K} \right)_j (w_{j-1} - w_j)_n - \left( \frac{t_{K+1}}{-L_{K+1}} \right)_j (w_j - w_{j+1})_n \right\} \\ &= \frac{2}{(L_K + L_{K+1})_j} \left\{ \left( \frac{t_{K+1}}{L_{K+1}} \right)_j (w_{j+1} - w_j)_n - \left( \frac{t_K}{L_K} \right)_j (w_j - w_{j-1})_n \right\} \end{aligned}$$

where, for example the term  $(w_{n+1})_j$  refers to the axial displacement of the point  $(j, n+1)$  and  $(L_k)_j$  refers to the interval in the direction parallel to the  $s$  coordinate in the neighborhood of the point  $j$  as indicated in Figure 4.

The first derivative of a function is given by Equation (21) to be

$$f'(u) = f(a_0, a_1) + (\alpha_0 + \alpha_1) f(a_0, a_1, a_2)$$

Consider a function  $f[t(u), r(u), \alpha(u)]$  which is known at  $u = a_0, a_1, \dots, a_n$ . It is desired to obtain the first derivative at a point  $x = (a_1 + a_2)/2$ . Inserting  $u = x$  in Equation (21), then

$$\begin{aligned} f'(x) &= \frac{f(a_0) - f(a_1)}{a_0 - a_1} + \left( \frac{a_1 - a_2}{2} - a_0 + \frac{a_1 + a_2}{2} - a_1 \right) \left( \frac{1}{a_0 - a_2} \right) x \\ &\quad \left( \frac{f(a_0) - f(a_1)}{a_0 - a_1} - \frac{f(a_1) - f(a_2)}{a_1 - a_2} \right) \\ &= \frac{f(a_2) - f(a_1)}{a_2 - a_1} \end{aligned}$$

In terms of the mesh network, the values of the function are given at the mid-points of each interval along the lines  $(n, n+1, \dots)$  parallel to the  $s$  axis as illustrated by Figure 4. The first derivative is desired at the node point  $(j, n)$  of the mesh. Therefore

$$\frac{d}{ds} f[t(s), r(s), \alpha(s)] = \left[ \frac{f(t, r, \alpha)_{k+1} - f(t, r, \alpha)_k}{(L_{k+1} + L_k)/2} \right]_j$$

The line integrals may be evaluated by means of the trapezoidal rule. The integral terms become

$$\oint w \frac{d}{ds} f(t, r, \alpha) ds = \sum_j [f(t, r, \alpha)_{K+1} - f(t, r, \alpha)_K]_j w_j$$

The differential Equation (16) may be transformed into a difference equation by expressing the differentials and integrals in terms of the differences that have been derived. For the point (j, n), the equation becomes

$$\begin{aligned} & \frac{E't}{G} \frac{(w_{n+1} + w_{n-1} - 2w_n)_j}{l^2} + \frac{2}{(L_{K+1} + L_K)_j} \left[ \left( \frac{t_{K+1}}{L_{K+1}} \right)_j (w_{j+1} - w_j)_n - \left( \frac{t_K}{L_K} \right)_j (w_j - w_{j-1})_n \right] \\ &= - \frac{2}{I_C} \frac{(t_{K+1} r_{K+1} - t_K r_K)_j}{(L_{K+1} + L_K)_j} \left[ \frac{T}{G} + \sum_j (t_{K+1} r_{K+1} - t_K r_K)_j w_j \right] \\ & \quad - \frac{2}{A_V} \frac{(t_{K+1} \sin \alpha_{K+1} - t_K \sin \alpha_K)_j}{(L_{K+1} + L_K)_j} \left[ \frac{V}{G} + \sum_j (t_{K+1} \sin \alpha_{K+1} - t_K \sin \alpha_K)_j w_j \right] \\ & \quad - \frac{2}{A_H} \frac{(t_{K+1} \cos \alpha_{K+1} - t_K \cos \alpha_K)_j}{(L_{K+1} + L_K)_j} \left[ \frac{H}{G} + \sum_j (t_{K+1} \cos \alpha_{K+1} - t_K \cos \alpha_K)_j w_j \right] \end{aligned}$$

Multiplying through by  $(L_{K+1} + L_K)_j / 2$ , and letting  $a_j = t(L_{K+1} + L_K)_j / 2$ , the expression becomes:

$$\begin{aligned} & \frac{E't a_j}{G l^2} (w_{n+1} + w_{n-1} - 2w_n)_j + \left( \frac{t_{K+1}}{L_{K+1}} \right)_j (w_{j+1} - w_j)_n - \left( \frac{t_K}{L_K} \right)_j (w_j - w_{j-1})_n \\ &= - \frac{1}{I_C} (t_{K+1} r_{K+1} - t_K r_K)_j \left[ \frac{T}{G} + \sum_j (t_{K+1} r_{K+1} - t_K r_K)_j w_j \right] \\ & \quad - \frac{1}{A_V} (t_{K+1} \sin \alpha_{K+1} - t_K \sin \alpha_K)_j \left[ \frac{V}{G} + \sum_j (t_{K+1} \sin \alpha_{K+1} - t_K \sin \alpha_K)_j w_j \right] \quad (23) \\ & \quad - \frac{1}{A_H} (t_{K+1} \cos \alpha_{K+1} - t_K \cos \alpha_K)_j \left[ \frac{H}{G} + \sum_j (t_{K+1} \cos \alpha_{K+1} - t_K \cos \alpha_K)_j w_j \right] \end{aligned}$$

where  $a_j$  = equivalent area resisting the normal stresses.

In the event that there is symmetry of the cross section and the boundary conditions, the difference equation may be simplified. In the

same manner as in Part II, symmetry about both principal shear axes permits the equation to be written as

$$\begin{aligned} & \frac{E' a_j}{G L^2} (w_{n+1} + w_{n-1} - 2w_n)_j + \left( \frac{t_{k+1}}{L_{k+1}} \right)_j (w_{j+1} + w_j)_n - \left( \frac{t_k}{L_k} \right)_j (w_j - w_{j-1})_n \\ & = 0 \end{aligned} \quad (24)$$

$$\text{or,} \quad = - \frac{1}{I_c} (t_{k+1} r_{k+1} - t_k r_k)_j \left[ \frac{T}{G} + \sum_j (t_{k+1} r_{k+1} - t_k r_k)_j w_j \right]$$

$$\text{or,} \quad = - \frac{1}{A_V} (t_{k+1} \sin \alpha_{k+1} - t_k \sin \alpha_k)_j \left[ \frac{V}{G} + \sum_j (t_{k+1} \sin \alpha_{k+1} - t_k \sin \alpha_k)_j w_j \right]$$

$$\text{or,} \quad = - \frac{1}{A_H} (t_{k+1} \cos \alpha_{k+1} - t_k \cos \alpha_k)_j \left[ \frac{H}{G} + \sum_j (t_{k+1} \cos \alpha_{k+1} - t_k \cos \alpha_k)_j w_j \right]$$

In the case of symmetry about the x axis, the equation becomes

$$\begin{aligned} & \frac{E' a_j}{G L^2} (w_{n+1} + w_{n-1} - 2w_n)_j + \left( \frac{t_{k+1}}{L_{k+1}} \right)_j (w_{j+1} - w_j)_n - \left( \frac{t_k}{L_k} \right)_j (w_j - w_{j-1})_n \\ & = - \frac{1}{A_H} (t_{k+1} \cos \alpha_{k+1} - t_k \cos \alpha_k)_j \left[ \frac{H}{G} + \sum_j (t_{k+1} \cos \alpha_{k+1} - t_k \cos \alpha_k)_j w_j \right] \end{aligned} \quad (25)$$

$$\text{or,} \quad = - \frac{1}{I_c} (t_{k+1} r_{k+1} - t_k r_k)_j \left[ \frac{T}{G} + \sum_j (t_{k+1} r_{k+1} - t_k r_k)_j w_j \right]$$

$$- \frac{1}{A_V} (t_{k+1} \sin \alpha_{k+1} - t_k \sin \alpha_k)_j \left[ \frac{V}{G} + \sum_j (t_{k+1} \sin \alpha_{k+1} - t_k \sin \alpha_k)_j w_j \right]$$

In the case of symmetry about the y axis, the equation becomes

$$\begin{aligned} & \frac{E' a_j}{G L^2} (w_{n+1} + w_{n-1} - 2w_n)_j + \left( \frac{t_{k+1}}{L_{k+1}} \right)_j (w_{j+1} - w_j)_n - \left( \frac{t_k}{L_k} \right)_j (w_j - w_{j-1})_n \\ & = - \frac{1}{A_V} (t_{k+1} \sin \alpha_{k+1} - t_k \sin \alpha_k)_j \left[ \frac{V}{G} + \sum_j (t_{k+1} \sin \alpha_{k+1} - t_k \sin \alpha_k)_j w_j \right] \end{aligned} \quad (26)$$

$$\text{or,} \quad = - \frac{1}{I_c} (t_{k+1} r_{k+1} - t_k r_k)_j \left[ \frac{T}{G} + \sum_j (t_{k+1} r_{k+1} - t_k r_k)_j w_j \right]$$

$$- \frac{1}{A_H} (t_{k+1} \cos \alpha_{k+1} - t_k \cos \alpha_k)_j \left[ \frac{H}{G} + \sum_j (t_{k+1} \cos \alpha_{k+1} - t_k \cos \alpha_k)_j w_j \right]$$

The difference equation is written in terms of differences of the variable at a discrete set of points. In cases where there is a variation of the variable between the points, it is necessary to approximate the variation by some consistent procedure. Consider the wall of the shell on which a mesh network has been superimposed. A curved element of variable thickness in a mesh interval may be approximated by a plane element of constant thickness. This implies that the values of  $t$ ,  $r$ , and  $\alpha$  are constant in each mesh interval. In Equation (23) the term  $a_j$  was defined as equal to  $t(L_{k+1} + L_k)/2$ , where  $a_j$  is the equivalent area resisting the normal stresses. This implies that the area corresponding to the normal stress  $\sigma$  at the point  $(j, n)$  is half of the area of the material in each interval neighboring the line  $j$  containing the point.

The section properties associated with the principal shear axes are given by Equation (8). The transformation of these equations into difference form gives

$$I_C = \sum_K t_K L_K r_K^2 \quad (27)$$

$$A_H = \sum_K t_K L_K \cos^2 \alpha_K$$

$$A_V = \sum_K t_K L_K \sin^2 \alpha_K$$

The deflections and rotations of the principal shear axis of the shell are given by Equation (13). The transformation of these equations into difference form gives,

$$\begin{aligned}
\frac{d\varphi}{dz} &= \frac{1}{I_c} \left[ \frac{T}{G} + \sum_j (t_{k+1} r_{k+1} - t_k r_k)_j w_j \right] \\
\frac{du}{dz} &= \frac{1}{A_H} \left[ \frac{H}{G} + \sum_j (t_{k+1} \cos \alpha_{k+1} - t_k \cos \alpha_k)_j w_j \right] \\
\frac{dv}{dz} &= \frac{1}{A_V} \left[ \frac{V}{G} + \sum_j (t_{k+1} \sin \alpha_{k+1} - t_k \sin \alpha_k)_j w_j \right]
\end{aligned} \tag{28}$$

The value of the total deflection or rotation is given by the summation of the terms along the z axis of the shell. The summation is given by the trapezoidal rule. For example the total rotation becomes

$$\begin{aligned}
\varphi &= \int_0^z \frac{d\varphi}{dz} dz \\
&= \sum_R \frac{1}{2} \left[ \left( \frac{d\varphi}{dz} \right)_{n-1} + \left( \frac{d\varphi}{dz} \right)_n \right] l
\end{aligned}$$

The displacements  $u_j$  and  $v_j$  of the surface of the shell are functions of the deflections and rotations of the principal shear axis, and may be easily shown to be

$$\begin{aligned}
u_j &= u - \varphi y \\
v_j &= v + \varphi x
\end{aligned} \tag{29}$$

The transformation of the differential equation (15) gives the following difference equation for the shear stress,

$$\begin{aligned}
\tau_k &= G \left[ \frac{1}{I_c} (w_j - w_{j-1}) + \frac{T r_k}{G I_c} + \frac{H \cos \alpha_k}{G A_H} + \frac{V \sin \alpha_k}{G A_V} \right. \\
&\quad + \frac{r_k}{I_c} \sum_j (t_{k+1} r_{k+1} - t_k r_k)_j w_j \\
&\quad + \frac{\cos \alpha_k}{A_H} \sum_j (t_{k+1} \cos \alpha_{k+1} - t_k \cos \alpha_k)_j w_j \\
&\quad \left. + \frac{\sin \alpha_k}{A_V} \sum_j (t_{k+1} \sin \alpha_{k+1} - t_k \sin \alpha_k)_j w_j \right]
\end{aligned} \tag{30}$$



The tangential path of integration for determining the shear in the K, Rth element (Figure 4) in Equation (30) may be either along the neighboring (n-1) or (n) th line. If the length of the interval approaches zero, the choice of the path is immaterial. However, for finite intervals the choice of the path affects the result, and by definition, the path chosen is along the (n)th line. In other words, the path is the line neighboring the shear element in the direction of the positive z axis. It is to be noted that the shear stress in each mesh interval is constant.

The normal stress along a line parallel to the z axis is given by Equation (4). By application of Newton's Equation (21) for the derivative, the normal stresses are given by the following difference equations:

$$\begin{aligned}(\sigma)_{n-1} &= \frac{E'}{2l} (-3w_{n-1} + 4w_n - w_{n+1})_j \\(\sigma)_n &= \frac{E'}{2l} (w_{n+1} - w_{n-1})_j \\(\sigma)_{n+1} &= \frac{E'}{2l} (3w_{n+1} - 4w_n + w_{n-1})_j\end{aligned}\tag{31}$$

where the subscript notation is in accordance with the nomenclature in Figure 4. It is to be noted, that as the shear stress in each mesh interval is constant, the variation of the normal stress along each line parallel to the z axis is linear.

The formulation of the finite difference problem for unstiffened shells may be applied to stiffened shells provided that two modifications are made to Equation (23). First, the equivalent area of the material resisting the normal stresses ( $a_j$ ) should include the stiffener area in addition to the wall area. Second, the modulus of elasticity E should be used in place of E'.

In order that the solution of the difference equations in a given domain  $D$  be unique, the location of the closed curve  $\Gamma$  bounding the domain and the values of the function or its derivatives must be assigned or determinable. In the cases to be considered, the location of the boundaries are assigned, and intersect nodes of the mesh. The boundary value problems to be considered are "mixed", as the values of the function are given over certain portions of the boundary, and the value of the first derivatives over the remainder. The details of the application of the boundary conditions are discussed in Parts IV and V.

#### IV. THE RELAXATION PROCEDURE FOR THE SOLUTION OF THE FINITE DIFFERENCE PROBLEM

An excellent introduction on the use of relaxation methods is given by Shaw (Reference 5). This section can only hope to point out the highlights of the procedure, as the serious user will have to master the technique by study of the literature.

The relaxation mesh of the finite difference procedure for the orthogonal shell is a right cylinder (since the displacements are a singly periodic function) with boundary conditions imposed at the two ends. Simplification of the mesh arises when the cross section of the beam and corresponding boundary conditions are symmetrical about one or both principal shear axes. In this case, the cylindrical mesh may be cut along a line corresponding to the intersection of a principal shear axis and the surface of the shell. The boundary condition along the edges of the cut is that the value of either the displacement or its derivative is zero. This is illustrated by Table 1. The cut cylindrical mesh is then unwrapped, and the mesh becomes a rectangle in the cartesian  $s, z$  plane. The boundary conditions along the ends of this rectangle are dependent on the particular problem.

The size of the initial mesh is dependent on the rate of change of the wanted function, the ease in "advancing to finer mesh", and the ease of application of "line" and "block" relaxation. The meshes used in

Parts VI and VII are examples of the usable size.

The initial assumptions of the function in the domain D should be made with care in order to avoid excessive labor. For the case of orthogonal shells, much aid may be obtained from simple bending and torsion theory.

In order to briefly illustrate the techniques used, the simple Poisson equation

$$\nabla^2 \phi(x, y) = F \quad (32)$$

will be considered. The procedure for the more complex integro-differential equation for shells is identical. Consider a square domain with square meshes of side  $h$  as shown in Figure 5(a) in which the nearby mesh nodes are identified by a letter system. The transformation of the differential Equation (32) gives the following difference equation for the point (0),

$$\phi_a + \phi_b + \phi_c + \phi_d - 4\phi_0 - h^2 F = E_0 \quad (33)$$

where

$\phi_0$  = the value of the "wanted" function at point 0

$E_0$  = error of the difference equation at point 0.

Consider that the boundary values are known for the mesh network shown in Figure 5(b), and assume initial values of the function in the domain. By the use of Equation (33), the errors are computed for each point in the set not on the boundary. The purpose of the method is to reduce the error to a value which will approach zero. This is done by the use of relaxation operators.

An example will illustrate the procedure for obtaining a relaxation operator. Assume a change in the value of the function at point (o) of  $\varphi = 1$ . The question arises, "What are the changes in the errors in the domain?". Inspection of Equation (33) shows that  $E_o$  changes by -4. The equations for the errors at the points a, b, c, d contain  $\varphi_o$ , and thus  $E_a, E_b, E_c, E_d$  change by 1. The "point" relaxation operator is diagrammatically shown in Figure 5(c). In the calculations, only the value of the total error should be recorded, whereas usually the increment is recorded in the case of the function  $\varphi$ . Note that the value of the function is written to the left of the vertical line, and the errors to the right of it. At the boundary where the value of the function is specified, the errors are not recorded.

Lines of symmetry may be used with boundary conditions where the derivative of the function is zero. With reference to Figure 5(d), consider that a solution of the problem is desired in the hatched region. If a change in the value of the function is made at a point (o) along a line adjacent to the line of symmetry, then a change is necessary at the corresponding point (o') on the other side of the symmetry line. The difference equations are unchanged except at the line of symmetry. For example at the point c, the difference equation becomes

$$\varphi_o + \varphi_f + 2\varphi_o - 4\varphi_c - h^2 F = E_c$$

The relaxation operators are unchanged except at the line adjacent to the line of symmetry. The modified operator is diagrammatically illustrated in Figure 5(e).

The procedure for reducing an error is to alter the value of the function at the point in such a manner so as to reduce the error. Usually the points with the largest errors are treated first. The totality of the errors is only reduced by "pushing some of them over the boundary". Any other operation has the effect of distributing them over a larger area. In order to speed up the process, "line" and "block" relaxation operators are used. These are the superposition of a number of adjacent point relaxation operators due to a simultaneous change of the function along a portion of a line or in an area. Usually, they are computed for a unit change of the function and the magnitude adjusted by a multiplier dependent on the totality of the errors. In addition, the practice of "over relaxation" is frequently used with relaxation operators. By these procedures, the errors may be reduced to nearly zero, and the approximate difference equations solved for any given mesh.

In order to obtain increased accuracy, it is necessary to decrease the size of the mesh. In practice, it seems best to commence the problem with a fairly coarse mesh, liquidate the errors everywhere, and then from this first approximation derive a trial solution on a net of finer mesh. As the mesh becomes finer, the resulting successive solutions give an indication of their convergence. The procedure is indicated in Figure 5(f). Let the horizontal and vertical solid lines be the net, of mesh size  $h$ , for which an approximate solution has been obtained. Then the net with the next finer mesh will be that at  $45^\circ$

formed by the broken lines. The mesh size will be  $h/\sqrt{2}$ . Then for the point  $O$  (for Poisson's equation) the difference equation is

$$\varphi_1 + \varphi_2 + \varphi_3 + \varphi_4 - 4\varphi_0 - \frac{h^2}{2} F = E_0$$

Assume the error is zero ( $E_0 = 0$ ), hence

$$\varphi_0 = \frac{1}{4} \left( -\frac{h^2 F}{2} + \varphi_1 + \varphi_2 + \varphi_3 + \varphi_4 \right)$$

This gives the trial points for the  $45^\circ$  mesh. This mesh may be liquified, and the procedure repeated to give a new  $90^\circ$  mesh, of mesh size  $h/2$ , and so on.

## V. GENERAL PROCEDURE FOR THE DETERMINATION OF STRESSES AND DEFLECTIONS FOR THIN-WALLED BEAMS

### 1. Orthogonal Beams

The stresses and deflections of a thin-walled orthogonal beam of uniform closed cross section may be determined by the application of the theory of shells. The procedure may be simplified in the event of symmetry of the cross section and symmetry of the boundary conditions of the beam about one or both of the principal shear axes. The beam is oriented by the coordinate system shown in Figure 1. The relaxation mesh corresponding to the beam is a right cylinder. In the event of symmetry, the simplification of the relaxation mesh and the boundary conditions along the edges of the mesh parallel to the  $z$  axis is illustrated by Table 1. The boundary conditions along the edges of the mesh parallel to the  $s$  coordinate are dependent upon the particular problem, and in the cases to be considered, are either on the value of the displacement ( $w$ ) or the first derivative of the displacement. The value of the first derivative of the displacement is expressed in difference form by Equation (31). The length of the intervals of the relaxation mesh and the corresponding idealization of the beam cross section are dependent upon the possibility of simplifying the difference equation, the rate of change of the wanted function, the ease in advancing to finer mesh, and the ease of application of line and block relaxation operators. The nodes and the intervals of the mesh are identified in accordance with



Figure 4. The behavior of the beam is governed by the applicable difference equation for the displacement ( $w$ ) given in Part III. The point relaxation operators are determined from the difference equation by the methods outlined in Part IV. The initial assumptions of the function in the mesh may be obtained from simple bending and torsion theory. The solution of the difference equations on the displacement are obtained by the procedures in Part IV. The stresses and deflections of the beam are obtained from the equations given in Part III.

The boundary conditions along the edges of the mesh parallel to the  $s$  coordinate are illustrated by considering the cases of the simply supported and cantilever beams.

a. Simply Supported Beam

The boundary conditions along the edges of the mesh parallel to the  $s$  coordinate are dependent upon the conditions at the ends of the actual beam. For the case of a simply supported beam with transverse loads, the axial stresses at the ends of the beam are zero. In the case of a simply supported beam with end moments, the axial stresses at the ends of the beam are known. In both cases, the stress may be expressed as a derivative of the displacement and transferred into difference form.

b. Cantilever Beam with an Orthogonal Support

The boundary conditions along the edges of the mesh parallel to the  $s$  coordinate are dependent upon the conditions at the ends of the

actual beam. For the case of a cantilever beam with transverse loading, the axial stresses at the free ends of the beam are zero. The boundary conditions for the fixed end of the beam are dependent upon the type of support. For a rigid support, the boundary condition is that the displacement is zero at the root. An example of this case is given in Part VI. For an elastic support, the boundary conditions require the compatibility of displacements and equilibrium of forces at the root. An example of this case is given in Part VII.

## 2. Cantilever Beam with a Rigid Oblique Support

The stresses and deflections of a swept, cantilever beam of uniform, thin-walled, closed cross section may be determined by the application of the theory of shells. Consider the problem of a cantilever beam on a rigid oblique support (AA'D'D) shown in Figure 6(a). The problem is equivalent to a cantilever beam with an orthogonal support (AA'E'E) shown in Figure 6(b), with the condition of no displacement ( $u_j = v_j = w_j = 0$ ) of the section AA'D'D.

The problem of the equivalent cantilever beam is the same as the problem of the orthogonal cantilever beam discussed in Part 1 of this section, with the following exceptions.

The first exception is that the boundary condition applied at the fixed end becomes a condition applied along a line in the domain adjacent to the boundary. In other words, it is required to distribute the values of the function along the boundary adjacent to the line in the domain such

that the desired conditions of the function are achieved along the specified line. The solution of the inverse problem may be obtained by relaxation methods, and is unique. Therefore, the equivalent beam problem may be treated in the same manner as before, with the displacement ( $w_j$ ) being the unknown function. It remains to discuss the question, in the framework of the orthogonal shell theory, how closely can the conditions along the section AA'D'D be satisfied? In answer to the question, it is obvious that the conditions on the displacement  $w_j$  may be exactly satisfied along the section AA'D'D. However, the displacements  $u_j$  and  $v_j$  are functions of the displacement  $w_j$ , the orientation of the orthogonal support AA'E'E, and the beam and loading conditions as shown by Equations (28) and (29). Consider the vertical displacement  $v_j$  along the section AA'D'D. The assumption in the formulation of the shell theory that the cross sections normal to the beam are preserved implies that cross sections oblique to the beam are not preserved. It follows, in general, that the condition on the vertical displacement along the section AA'D'D may only be satisfied at 2 points on the contour. In particular, for a wing of conventional box section, the conditions on  $v_j$  may only be satisfied at the spars. Consider the lateral displacement  $u_j$  along the section AA'D'D. The condition may be satisfied for a point along AA', but only by chance for any other point along AA'D'D. However, the effect of the error in  $u_j$  is assumed to be small, and is neglected in the analysis. Therefore, in the frame-

work of the orthogonal shell theory the condition on the displacement  $w_j$  is satisfied, and the condition on  $u_j$  and  $v_j$  is approximately satisfied. The condition on  $v_j$  may be satisfied if the assumption on the preservation of the cross section in the root region is relaxed. Consider a finite number of normal forces applied along the lines AD and A'D'. If the magnitudes of the normal forces are such that the deflections ( $v_j$ ) are zero, then the conditions on  $v_j$  are satisfied. However, it turns out that the deflections ( $v_j$ ) along the cross section AA'D'D are small, and the effects may be neglected.

The second exception is that the deflections of the beam are obtained in the same manner as in Part 1 of this section, with the addition of a solid body translation and rotation to satisfy the conditions on the displacements  $u_j$  and  $v_j$  at the spars.

### 3. Beam on Multiple Supports Representing a Sweptback Wing with a Carry Through Bay.

The stresses and deflections of a beam on multiple supports representing a sweptback wing with a carry through bay may be determined by the application of the theory of shells. Consider the problem of the sweptback wing shown in Figure 7(a). The wing is composed of an outer panel cantilevered obliquely to a simply supported inner panel. The intersection of the panels introduces a redundancy that may be removed by making a cut along the intersection. As a result, the problem is equivalent to considering the outer panel as a

cantilevered shell with an orthogonal support (AA'E E) and the inner panel as a simply supported shell, as shown in Figure 7(b). The conditions of compatibility of displacements and equilibrium of forces of the shells are required to be satisfied along the section AA'D'D.

The problems of the equivalent wing comprising the equivalent cantilever beam and the simply supported beam are the same as the problems discussed in parts 1(a) and 2 of this section, with the exception of the boundary conditions imposed on the equivalent wing, and the elasticity of the oblique support (AA'D'D).

For the moment, consider the boundary conditions on the wing, assuming rigid wing supports. The boundary conditions on the wing are dependent upon the load distribution. Any arbitrary load distribution may be split up into its symmetrical and antisymmetrical parts. In the symmetrical case, the slope of the wing at the center and the vertical deflection at the wing supports are zero. For the antisymmetrical case, the vertical deflections of the wing at the center and at the wing supports are zero. Thus, for both cases, the vertical deflection of the wing at the supports is zero and for transverse loading the normal stresses at the free ends are zero. The displacements ( $w$ ) and normal stresses ( $\sigma$ ) are zero at the center of the wing for the symmetrical and antisymmetrical cases respectively.

Consider the elasticity of the oblique support (AA'D'D). The idealized support structure is composed of a fuselage rib (AA'D'D), an inboard orthogonal wing rib (HH'D'D), and the joints of the sheet and stiffeners

between the inner and outer shells as shown in Figure 7(a). In order to investigate the effects of the ribs the assumption of the preservation of the cross sections of the shells in the support region is relaxed. It is assumed that the fuselage rib is infinitely stiff in its own plane and free to warp out of its plane. In addition, it is assumed that the wing rib is elastic, pin-ended at HH', and that the shear loads on the top and bottom rib flanges may be neglected.

As the equations governing the behavior of the structure are linear, the method of influence coefficients may be used to determine the stresses and deflections at any point. The stresses and deflections are given by

$$\begin{aligned}\sigma_m &= \sum_{n=1}^r \sigma_{m,n}^{\sigma,F} F_n \\ \delta_m &= \sum_{n=1}^r \delta_{m,n}^{\delta,F} F_n\end{aligned}\tag{34}$$

where

$\sigma_m, \delta_m$  = stress and deflection at point  $m$

$\sigma_{m,n}^{\sigma,F}, \delta_{m,n}^{\delta,F}$  = stress and deflection influence coefficients for the behavior at  $m$  due to a unit load at point  $n$ .

$F_n$  = load at point  $n$

The influence coefficients are determined for the behavior of the equivalent wing with no wing rib under the action of external loads, and under the action of loads imposed by the wing rib. The procedure for determining the influence coefficients for the external loading and the rib loading

are discussed in the following.

Consider the behavior of the wing with no wing rib under the action of external loads. Orient the equivalent cantilever beam (outer panel) and the simply supported beam (inner panel) as shown in Figure 7(b). The corresponding relaxation meshes divide up the surface of the wing into a series of stiffener and sheet elements. Consider the compatibility of the displacements of a point  $(j, n)$ . The displacements  $(u_j)_0$  and  $(w_j)_0$  of the  $j$ th stringer of the outer panel along the outer panel coordinate axes  $(x)_0$  and  $(z)_0$  respectively, are resolved along the inner panel coordinate axes  $(x)_i$  and  $(z)_i$  as follows:

$$(w_j)_i = (w_j)_0 \cos \psi + (u_j)_0 \sin \psi$$

$$(u_j)_i = (u_j)_0 \cos \psi - (w_j)_0 \sin \psi$$

The assumption of a rigid fuselage rib (AA'D'D) implies that  $(u_j)_i = 0$ , whence

$$(w_j)_i = (w_j)_0 / \cos \psi \quad (35)$$

This establishes the relationship between the displacements  $(w_j)$  of the inner and outer panels.

The condition of equilibrium of forces must be satisfied at the joint in order to uniquely determine the displacements. The forces acting at the joints of the stiffener and sheet elements are shown in Figure 7(c). The stresses in the outer panel sheet elements may be resolved into directions normal and parallel to the fuselage rib. The portion of the force normal to the fuselage rib that is contributed by the sheet is pro-

portional to the resolved normal stress  $\sigma'_z$ . The resolved normal stress is given in Timoshenko (Chapter 1, Reference 6) to be

$$\sigma'_z = \sigma_z \cos^2 \lambda + \sigma_s \sin^2 \lambda - 2 \tau_{sz} \sin \lambda \cos \lambda$$

where  $\lambda$  = angle of resolution of the stress.

By Equation (1)

$$\sigma_s = \mu \sigma_z$$

whence

$$\sigma'_z = \sigma_z (\cos^2 \lambda + \mu \sin^2 \lambda) - \tau_{sz} \sin 2\lambda \quad (36)$$

For a swept back wing with a carry through bay with a uniform cross section in each panel, the angle of resolution is

$$\lambda = \psi / \cos \alpha$$

where  $\psi$  = angle of sweep

It follows that the portion of the force transmitted across the fuselage rib by the outer panel sheet element is,

$$\left( \sigma'_z \frac{Lt}{\cos \lambda} \right)_0$$

The force is resolved parallel to the  $(z)_i$  axis to give the following contribution by the sheet element.

$$\left( \sigma'_z \frac{Lt}{\cos \lambda} \right)_0 \cos \beta$$

where  $\beta = \psi / \sin \alpha$  = included angle between outer sheet element and  $(z)_i$  axis.

The force transmitted across the fuselage rib by the stiffeners is

$(\sigma_z a_{st})_j$ , where  $a_{st}$  is the area of the stiffener element. The



force is resolved parallel to the  $(z)_i$  axis to give the following contribution by the stiffener element.

$$(\sigma_z a_{SH})_0 \cos \psi$$

Since it was assumed that half of the width of the sheet each side of the stiffener acts with the stiffener, the following equation is obtained for the equilibrium of forces at the point  $(j, n)$ ,

$$\begin{aligned} (\sigma_j a_j)_i = & \left[ (\sigma_z a_{ST})_j \right]_0 \cos \psi + \frac{1}{z} \left[ (\sigma'_z \frac{Lt}{\cos \lambda} \cos \beta)_{k+1} \right. \\ & \left. + (\sigma'_z \frac{Lt}{\cos \lambda} \cos \beta)_k \right]_0 \end{aligned} \quad (37)$$

where  $\sigma'_z$  is given by Equation (36). The normal and shear stresses may be written in terms of the displacements  $(w_j)$ , the beam loading, and geometrical characteristics by means of Equations (30) and (31). It follows that by using the boundary conditions on the wing and the equations of compatibility and equilibrium of the joint, the difference equations for the displacements may be solved. The stresses and deflections of the beam are determined, and the influence coefficients given by Equation (34).

Consider the behavior of the wing under the action of loads imposed by the wing rib. To account for the effects of the wing rib, cut the rib at HH', and apply an equal and opposite redundant load  $P$  to the rib and to the spar as shown in Figure 7(d). The load  $P$  on the rib at HH' applies a moment at DD' to the rear spar of the inner panel equal to

$$M = P c \sin \psi$$

where  $c$  = normal chord of the outer panel. The load  $P$  on the outer

panel is equivalent to a vertical and a torque load applied at the cross section HH'D'D. The boundary conditions on the displacements and on the forces at the joint are the same as for the case of the external loads (Equations (35) and (37)), with the exception of the force equation for the rear spar flange. For this case, Equation (37) for the equilibrium of forces includes an additional term in the right hand side to account for the moment applied by the rib. The expression becomes

$$(\sigma_j a_j)_i = \frac{P c \sin \psi}{h} + [(\sigma_z a_{ST})_j]_0 \cos \psi \quad (38)$$

$$+ \frac{1}{2} \left[ (\sigma_z' \frac{Lt}{\cos \lambda} \cos \beta)_{K+1} + (\sigma_z' \frac{Lt}{\cos \lambda} \cos \beta)_K \right]_0$$

where  $h$  = depth of beam cross section at root of rear spar. It follows that the stresses and deflections of the beam may be determined for a given load  $P$ , whence the influence coefficients may be obtained by Equation (34).

The value of the redundant load  $P$  imposed by the wing rib is determined by considering the compatibility of deflections at the cut. The deflection of the outer panel front spar must be equal to the deflection of the wing rib at the point H. This is given by

$$\delta_H = \delta_{H, f_n}^{\delta, F}(V, H, T) F_n(V, H, T) + \delta_{H, f_n}^{\delta, F}(V, H, T) F_n(P, M) \quad (39)$$

where  $f_n(V, H, T)$ ,  $F_n(V, H, T)$ , etc., represent the loading conditions. The deflection of the wing rib at the point H is a function of the rotation of the rear spar of the inner panel and the elasticity of the rib. The deflection is given by

$$\delta_H = \left[ \theta_{D, F_n}^{\delta, F} (V, H, T) F_n (V, H, T) + \theta_{D, M}^{\delta, F} M \right] c \sin \psi + \frac{1}{3} \frac{P c^3}{(EI)_{\text{wing rib}}} \quad (40)$$

where  $\theta_{m, n}^{\delta, F}$  = rotation influence coefficient for the behavior at  $m$  due to a unit moment at point  $n$ .

The value of  $P$  may be determined by equating Equations (39) and (40).

The stresses and deflections of the wing under external load including the effects of the wing rib are given by Equation (34). An example is given in Part VII.

## VI. COMPARISON OF THE FINITE DIFFERENCE METHOD AND THE ANALYTICAL SOLUTIONS FOR A CANTILEVER BEAM WITH A RIGID ORTHOGONAL SUPPORT

The problem of determining the stresses and deflections of a thin-walled beam of uniform thickness subject to variable twist has been formulated by von Karman and Chien (Reference 7). From the formulation, an analytical solution was developed for a beam with a doubly symmetric cross section, and in particular, an example was worked out for a semi-infinite beam of rectangular cross section on a rigid support subject to end twist.

The formulation of the problem given in Part II is in agreement with the formulation by Karman and Chien. Therefore, it is of interest to compare the finite difference and analytical solutions for a representative beam. Consider the tube of rectangular cross section shown in Figure 8(a). The tube has a length of 25.4 in., a cross section 2 in. x 8 in., and a wall thickness of one-eighth inch. The tube is loaded by an end torque of 29,600 inch-pounds. The cross section and boundary conditions are symmetrical about both principal shear axes, and therefore permit maximum simplification of the procedures. The tube is oriented by the coordinate system shown in Figure 8(a) and the simplified relaxation mesh for this case is given by Table 1. As a result the mesh corresponds to the upper left hand quadrant of the cross section. The boundary condition along the edges of the mesh parallel to the z axis is that the dis-

placement ( $w$ ) is zero. The boundary conditions along the edges of the mesh parallel to the  $s$  coordinate corresponding to the fixed and free ends of the beam are that the displacement ( $w$ ) and the derivative of the displacement ( $\sigma$ ) are zero respectively. This is illustrated in Figure 8(b). The length of the intervals of the relaxation mesh and idealization of the cross section may be chosen so as to simplify the difference Equation (24). It will be seen that it is desirable to let  $L_{k+1} = L_k = L$ , and

$$\frac{E'q_j L}{G l^2 t} = 1 \quad (41)$$

Assuming,  $\mu = .3$ , and since  $a_j = Lt$ , the relationship between the intervals is given by

$$l = 1.690L$$

In this problem, it is relatively easy to advance to finer mesh and employ line and block relaxation techniques. As a result, the interval  $L = 1$  in. is chosen for the initial mesh for the entire domain. Subsequently, the mesh size is advanced to  $L = 1/2$  inch for the half of the domain corresponding to the root region, and to  $L = 1/4$  inch for the domain corresponding to the corner of the cross section in the root region. The advance to finer mesh employs the procedures outlined in Part IV, and is illustrated in Figure 8(b). The nodes and intervals of the mesh are identified in accordance with Figure 4.

The difference equation for a beam under torsion with doubly symmetrical cross section and boundary condition is

$$\begin{aligned} & \frac{E' d_j}{G L^2} (W_{n+1} + W_{n-1} - 2W_n)_j + \left(\frac{t_{k+1}}{L_{k+1}}\right) (W_{j+1} - W_j)_n - \left(\frac{t_k}{L_k}\right) (W_j - W_{j-1})_n \quad (24) \\ & = -\frac{1}{I_c} (t_{k+1} r_{k+1} - t_k r_k) \left[ \frac{T}{G} + \sum_j (t_{k+1} r_{k+1} - t_k r_k)_j W_j \right] \end{aligned}$$

The equation is simplified by the choice of the mesh intervals. Applying Equation (41), the result is

$$\begin{aligned} & (W_{n+1} + W_{n-1})_j + (W_{j+1} + W_{j-1})_n - 4W_{j,n} \quad (42) \\ & = -\frac{L}{I_c} (r_{k+1} - r_k)_j \left[ \frac{T}{G} + t \sum_j (r_{k+1} - r_k)_j W_j \right] \end{aligned}$$

For every region in the domain except the region corresponding to the corners of the tube, the equation reduces to the Laplace equation,

$$(W_{n+1} + W_{n-1})_j + (W_{j+1} + W_{j-1})_n - 4W_{j,n} = 0 \quad (43)$$

For the region in the domain corresponding to the corner of the tube, Equation (42) becomes

$$(W_{n+1} + W_{n-1})_j + (W_{j+1} + W_{j-1})_n - 4W_{j,n} = -L \left( \frac{2.31}{10^3} + 0.45 W_{j,n} \right) \quad (44)$$

where the numerical calculations are given in Appendix A. The relaxation technique is facilitated if decimal values of the variable are avoided, so let

$w' = w \times 10^6$ . Whence Equation (44) becomes

$$(W'_{n+1} + W'_{n-1})_j + (W'_{j+1} + W'_{j-1})_n - (4 - 0.45) W'_{j,n} = -2310 L \quad (45)$$

The difference equations corresponding to the mesh sizes are obtained by inserting the value of the interval (L) into Equation (45). The equation becomes,

$$(W'_{n+1} + W'_{n-1})_j + (W'_{j+1} + W'_{j-1})_n - K_1 W'_{j,n} = -K_2 \quad (46)$$

where  $K_1 = 3.55, 3.775, 3.8875$  and  $K_2 = 2310, 1155, 577$  for  $L = 1, 1/2$  and  $1/4$  inches respectively.

The point relaxation operators are determined by the procedures outlined in Part IV. Diagrammatically, the relaxation operators are shown in Figure 8(c). By the simple torsion theory, the initial displacements ( $w$ ) were assumed to be zero for the coarse mesh. The solutions of the difference Equations (43) and (46) in the domain corresponding to the upper left hand quadrant of the cross section with the applicable boundary conditions are obtained by the procedures in Parts IV and V.

The final values of the displacement ( $w$ ) for the rectangular tube under torsion are shown in Figure 9. The values of the normal stress are calculated from the displacements by Equation (31), and are shown in Figure 9. The values of displacement and stress determined with the fine mesh ( $L = 1/2$  in.) are plotted as a function of the tangential coordinate in Figures 10 and 11 respectively. The normal stresses along the corner of the tube are plotted as a function of the axial coordinate in Figure 12. The normal stresses at the support for various mesh sizes are compared to the results of the analytical solution by von Karman and Chien by plotting the stresses as a function of the mesh size in Figure 13.

The comparison of the stresses determined analytically and by the finite differences method show good agreement, with a possible exception of the region in the neighborhood of the corner of the tube at the support.

In this region, the large gradients of the normal stress, both in the axial and tangential directions, probably account for the discrepancy. An additional advance to a finer mesh would undoubtedly improve the agreement, but in view of the fact that the mesh interval is already within 5 percent of the width of the tube, it does not appear to be of practical importance to do so. This example illustrates the distribution of the "bending stresses due to torsion" in the support region of the tube, and points out the necessity of an accurate knowledge of the support conditions if precise stress data are desired.



VII. COMPARISON OF THE THEORETICAL SOLUTIONS AND  
EXPERIMENTAL DATA FOR A SWEPT BACK WING WITH A  
CARRY THROUGH BAY UNDER SYMMETRICAL BENDING

The National Advisory Committee for Aeronautics has conducted a series of experimental investigations on the behavior of an untapered box beam, representing the main structural component of a full span, two spar,  $45^{\circ}$  swept wing with a carry through bay. The investigation was reported in references (8) and (9) for the cases of symmetrical and antisymmetrical bending and torsion respectively. The full span model was carefully constructed, and included complete instrumentation to record the normal and shear stresses, in addition to the distortions of the structure. As a result, the NACA experimental data is considered to be unusually reliable, and is compared to the theoretical difference solution for symmetrical bending in order to establish the validity of the theoretical assumptions.

The experimental wing was constructed of aluminum alloy with the swept-back parts consisting of two boxes with their longitudinal axes at right angles, joined by and continuous with a short rectangular carry through bay representing that part of the wing inside the fuselage. The details of the experimental swept-back box beam are shown in Figure 14. The wing was loaded in symmetrical bending with a downward end shear of 2500 pounds acting through the principal shear axes of the tip cross section.

The procedure for theoretically determining the stresses and deflections of the swept wing follow the methods given in Part 3 of Part V. The swept wing is equivalent to a cantilevered shell with an orthogonal support and a shell on a simple support. The beams are oriented by the coordinate system shown in Figure 7(b). The cross section and boundary conditions are symmetrical about the x axis, and therefore permit a simplification of the procedures. The simplified relaxation mesh for this case is given by Table 1. As a result, the mesh corresponds to the upper half of the cross section. Since the purpose of this investigation is to establish a satisfactory minimum idealization of the swept wing in addition to establishing the validity of the theoretical assumptions, the cross section is idealized into four, six, and ten stiffener or flange elements.

The relaxation mesh for the inner and outer panels are shown in Figure 15(a), (b), and (c) for the four, six and ten element beams respectively. The mesh lines (j) parallel to the z axis correspond to the boundaries, the flanges ( $F_1, F_2$ ) or to the stringers (S). The intervals between the lines corresponding to the flanges and stringers are constant. The mesh lines parallel to the s coordinate are located by virtue of the desired intervals between the mesh lines. For instance, there are three mesh lines (n) of equal interval in the inner panel in order that the difference equations for stresses (31) may be used, and the intervals between the mesh lines (n) in the outer panel are equal to the interval

between the stiffeners and flanges. As it will be seen later, it is desirable to adopt two methods of identifying the modes and intervals of the mesh. For the difference equation, the mesh is identified in accordance with Figure (4) with the addition that the mesh lines parallel to the  $z$  axis are annotated  $F_1, F_2, S$ , etc. corresponding to the flanges and stringers. For the equations of equilibrium and compatibility, the mesh nodes in the neighborhood of the joint are identified by numbers. The identification of the meshes is illustrated in Figures 15(a), (b) and (c).

The distribution of material for the idealized cross section is governed by the assumptions made in Parts II and III. The total areas of the idealized and actual stiffeners and flanges are equal, with the exception that the idealized flanges contain the equivalent spar web material and the sheet material attached to the flange. The equivalent spar web material is that equivalent area representing the moment carrying capacity of the webs, and for each flange is equal to one sixth of the cross sectional area of the actual web. The areas of the idealized and actual sheet are equal. The concept of effective width has not been introduced, primarily to avoid inconsistencies at the oblique boundary. The numerical calculations for the idealization are carried out in Appendix B. 1, and the idealized cross sections are illustrated in Figure 16.

The idealized support structure discussed in Part 3 of Part V is composed of a fuselage rib, an inboard orthogonal wing rib, and the

joints of the sheet and stiffeners between the inner and outer shells as shown in Figure 7(a).

It is now desirable to consider the boundary conditions. From Table 1, the boundary condition along the edges of the mesh parallel to the  $z$  axis is that the displacement ( $w$ ) is zero. The boundary conditions along the edges of the mesh parallel to the  $s$  coordinate are dependent upon the boundary conditions on the wing and the conditions at the intersection of the inner and outer shells.

The boundary conditions for the wing loaded in symmetrical bending are that the displacements are zero at the center of the carry through bay and the stresses are zero at the tip of the wing. This is illustrated in Figure 15. With regard to the boundary condition applied at the tip of the wing, there is one important point to be brought up. In thin-walled beams, the "disturbances" due to the oblique support are nearly "damped" out in about one (normal) chord length from the support. As a result, the final convergence of the solution of the difference equations is greatly speeded up if the boundary conditions are initially applied at a cross section one chord length from the support. The boundary conditions are determined by elementary beam theory. The resulting wing is called a "clipped" wing, and this procedure is used for the six and ten element beams. The numerical calculations for this boundary condition are carried out in Appendix B. 2.

Boundary conditions are imposed on the compatibility of displacements

and equilibrium of forces at the intersection of the inner and outer shells. The compatibility of displacements is given by Equation (35). In the wing with an angle of sweep of  $45^\circ$ , the equation becomes

$$(w_j)_i = 1.414 (w_j)_o \quad (47)$$

As discussed in Part 3 of Part V, the conditions on the equilibrium of forces, and in addition, the difference equation are dependent upon whether the behavior of the wing under the action of external loads or rib loads is being considered. As a result, these equations are obtained for a general loading, with the treatment of the particular loading conditions discussed as required. Hence, the equation of equilibrium of forces at the point  $(j, n)$  is

$$\begin{aligned} (\sigma_j a_j)_i = & \frac{Pc \sin \psi}{h} + [(\sigma_z a_{ST})_j]_o \cos \psi \\ & + \frac{1}{2} \left[ (\sigma'_z \frac{Lt}{\cos \lambda} \cos \beta)_{K+1} + (\sigma'_z \frac{Lt}{\cos \lambda} \cos \beta)_K \right]_o \end{aligned} \quad (38)$$

where  $\sigma'_z = \sigma_z (\cos^2 \lambda + \mu \sin^2 \lambda) - \tau_{sz} \sin 2\lambda$

$$\lambda = \psi / \cos \alpha \quad (37)$$

$$\beta = \psi / \sin \alpha$$

In the idealized cross section, the spar web does not transmit normal stress. Thus, only the elements in the idealized cover of the box contribute to the equilibrium equation. Hence substituting Equation (37) into Equation (38), the result is

$$\begin{aligned} (\sigma_j a_j)_i = & 3P + 0.707 [(\sigma_z a_{ST})_j]_o \\ & + 0.03535 \left\{ [(1.656 \sigma_z - \tau_{sz})L]_{K+1} + [(1.656 \sigma_z - \tau_{sz})L]_K \right\} \end{aligned} \quad (48)$$

where

$$\begin{aligned} \mu &= .312 && \text{(Ref. Appendix 3.3)} \\ c &= 29.7 \text{ in.} \\ h &= 7 \text{ in.} \\ t &= 0.050 \text{ in.} && \text{(Ref. Figure 15)} \\ \lambda &= \psi = 45 \text{ deg.} \\ \beta &= 0 \end{aligned}$$

By Equation (30), the shear stress ( $\tau_{sz}$ ) for the upper cover sheet of the outer panel becomes

$$\tau_{sz} = 4 \times 10^6 \left[ \frac{1}{L_K} (w_j - w_{j-1}) + \frac{3.5T}{4 \times 10^6 \times 277.2} + \frac{3.5}{277.2} (-1.966 (w_{F_1} - w_{F_2})) \right]$$

$$E = 10.5 \times 10^6 \text{ psi}$$

where

$$G = 4 \times 10^6 \text{ psi} \quad \text{(Ref. Appendix B.3)}$$

$$I_c = 277.2 \text{ in.}^4$$

$$\sum_j (t_{k+1} r_{k+1} - t_k r_k)_j w_j = -1.966 (w_{F_1} - w_{F_2})$$

$$r_k = 3.5 \text{ in.} \quad \text{(Ref. Figure 15)}$$

The relaxation technique is facilitated if decimal values of the variable are avoided, so let  $w' = w \times 10^5$ , whence

$$\tau_{sz} = 0.01262T - \frac{40}{L_K} \left[ w'_{j-1} - w'_j + 0.0248 L_K (w'_{F_1} - w'_{F_2}) \right] \quad (49)$$

The difference equation for a beam under vertical shear and torsion with the cross section and boundary conditions symmetrical about the

x axis is

$$\begin{aligned} & \frac{E a_j}{G \rho^2} (W_{n+1} + W_{n-1} - 2W_n)_j + \left( \frac{t_{k+1}}{L_{k+1}} \right) (W_{j+1} - W_j)_n - \left( \frac{t_k}{L_k} \right)_j (W_j - W_{j-1})_n \quad (25) \\ & = -\frac{1}{I_c} (t_{k+1} r_{k+1} - t_k r_k)_j \left[ \frac{T}{G} + \sum_j (t_{k+1} r_{k+1} - t_k r_k)_j w_j \right] \\ & \quad - \frac{1}{A_v} (t_{k+1} \sin \alpha_{k+1} - t_k \sin \alpha_k)_j \left[ \frac{V}{G} + \sum_j (t_{k+1} \sin \alpha_{k+1} - t_k \sin \alpha_k)_j w_j \right] \end{aligned}$$

The additional section properties associated with the principal shear axes, and the summation terms are evaluated in Appendix B.3 to give

$$I_c = 528.2 \quad \text{in.}^4 \quad \text{inner panel}$$

$$A_v = 1.092 \text{ in.}^2 \quad \text{inner and outer panels}$$

$$\sum_j (t_{k+1} r_{k+1} - t_k r_k)_j w_j = -2.910 (W_{F_1} - W_{F_2}) \quad \text{inner panel}$$

$$\sum_j (t_{k+1} \sin \alpha_{k+1} - t_k \sin \alpha_k)_j w_j = -0.156 (W_{F_1} + W_{F_2}) \quad \text{inner and outer panels}$$

$$l = 7.5 \text{ in.} \quad \text{inner panel}$$

substituting into Equation (25), and recalling that  $w' = w \times 10^5$ , the expression for the inner panel is

$$\begin{aligned} & .0466 a_j (W'_{n+1} + W'_{n-1} - 2W'_n)_j + \left( \frac{t_{k+1}}{L_{k+1}} \right) (W'_{j+1} - W'_j)_n - \left( \frac{t_k}{L_k} \right)_j (W'_j - W'_{j-1})_n \\ & = -\frac{1}{528.2} (t_{k+1} r_{k+1} - t_k r_k)_j \left[ \frac{T}{40} - 2.910 (W'_{F_1} - W'_{F_2})_n \right] \quad (50) \\ & \quad - \frac{1}{1.092} (t_{k+1} \sin \alpha_{k+1} - t_k \sin \alpha_k)_j \left[ \frac{V}{40} - 0.156 (W'_{F_1} + W'_{F_2})_n \right] \end{aligned}$$

similarly Equation (25) for the outer panel becomes

$$\begin{aligned}
& \frac{2.62 a_j}{l^2} (W'_{n+1} + W'_{n-1} - 2W'_n)_j + \left(\frac{t_{k+1}}{L_{k+1}}\right)_j (W'_{j+1} - W'_j)_n - \left(\frac{t_k}{L_k}\right)_j (W'_j - W'_{j-1})_n \\
& = - \frac{1}{277.2} (t_{k+1} r_{k+1} - t_k r_k)_j \left[ \frac{T}{40} - 1.966 (W'_{F_1} - W'_{F_2})_n \right] \\
& \quad - \frac{1}{1.092} (t_{k+1} \sin \alpha_{k+1} - t_k \sin \alpha_k)_j \left[ \frac{V}{40} - 0.156 (W'_{F_1} + W'_{F_2})_n \right]
\end{aligned} \tag{51}$$

Now that the equations of equilibrium of forces and the difference equations for the general loading condition for the swept wing have been derived, the particular loading conditions may be investigated. As indicated in part 3, Part V, the behavior of the wing with an elastic wing rib may be determined by the method of influence coefficients. The influence coefficients are determined for the behavior of the equivalent wing with no wing rib under the action of external loads and under the action of loads imposed by the wing rib. The case of the four-element beam is discussed in detail in this section, and the details for the six and ten-element cases are given in the appendices.

Consider the behavior of the wing with no wing rib under the action of external loads. The compatibility of displacements of the joint are given by Equation (47) to be

$$\begin{aligned}
W_3 &= 1.414 W_5 \\
W_4 &= 1.414 W_8
\end{aligned} \tag{52}$$

The equilibrium of the joint is governed by Equations (48) and (49). For this case  $P = T = 0$  and the section dimensions are given in Figure 15(a). Inserting Equation (49) into (48), the expression becomes



$$2.156 (\sigma_j)_i = .707(1.111)(\sigma_j)_o + .03535(29.7) \left\{ .656 (\sigma_j)_o + \frac{40}{29.7} [w'_{F_1} - w'_{F_2} + .0248(29.7)(w'_{F_1} - w'_{F_2})] \right\} \quad (53)$$

$$(\sigma_j)_i = .684 (\sigma_j)_o + 1.137 (w'_{F_1} - w'_{F_2})$$

substitute the expressions for displacements in terms of the stresses given by Equation (31) into Equation (53), and obtain for flange  $F_1$ ,

$$\frac{10.5 \times 10^6}{2 \times 7.5 \times 10^5} (3w'_3 - 4w'_1) = .684 \times \frac{10.5 \times 10^6}{2 \times 29.7 \times 10^5} (-3w'_5 + 4w'_7 - w'_9) + 1.137 (w'_7 - w'_8)$$

Inserting the compatibility relationship for  $w'_3$  given by Equation (52) into the above equation gives

$$-w'_5 + .8403w'_1 + .1793w'_7 - .03628w'_9 - .03412 w'_8 = 0 \quad (54)$$

Similarly, the expression for the flange  $F_2$  is

$$w'_8 + .9082 w'_2 + .03921 (w'_{10} - w'_6) + .03688 w'_7 = 0 \quad (55)$$

The difference equations for the inner and outer panels are given by Equations (50) and (51) respectively. The section dimensions are given in Figure 15(a). For the inner panel,  $V = T = 0$ , and the equation for flange  $F_1$  becomes

$$\begin{aligned} & (.0466)(2.156)(w'_{n+1} + w'_{n-1} - 2w'_n)_j + \left( \frac{.050}{41.8} \right) (w'_{F_2} - w'_{F_1})_n - \left( \frac{.078}{3.5} \right) (w'_{F_1})_n \\ & = - \frac{1}{528.2} (.050 \times 3.5 - .078 \times 20.9) (-2.910) (w'_{F_1} - w'_{F_2})_n \\ & \quad - \frac{1}{1.092} (-.078) (-.156) (w'_{F_1} + w'_{F_2})_n \end{aligned}$$

Simplifying, and as  $(w_{n-1})_j = 0$  by boundary conditions,

$$-(W'_{F_1})_n + .0210 (W'_{F_2})_n + .489 (W'_{n+1})_{F_1} = 0 \quad (56)$$

Similarly for flange  $F_2$ ,

$$-(W'_{F_2})_n + .0210 (W'_{F_1})_n + .489 (W'_{n+1})_{F_2} = 0 \quad (57)$$

For the outer panel, the equation for flange  $F_1$  becomes

$$\begin{aligned} & \frac{2.62 \times 1.853}{(29.7)^2} (W'_{n+1} + W'_{n-1} - 2W'_n)_j + \frac{.050}{29.7} (W'_{F_2} - W'_{F_1})_n - \frac{.078}{3.5} (W'_{F_1})_n \\ & = -\frac{1}{277.2} (.050 \times 3.5 - .078 \times 14.85) \left[ \frac{T}{40} - 1.966 (W'_{F_1} - W'_{F_2})_n \right] \\ & \quad - \frac{1}{1.092} (-.078) \left[ \frac{V}{40} - .156 (W'_{F_1} + W'_{F_2})_n \right] \end{aligned}$$

Simplifying

$$-(W'_{F_1})_n + .346 (W'_{F_2})_n + .326 (W'_{n+1} + W'_{n-1})_{F_1} - .1058 V - .00525 T = 0 \quad (58)$$

Similarly for flange  $F_2$

$$-(W'_{F_2})_n + .346 (W'_{F_1})_n + .326 (W'_{n+1} + W'_{n-1})_{F_2} - .1058 V + .00525 T = 0 \quad (59)$$

The loading condition for the outer panel is  $V = 2500$  pounds and  $T = 0$ .

Inserting the loading conditions, the equations for flange  $F_1$  and  $F_2$

become respectively

$$\begin{aligned} & -(W'_{F_1})_n + .346 (W'_{F_2})_n + .326 (W'_{n+1} + W'_{n-1})_{F_1} + 265 = 0 \quad (60) \\ & -(W'_{F_2})_n + .346 (W'_{F_1})_n + .326 (W'_{n+1} + W'_{n-1})_{F_2} + 265 = 0 \end{aligned}$$

Likewise the equations for the six and ten-element beams may be derived. These equations are given in Appendix B. 4.

The relaxation operators are determined from the difference equation by the procedures outlined in Part IV. Diagrammatically, the point relaxation operators for the inner and outer panels are shown in Figure 17. The initial displacements ( $w$ ) for the mesh were obtained by simple bending theory. The solutions of the difference equations in the domain corresponding to the upper half of the cross section with the applicable boundary conditions on the value and derivative of the displacement are obtained by the procedures in Parts IV and V. The final values of displacement for the swept wing with no wing rib under symmetrical bending are shown in Figure 18. The values of the normal stress are calculated from the displacements by Equation (31), and are shown in Figure 18. The deflection and rotation of the beam are calculated by Equation (28), with  $u_j = v_j = 0$  at AA' and DD', and are given in Table 2.

Consider the behavior of the wing under loads imposed by the wing rib. With reference to Part 3, Part V, the action of the wing rib is to apply a vertical load  $P$  at HH' and a moment ( $M = Pc \sin \psi$ ) at DD'. The vertical load  $P$  at HH' is equivalent to a vertical and a torque load applied at the cross section HH'D'D. The loading of the inner panel is  $V = T = 0$ . Since the experimental value for  $P$  is approximately 1000 pounds, let the loading of the outer panel be  $P = V = 1000$  pounds,  $T = 14,850$  in. pounds for the cross section HH'D'D and inboard, and  $V = T = 0$  outboard of section HH'D'D. The compatibility of displacements

of the joint are unaffected by the loading, and are given by Equation (52).

The equilibrium of the joint is governed by Equations (48) and (49).

Inserting the proper constants, Equation (49) becomes

$$\tau_{sz} = 187 - 2.34(w'_{F_1} - w'_{F_2}) \quad (61)$$

Equation (61) may be substituted into Equation (48) to obtain the equation of equilibrium of forces

$$2.156 (\sigma_j)_i = 3P + .707 (1.11) (\sigma_j)_o + .03535(29.7) \\ \left[ .656 (\sigma_j)_o - 187 + 2.34 (w'_{F_1} - w'_{F_2}) \right] \quad (62)$$

$$(\sigma_j)_i = 1.393P + .684 (\sigma_j)_o + 1.137 (w'_{F_1} - w'_{F_2}) - 91$$

The term including  $P$  is only applicable to the equilibrium equations for the rear flange. Substitute the expressions for displacements in terms of the stresses given by Equation (31) into Equation (62), and obtain for flange  $F_1$

$$\frac{10.5 \times 10^6}{2 \times 7.5 \times 10^5} (3w'_3 - 4w'_1) = .684 \times \frac{10.5 \times 10^6}{2 \times 29.7 \times 10^5} (-3w'_5 + 4w'_7 - w'_9) \\ + 1.137 (w'_7 - w'_8) - 91$$

Inserting the compatibility relationship for  $w'_3$  given by Equation (52)

into the above equation gives

$$-w'_5 + .8403 w'_1 + .1793 w'_7 - .03628 w'_9 - .03412 w'_8 - 3 = 0. \quad (63)$$

Similarly, the expression for the flange  $F_2$  is

$$-w'_8 + .9082 w'_2 + .03921 (w'_{10} - w'_6) + .03688 w'_7 + 42 = 0 \quad (64)$$

The difference equations for the inner and outer panels are given by Equations (50) and (51) respectively. For the inner panel,  $V = T = 0$ , and the equations for flanges  $F_1$  and  $F_2$  are given by Equations (56) and (57). For the outer panel, there are two loading conditions. In the cross section HH'D'D and inboard, the loading is  $V = 1000$  pounds and  $T = 14,500$  inch-pounds. Inserting the loading conditions into Equations (58) and (59), the equations for flanges  $F_1$  and  $F_2$  become respectively

$$\begin{aligned} -(W'_{F_1})_n + .346 (W'_{F_2})_n + .326 (W'_{n+1} + W'_{n-1})_{F_1} - 184 &= 0 \\ -(W'_{F_2})_n + .346 (W'_{F_1})_n + .326 (W'_{n+1} + W'_{n-1})_{F_2} - 28 &= 0 \end{aligned} \quad (65)$$

Outboard of section HH'D'D, the loading is  $V = T = 0$ . Inserting the loading conditions into Equations (58) and (59), the equations for the flanges  $F_1$  and  $F_2$  become respectively

$$\begin{aligned} -(W'_{F_1})_n + .346 (W'_{F_2})_n + .326 (W'_{n+1} + W'_{n-1})_{F_1} &= 0 \\ -(W'_{F_2})_n + .346 (W'_{F_1})_n + .326 (W'_{n+1} + W'_{n-1})_{F_2} &= 0 \end{aligned} \quad (66)$$

Likewise the equations for the six-element beam may be derived. These equations are given in Appendix B.5.

The relaxation operators are unaffected by the loading, and are shown in Figure 17. The solutions of the difference equations in the domain corresponding to the upper half of the cross section with the applicable boundary conditions on the value and the derivative of the displacement are obtained by the procedures in Parts IV and V. The final values of the

displacement for the swept wing under loads imposed by the wing rib are shown in Figure 19. The values of the normal stress are calculated from the displacements by Equation (31), and shown in Figure 19.

The deflection and rotation of the beam are calculated by Equation (28), with  $u_j = v_j = 0$  at AA' and DD', and are given in Table 2.

The value of the redundant load  $P$  imposed by the wing rib is determined by considering the compatibility of deflections at the cut. The deflection of the outer panel front spar must be equal to the deflection of the wing rib at the point H. The deflection of the outer panel front spar at the point H is given by Equation (39) to be

$$\delta_H = -.043 + 14.85(-.00295) + \left[ .012 + 14.85(0.0078) \right] \frac{P}{1000} \quad (67)$$

where the incremental deflections are given by Equation (29) and Table 2. Similarly, the deflection of the wing rib at the point H is given by

Equation (40) to be

$$\delta_H = (29.7)(.707) \left[ \frac{-1244}{10^5} \frac{1}{(3.5)} - \frac{30}{10^5} \frac{1}{(3.5)} \frac{P}{1000} \right] - \frac{P(29.7^3)}{3(6.63)(30 \times 10^6)} \quad (68)$$

where the rotations are obtained from the displacements given in Figures 18 and 19. The value of  $P = 167$  pounds is obtained by equating Equations (67) and (68). Likewise the value of the redundant load  $P$  may be determined for the six-element beam. This is computed in Appendix B.6.

The stresses and deflections of the wing under external load including the effects of the wing rib are given by application of Equation (34). The

final values of normal stresses and deformations for the swept wing with a wing rib are shown in Figure 20 and Table 2 respectively.

The axial distribution of the normal stresses for the four, six and ten-element beams for the normal and "clipped" cases is shown in Figure 21(a), (b) and (c). The normal stresses at various cross sections are compared to the experimental data in Figure 22. The deflection and rotation deformations are compared to the experimental data in Figure 23.

The stresses as theoretically determined by the use of an idealized six-element beam show good agreement with experimental data. The stresses determined using a four-element beam do not show the effects of shear lag, and therefore do not have the desired characteristics. However it is to be pointed out that the maximum stresses are closely approximated by this simple idealization. The stresses determined by using a ten-element beam are in close agreement with the stresses given by the six-element beam with the exception of the low stress region in the neighborhood of the front flange joint.

The comparison of the deformations determined by the method of finite differences with the experimental data shows good agreement for the deflections and fair agreement for the rotations. The less accurate solution for the beam rotations is probably due to the assumption of a rigid fuselage rib. A preliminary investigation revealed that the assumption of an elastic fuselage rib improves the agreement. The procedure for taking into account the elasticity of the fuselage rib is

identical to the methods outlined in Part V, with the exception that the equations of equilibrium of forces and compatibility of displacements in the transverse direction are not eliminated, and require the consideration of the elasticity of the fuselage rib. Since the bending loads in the fuselage rib are high, the problem of approximating the rib loads by a number of concentrated forces is important.



## VIII. CONCLUSION

The method is a rational engineering approach to the problem of determining the stresses and deflections of unswept and swept, thin-walled beams of uniform closed cross section. The cross section, loading distribution, and boundary conditions are assumed to be arbitrary. The method is based on the differential equation governing the behavior of orthogonal elastic shells. The differential equation is transformed into a difference equation, and the solution is obtained by the relaxation technique. The comparison of the theoretical solution and experimental data for a swept back wing with a carry through bay under symmetrical bending showed good agreement.

As a result of the investigation, it is apparent that the swept wing with a carry through bay may be idealized by intersecting orthogonal shells, with elastic fuselage and inboard wing ribs. In the event that there is sufficient interest, it would be desirable to conduct further investigations in order to broaden the field of applicability of this method. The effects of symmetrical and antisymmetrical loading, taper of the cross section, and the influence of rib rigidity on rotational deformations have not been investigated with any completeness. For these conditions, it would be desirable to indicate the relationship between the idealization of the beam and the accuracy of the solution. In addition, there is the

possibility that cut outs and temperature effects may be studied by modification of the theory. In conclusion, it is believed that the method provides a more accurate and rapid means of investigating the behavior of thin-walled beams than was previously available.

## REFERENCES

1. Bescoter, S. U. Secondary Stresses in Thin-Walled Beams With Closed Cross Sections. Ph.D. Thesis, California Institute of Technology, 1950.
2. Duberg, J. E. A Numerical Procedure for the Stress Analysis of Stiffened Shells. J. Aero Sci., Vol. 16, No. 8, pp. 451-462, August 1949.
3. Southwell, R. V. Relaxation Methods in Theoretical Physics. Oxford University Press, 1946.
4. Whittaker, E. and Robinson, G. The Calculus of Observations. Blackie and Son Limited, London and Glasgow, 4th Edition, Reprinted 1948.
5. Shaw, F. S. An Introduction to Relaxation Methods. Report SM. 78, Aeronautical Laboratory, Fishermen's Bend, Melbourne, Australia, September 1946.
6. Timoshenko, S. Theory of Elasticity. McGraw-Hill Book Company, Inc., New York and London, 1934.
7. von Kármán, Th. and Chien, W. Z. Torsion with Variable Twist. J. Aero. Sci., Vol. 13, No. 10, pp. 503-510, October 1946.
8. Zender, G. and Libove, Charles Stress and Distortion Measurements in a 45° Swept Box Beam Subject to Bending and Torsion. NACA T.N. 1525, March 1948.
9. Zender, G. and Heldenfels, R. Stress and Distortion Measurements in a 45° Swept Box Beam Subjected to Antisymmetrical Bending and Torsion. NACA T.N. 2054, April 1950.

## LIST OF APPENDICES

Number	Title	Page
A	Numerical Data for Rectangular Tube Under Torsion.	67
B	Numerical Data for Swept Box Beam Under Symmetrical Bending.	68
B.1	Idealized Cross Sections of Swept Beam.	68
B.2	Clipped Wing Boundary Conditions for Six and Ten-Element Beams.	70
B.3	Evaluation of Section Constants	71
B.4	Boundary Conditions and Difference Equations for the Behavior of the Wing With No Wing Rib Under External Loads for the Six and Ten-Element Beams.	72
B.5	Boundary Conditions and Difference Equations for the Behavior of the Wing Under Loads Imposed by the Wing Rib for the Six-Element Beam.	75
B.6	Determination of the Redundant Rib Load for the Six-Element Beam.	76

## APPENDIX A

## NUMERICAL DATA FOR RECTANGULAR TUBE UNDER TORSION

The difference equation governing the behavior of the rectangular tube is given by Equation (42). The equation is

$$\begin{aligned} & (w_{n+1} + w_{n-1})_j + (w_{j+1} + w_{j-1})_n - 4w_{j,n} \\ & = - \frac{L}{I_c} (r_{k+1} - r_k)_j \left[ \frac{T}{G} + t \sum_j (r_{k+1} - r_k)_j w_{j,n} \right] \end{aligned} \quad \text{A-1}$$

The constants in the equation may be evaluated as follows. By Equation (27)

$$I_c = \sum_j t_k r_k^2 L_k = \frac{2}{8} (8 \times 1 + 2 \times 4^2) = 10 \text{ in.}^4$$

The cross section of the tube and the boundary conditions are doubly symmetric. Therefore under torsion, the displacements ( $w_j$ ) at the corners are doubly antisymmetric. Hence

$$\sum_j (r_{k+1} - r_k)_j w_{j,n} = 4(4-1)w_{j,n} = 12w_{j,n}$$

where  $w_j$  is the displacement of the corner of the upper left hand quadrant of the tube. The external torque applied to the cross section is 29,600 inch-pounds. Let  $E = 10^7$  psi,  $\mu = .3$  whence  $G = E/2(1+\mu) = 10^7/2.6$ .

Inserting the numerical values, Equation (42) becomes

$$\begin{aligned} & (w_{n+1} + w_{n-1})_j + (w_{j+1} + w_{j-1})_n - 4w_{j,n} \\ & = - \frac{L}{10} (4-1) \left[ \frac{(29,600)(2.6)}{10^7} + \frac{1}{8} (12) w_{j,n} \right] \\ & = -L \left[ \frac{2.31}{10^3} + .45 w_{j,n} \right] \end{aligned} \quad \text{A-2}$$

This corresponds to Equation (44) in Part VI.

APPENDIX B  
 NUMERICAL DATA FOR SWEPT BOX BEAM UNDER  
 SYMMETRICAL BENDING

B.1 Idealized Cross Sections of Swept Beam

The details of the NACA swept box beam are shown in Figure 14. The numerical calculations for idealizing the cross sections of the swept beam are carried out in the following.

Outer Panel

The idealized outer shell has a length of  $118\text{-}3/4$  inches and a 7 inch by 29.7 inch rectangular cross section. The choice fortuitously makes the length equal to four times the chord. The cross-sectional area of the elements are as follows:

$$\text{Area of each cover sheet (normal to z axis)} = 29.7 \times .050 = 1.485 \text{ sq. in.}$$

$$\text{Area of each spar web} = 7 \times .078 = 0.546 \text{ sq. in.}$$

$$\text{Total stiffener area per cover} = 14(1 - 1/2 \times 1/16) = 1.312 \text{ sq. in.}$$

$$\text{Area of each idealized flange} = \text{actual flange area} + \text{equivalent spar}$$

$$\text{web area} + \text{area of sheet effectively attached to flange}$$

$$= 2 \frac{1}{2} \times \frac{1}{8} + .546 \times \frac{1}{6} + (31 \frac{3}{4} - 29.7) \left( \frac{.050}{2} \right)$$

$$= 0.455 \text{ sq. in.}$$

Also, moment of inertia of section

$$= 2(2 \times .455 + 1.312 + .050 \times 29.7)(3.5)^2$$

$$= 90.8 \text{ in.}^4$$

### Inner Panel

The idealized inner panel is composed of one half of the carry through bay, and has a length of 15 inches and a 7 inch x 41.8 inch rectangular cross section. (Ref. NACA Langley Field Drawing No. LD-14839. The distance between the outside edges of flange angles =  $43 \frac{55}{64}$  inches. Whence  $43 \frac{55}{64} - (31 \frac{3}{4} - 29.7) = 41.8$  in. The cross sectional areas of the elements are as follows:

Area of each cover sheet (normal to z axis) =  $41.8 \times .050 = 2.090$  sq. in.

Area of each spar web = 0.546 sq. in.

Total stiffener area per cover = 1.312 sq. in.

Area of each idealized flange = 0.455 sq. in.

The idealized cross section of the beam contains stiffeners and flanges that transmit axial loads, cover sheets that transmit axial and shear loads, and spar webs that transmit only shear loads. The cross-sectional areas may be essentially divided into the areas resisting the axial loads, and the areas resisting the shear loads. The areas resisting the axial loads are made up of equivalent areas of elements ( $a_j$ ) which are composed of the area of the stiffener element ( $a_{ST}$ ) and the area of the cover sheet element ( $a_{SH}$ ) resisting the normal stress. The areas resisting the shear loads are the actual areas of the sheet. As a result, the idealized cross section is made up of equivalent areas of elements resisting the normal stress, and the sheet areas resisting the shear stress. In actuality, the resulting section is the

same as would be obtained by the effective width concept, except that the effective width concept would be inconsistent at an oblique boundary where the sheet stresses are resolved as shown in Figure 7(c).

The following example illustrates the idealization into a six-element beam. Assume that the distribution of the stiffener area across the cover is uniform. As indicated in Part III, assume that the area of the cover sheet acting in conjunction with the stiffener area is half of the area of the sheet material in each interval neighboring the stiffener. Thus the flange and stiffener areas become for the outer panel,

$$a_{\text{flange}} = \left(0.455 + \frac{1.312}{4}\right) + \left(\frac{1.485}{4}\right)$$

$$= .783 + .371 = 1.154 \text{ sq. in.}$$

$$a_{ST} = \frac{1.312}{2} + \frac{1.485}{2}$$

$$= .656 + .742 = 1.398 \text{ sq. in.}$$

The idealized cross sections are illustrated in Figure 16.

## B.2 "Clipped" Wing Boundary Conditions for Six and Ten-Element Beams

The outer panel is clipped a distance of 59.6 in. from the actual tip as illustrated in Figures 15(b) and (c). The boundary condition on the stress at the tip of the clipped wing is determined by elementary beam theory. For a vertical shear of 2500 pounds applied at the tip of



the actual wing, the normal stress at the tip of the clipped wing is

$$\sigma = \frac{My}{I} = \frac{59.6 \times 2500 \times 3.5}{90.8} = 5724 \text{ psi.}$$

Let the mesh line corresponding to the tip of the clipped wing be (n).

Then by Equation (31)

$$\sigma_n = \frac{E}{2l} (W_{n+1} - W_{n-1})_j = \frac{105}{2l} (W'_{n+1} - W'_{n-1})_j = 5724$$

Thus

$$\begin{aligned} (W'_{n+1})_j &= \frac{5724 \times 2l}{105} + (W'_{n-1})_j \\ &= 109l + (W'_{n-1})_j \end{aligned}$$

This condition is substituted in the difference equations corresponding to the tip of the clipped wing. The procedure then follows the methods outlined in Part IV.

### B.3 Evaluation of Section Constants

In order that the comparison between the theory and experiment may be made on the same basis, let  $E = 10.5 \times 10^6$  psi,  $G = 4 \times 10^6$  psi, and  $\mu = \frac{E}{2G} - 1 = 0.312$ . It is to be noted that this modulus (E) is different from the modulus used in Appendix A.

The section properties associated with the principal shear axes are given by Equation (27). Evaluation of the constants for the inner and outer panels gives,

$$\begin{aligned} I_C &= \sum_K t_K L_K r_K^2 \\ &= 2 (.050 \times 41.8 \times 3.5^2 + .078 \times 7 \times 20.9^2) = 528.2 \text{ in.}^4 \text{ (inner panel)} \\ &= 2 (.040 \times 29.7 \times 3.5^2 + .078 \times 7 \times 14.85^2) = 277.2 \text{ in.}^4 \text{ (outer panel)} \end{aligned}$$

$$\begin{aligned} A_V &= \sum_K t_K L_K \sin^2 \alpha_K \\ &= 2 \times .078 \times 7 = 1.092 \text{ in.}^2 \text{ (inner and outer panel)} \end{aligned}$$

For the NACA swept wing under vertical shear and torsion, the displacements are antisymmetrical about the x axis. Therefore, evaluation of the summation terms in the difference equation for the inner and outer panels gives

$$\begin{aligned} \sum_j (t_{KH} r_{KH} - t_K r_K)_j w_j &= 2(.050 \times 3.5 - .078 \times 20.9)(w_{F_1} - w_{F_2}) \\ &= -2.910(w_{F_1} - w_{F_2}) \text{ (inner panel)} \\ &= 2(.050 \times 3.5 - .078 \times 14.85)(w_{F_1} - w_{F_2}) \\ &= -1.966(w_{F_1} - w_{F_2}) \text{ (outer panel)} \\ \sum_j (t_{KH} \sin \alpha_{KH} - t_K \sin \alpha_K)_j w_j &= 2(-.078)(w_{F_1} + w_{F_2}) \\ &= -.156(w_{F_1} + w_{F_2}) \text{ (inner and outer} \\ &\quad \text{panel)} \\ \sum_j (t_{KH} \cos \alpha_{KH} - t_K \cos \alpha_K)_j w_j &= 0 \text{ (inner and outer panel)} \end{aligned}$$

#### B.4 Boundary Conditions and Difference Equations for the Behavior of the Wing With No Wing Rib Under External Loads for the Six and Ten-Element Beams

The boundary conditions and difference equations for the behavior of the wing for the six and ten-element beams are obtained by the procedures in Part VII. The notation is given in Figures 15(b) and (c).

For the six-element beam, the compatibility of displacements of the joint are given by Equation (47) to be

$$\begin{aligned} w'_4 &= 1.414 w'_7 \\ w'_5 &= 1.414 w'_{11} \\ w'_6 &= 1.414 w'_{15} \end{aligned}$$

The equations of equilibrium are governed by Equations (48) and (49), and become

$$-w'_7 + .7569 w'_1 + .3031 w'_{10} - .06575 w'_{13} - .02929 w'_{11} - .01078 w'_{12} = 0$$

$$-w'_{11} + .9173 w'_2 + .1057 w'_{14} - .0785 w'_8 + .03725 (w'_{10} - w'_{15}) + .01002 (w'_{13} - w'_{12}) = 0$$

$$-w'_{15} + .8981 w'_3 + .07801 (w'_{13} - w'_{12}) + .03475 w'_{14} + .01279 w'_{13} = 0$$

The difference equations for the inner and outer panels are given by Equations (50) and (51) respectively. For the inner panel, the expressions are

$$-(w'_F)_n + .0246 (w'_{F_2})_n + .0188 (w'_S)_n + .478 (w'_{n+1})_{F_1} = 0$$

$$-(w'_S)_n + .01464 (w'_F + w'_{F_2})_n + .486 (w'_{n+1})_S = 0$$

$$-(w'_{F_2})_n + .0246 (w'_F)_n + .0188 (w'_S)_n + .478 (w'_{n+1})_{F_2} = 0$$

Similarly, for the outer panel

$$-(w'_F)_n + .096 (w'_S)_n + .392 (w'_{n+1} + w'_{n-1})_{F_1} + .1192 (w'_{F_2})_n + 128 = 0$$

$$-(w'_S)_n + .0842 (w'_F + w'_{F_2}) + .416 (w'_{n+1} + w'_{n-1})_S = 0$$

$$-(w'_{F_2})_n + .096 (w'_S)_n + .392 (w'_{n+1} + w'_{n-1})_{F_2} + .1192 (w'_F)_n + 128 = 0$$

For the ten-element beam, the compatibility of displacements at the joint are given by Equation (47) to be

$$w'_6 = 1.414 \quad w'_{11}$$

$$w'_7 = 1.414 \quad w'_{17}$$

$$w'_8 = 1.414 \quad w'_{23}$$

$$w'_9 = 1.414 \quad w'_{29}$$

$$w'_{10} = 1.414 \quad w'_{35}$$

The equations of equilibrium are governed by Equations (48) and (49), and become

$$\begin{aligned}
 -w'_{11} + .6310 w'_1 + .4837 w'_{16} - .1109 w'_{21} - .0362 w'_{17} - .0067 w'_{20} &= 0 \\
 -w'_{17} + .8931 w'_2 + .2059 w'_{22} - .1528 w'_{12} + .0628 w'_{16} - .0531 w'_{23} \\
 + .0098 (-w'_{20} + w'_{21} - w'_{25}) &= 0 \\
 -w'_{23} + .8931 w'_3 + .2059 w'_{28} - .1528 w'_{18} + .0531 (w'_{22} - w'_{29}) \\
 + .0098 (w'_{21} - w'_{25} + w'_{26} - w'_{30}) &= 0 \\
 -w'_{29} + .8931 w'_4 + .2059 w'_{34} - .1528 w'_{24} + .0531 w'_{28} - .0628 w'_{35} \\
 + .0098 (w'_{26} - w'_{30} + w'_{31}) &= 0 \\
 -w'_{35} + .8863 w'_5 + .1549 (w'_{40} - w'_{30}) + .0509 w'_{34} + .0094 w'_{31} &= 0
 \end{aligned}$$

The difference equations for the inner and outer panels are given by Equations (50) and (51) respectively. For the inner panel, the expressions are

$$\begin{aligned}
 -(w'_F)_n + .0348 (w'_F)_n + .0532 (w'_S)_n + .456 (w'_{n+1})_F &= 0 \\
 -(w'_S)_n + .0538 (w'_{S_2} + w'_F)_n + .446 (w'_{n+1})_{S_1} &= 0 \\
 -(w'_{S_2})_n + .0538 (w'_{S_3} + w'_S)_n + .446 (w'_{n+1})_{S_2} &= 0 \\
 -(w'_{S_3})_n + .0538 (w'_F + w'_{S_2})_n + .446 (w'_{n+1})_{S_3} &= 0 \\
 -(w'_{F_2})_n + .0348 (w'_F)_n + .0532 (w'_S)_n + .456 (w'_{n+1})_{F_2} &= 0
 \end{aligned}$$

Similarly, for the outer panel

$$\begin{aligned}
 -(w'_F)_n + .0477 (w'_F)_n + .0769 (w'_S)_n + .438 (w'_{n+1} + w'_{n-1})_F + 51 &= 0 \\
 -(w'_S)_n + .0842 (w'_{S_2} + w'_F)_n + .415 (w'_{n+1} + w'_{n-1})_{S_1} &= 0 \\
 -(w'_{S_2})_n + .0842 (w'_{S_3} + w'_S)_n + .415 (w'_{n+1} + w'_{n-1})_{S_2} &= 0 \\
 -(w'_{S_3})_n + .0842 (w'_F + w'_{S_2})_n + .415 (w'_{n+1} + w'_{n-1})_{S_3} &= 0 \\
 -(w'_{F_2})_n + .0477 (w'_F)_n + .0769 (w'_S)_n + .438 (w'_{n+1} + w'_{n-1})_{F_2} + 51 &= 0
 \end{aligned}$$

B. 5 Boundary Conditions and Difference Equations for the Behavior of the Wing Under Loads Imposed by the Wing Rib for the Six-Element Beam

The boundary conditions and difference equations for the behavior of the wing for the six-element beam are obtained by the procedures in Part VII. The notation is given in Figure 15(b). The compatibility of displacements of the joint are given by Equation (47) to be

$$w'_4 = 1.414 w'_7$$

$$w'_5 = 1.414 w'_{11}$$

$$w'_6 = 1.414 w'_{15}$$

The equations of equilibrium are governed by Equations (48) and (49), and become

$$-w'_7 + .7569 w'_1 + .3031 w'_{10} - .06575 w'_{13} - .02929 w'_{11} - .01078 w'_{12} - 2 = 0$$

$$-w'_{11} + .9173 w'_2 + .1057 w'_{14} - .0785 w'_8 + .03725 (w'_{10} - w'_{15}) + .01002 (w'_{13} - w'_{12}) - 4 = 0$$

$$-w'_{15} + .8981 w'_3 + .07801 (w'_{16} - w'_{12}) + .03475 w'_{14} + .01279 w'_{13} + 72 = 0$$

The difference equations for the inner and outer panels are given by Equations (50) and (51) respectively. For the inner panel, the expressions are

$$-(w'_{F_1})_n + .0246 (w'_{F_2})_n + .0188 (w'_s)_n + .478 (w'_{n+1})_{F_1} = 0$$

$$-(w'_s)_n + .01464 (w'_{F_1} + w'_{F_2})_n + .486 (w'_{n+1})_s = 0$$

$$-(w'_{F_2})_n + .0246 (w'_{F_1})_n + .0188 (w'_s)_n + .478 (w'_{n+1})_{F_2} = 0$$

However, for the outer panel, the loading condition is not constant, and two systems of equations are required. In the cross section HH'D'D and inboard, the equations are

$$-(W'_F)_n + .096 (W'_S)_n + .392 (W'_{n+1} + W'_{n-1})_F + .1192 (W'_{F_2})_n - 89 = 0$$

$$-(W'_S)_n + .0842 (W'_F + W'_{F_2})_n + .416 (W'_{n+1} + W'_{n-1})_S = 0$$

$$-(W'_{F_2})_n + .096 (W'_S)_n + .392 (W'_{n+1} + W'_{n-1})_{F_2} + .1192 (W'_{F_1})_n - 13 = 0$$

Outboard of the cross section HH'D'D, the equations are the same as above with the exception that the constant terms are omitted.

#### B.6 Determination of Redundant Rib Load (P) for the Six-Element Beam

The value of the redundant load P imposed by the wing rib is determined by considering the compatibility of the deflections of the rib and the spar at point H. The deflection of the outer panel front spar at the point H is given by Equation (39) to be

$$\delta_H = -.0351 + 14.85(-.00237) + \left[ .009 + 14.85(.00061) \right] \frac{P}{1000} \quad (\text{B.1})$$

where the incremental deflections are given by Equation (29) and Table 2. Similarly the deflection of the wing rib at the point H is given by Equation (40) to be

$$\delta_H = (29.7) (.707) \left[ \frac{-1328}{10^5 (3.5)} - \frac{157}{10^5 (3.5)} \frac{P}{1000} \right] \frac{P (29.7^3)}{3 (6.63) (30 \times 10^6)} \quad (\text{B.2})$$

where the rotations are obtained from the displacements given in Figures (18) and (19). The value of P = -135 pounds is obtained by equating Equations (B.1) and (B.2).

## LIST OF TABLES

TABLE NUMBER		PAGE
1	Morphology of Single Cell Relaxation Meshes	78
2	Deflections and Rotations of Outer Panel of Swept Wing	80

TABLE 1

Morphology of Single Cell Relaxation Meshes

The relaxation mesh for the general orthogonal shell with arbitrary boundary conditions is a right cylinder. The mesh may be simplified if the cross section and boundary conditions are symmetric about one or both of the principal shear axes of the shell. This is illustrated by the following table. The regions corresponding to the simplified mesh are cross hatched, and the boundary conditions for the edges of the mesh parallel to the z axis are shown.



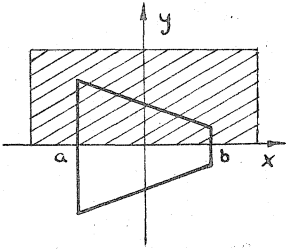
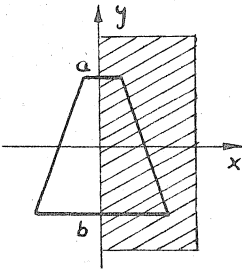
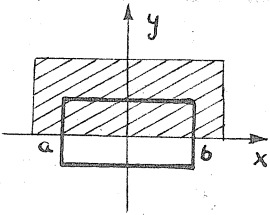
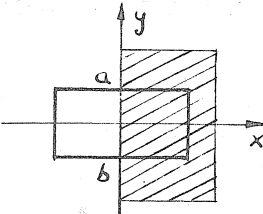
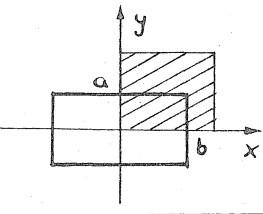
Cross sectional shape	End constraint	Boundary conditions along the edge of the mesh parallel to the z axis			
		Edge	Loading		
			Torsion	Vertical shear	Horizontal shear
Symmetric about x axis 	Symmetric about x axis	a, b	$w = 0$	$w = 0$	$\frac{\partial w}{\partial s} = 0$
Symmetric about y axis 	Symmetric about y axis	a, b	$w = 0$	$\frac{\partial w}{\partial s} = 0$	$w = 0$
Doubly Symmetric 	Symmetric about x axis	a, b	$w = 0$	$w = 0$	$\frac{\partial w}{\partial s} = 0$
	Symmetric about y axis	a, b	$w = 0$	$\frac{\partial w}{\partial s} = 0$	$w = 0$
	Doubly symmetric	a	$w = 0$	$\frac{\partial w}{\partial s} = 0$	$w = 0$
		b	$w = 0$	$w = 0$	$\frac{\partial w}{\partial s} = 0$

TABLE 2  
DEFLECTION AND ROTATION OF OUTER PANEL OF  
THE SWEPT WING

The deflections and rotations of the outer panel of the swept wing are obtained for the four and six element beams by the procedures in Part II, with the boundary conditions ( $u_j = v_j = 0$  at AA' and DD') satisfied at the supports. The results are shown in tabular form in the following.

4 Element Beam

Distance From Tip (in)	External Load No Wing Rib		Rib Load P = 1000		Rib Load P = 167		External Load With Wing Rib	
	Deflection (in)	Rotation (radians)	Deflection (in)	Rotation (radians)	Deflection (in)	Rotation (radians)	Deflection (in)	Rotation (radians)
118.8	-.029	.00196	.008	-.00055	.0013	-.00009	-.028	.00187
89.1	-.043	-.00295	.012	.00078	.0020	.00013	-.041	-.00282
59.4	-.259	-.00422	.025	.00135	.0042	.00023	-.255	-.00399
29.7	-.608	-.00455	.035	.00145	.0058	.00024	-.602	-.00431
0	-1.023	-.00466	.044	.00149	.0073	.00025	-1.016	-.00441

6 Element Beam

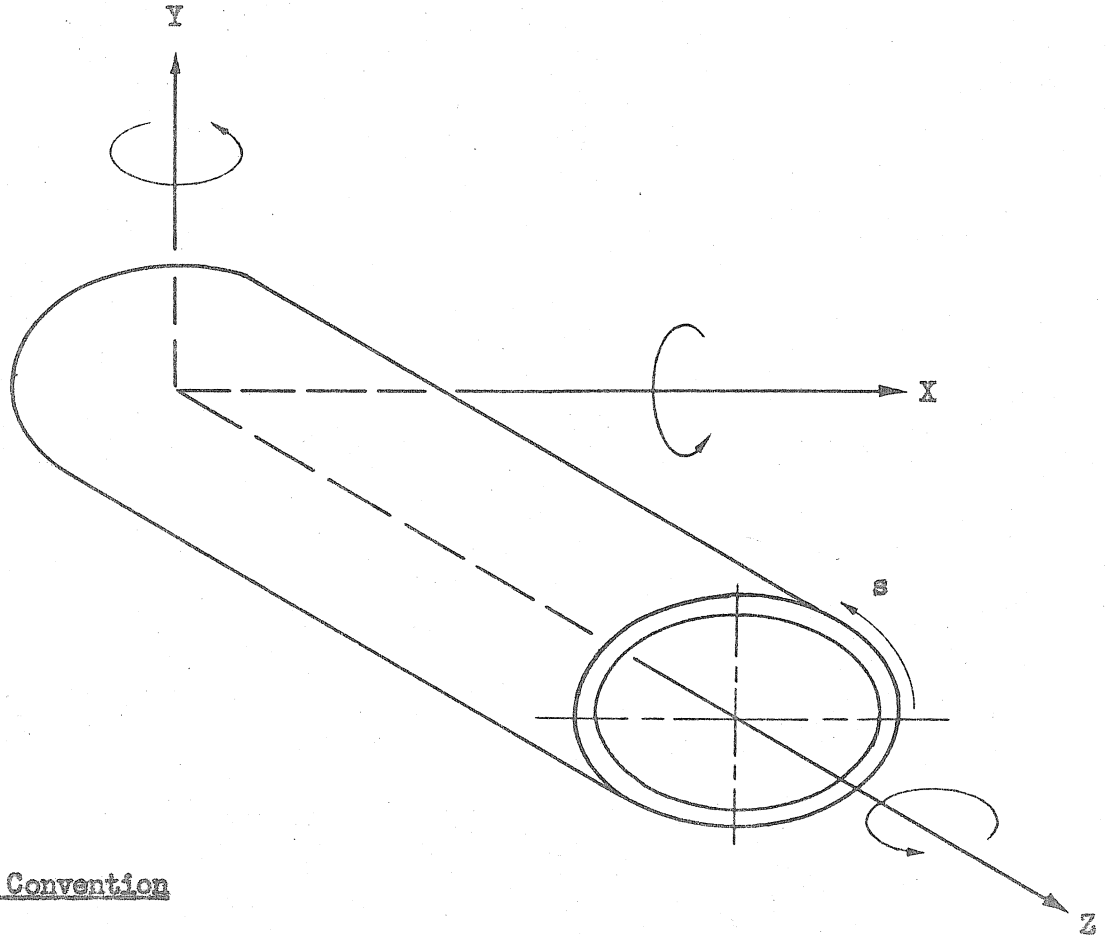
Distance From Tip (in)	External Load No Wing Rib		Rib Load P = 1000		Rib Load P = -135lb.		External Load With Wing Rib	
	Deflection (in)	Rotation (radians)	Deflection (in)	Rotation (radians)	Deflection (in)	Rotation (radians)	Deflection (in)	Rotation (radians)
118.80	-.0446	.00301	.0137	-.00092	-.0018	.00012	-.0464	.00313
103.95	-.0016	-.00081	.0071	.00001	-.0010	.00000	-.0026	-.00081
89.10	-.0351	-.00237	.0090	.00061	-.0012	-.00008	-.0363	-.00245
74.25	-.1275	-.00300	.0117	.00091	-.0016	-.00012	-.1291	-.00312
59.40	-.2658	-.00326	.0124	.00099	-.0017	-.00013	-.2675	-.00339
44.55	-.4396	-.00337	.0129	.00103	-.0017	-.00014	-.4413	-.00351
29.70	-.6398	-.00341	.0133	.00104	-.0018	-.00014	-.6416	-.00355
14.85	-.8568	-.00343	.0136	.00105	-.0018	-.00014	-.8586	-.00357
0	-1.0827	-.00344	.0138	.00105	-.0019	-.00014	-1.0846	-.00358

## LIST OF FIGURES

FIGURE NUMBER		PAGE
1	Coordinate System for Orthogonal Shell	85
2	Forces Acting on a Wall Element	86
3	Tangential Displacements	87
4	Mesh for Difference Equation	88
5	Relaxation Technique	89
6	Cantilever Beam on an Oblique Support	90
7	Swept Wing With a Carry Through Bay	91 - 94
8	Rectangular Tube Under Torsion	95 - 97
9	Final Values of Axial Displacements and Stresses for Rectangular Tube Under Torsion	98 - 100
10	Tangential Distribution of Axial Displacement for Rectangular Tube Under Torsion	101
11	Tangential Distribution of Normal Stress for Rectangular Tube Under Torsion	102
12	Axial Distribution of Normal Stress at Corner of Rectangular Tube Under Torsion	103
13	Normal Stress at the Support for Various Mesh Sizes for Rectangular Tube Under Torsion	104
14	Details of N. A. C. A. Swept Box Beam	105
15	Relaxation Mesh and Boundary Conditions for Swept Beam	106 - 108
16	Idealized Cross Sections of Swept Beam	109

## LIST OF FIGURES - Continued

FIGURE NUMBER		PAGE
17	Point Relaxation Operators for Swept Beam	110
18	Final Values of Axial Displacements and Stresses for the Swept Wing with No Wing Rib Under Symmetrical Bending	111 - 114
19	Final Values of Axial Displacements and Stresses for the Swept Wing Under the Loads Imposed by the Wing Rib	115 - 117
20	Final Values of Normal Stress for the Swept Wing With A Wing Rib Under Symmetrical Bending	118, 119
21	Stringer and Flange Stresses of Sweptback Box Beam For Tip Bending Load	120 - 125
22	Tangential Distribution of Normal Stress for the Swept Wing Under Symmetrical Bending	126 - 132
23	Deformations of Swept Wing Under Symmetrical Bending	133, 134



Sign Convention

Positive Forces are in direction of axes  
 Positive Moments are given by right hand rule  
 Positive Normal Stresses are tensile  
 Positive Shear Stresses result from positive torque

FIGURE 1

COORDINATE SYSTEM FOR ORTHOGONAL SHELL

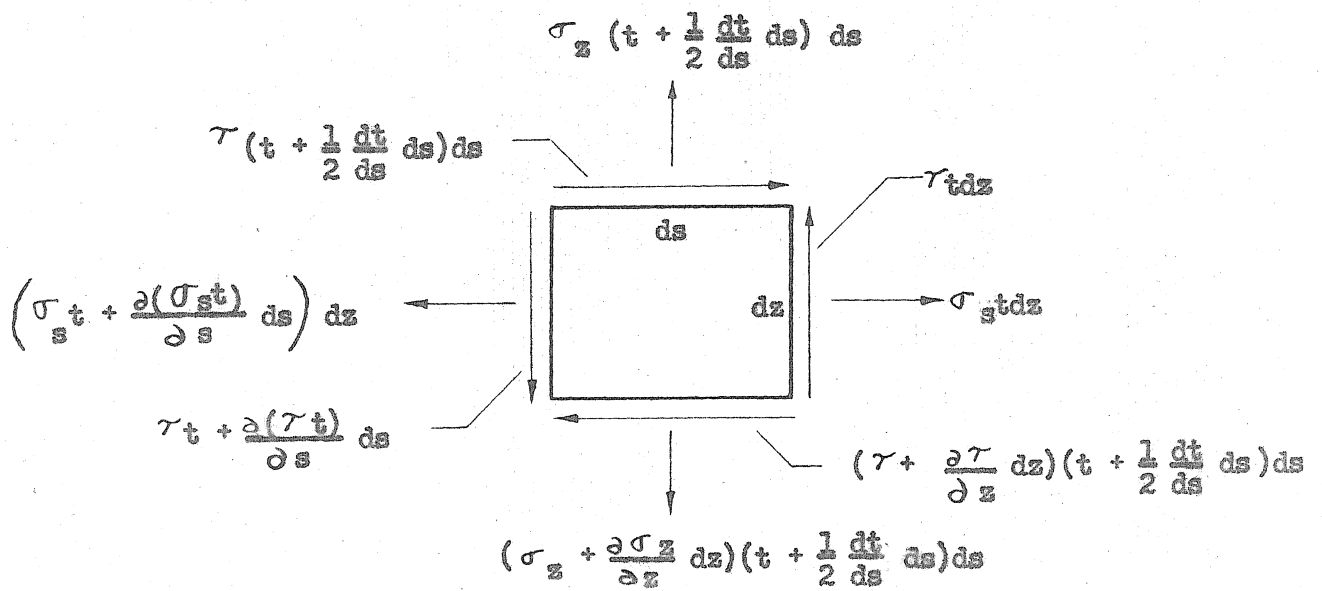
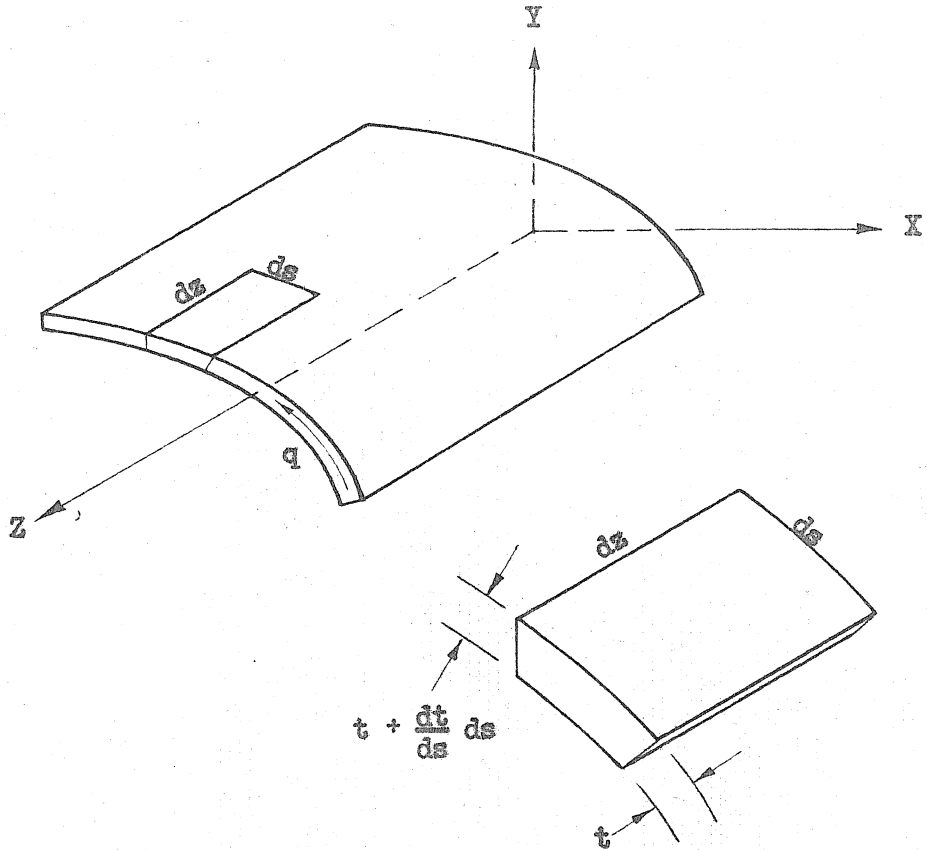
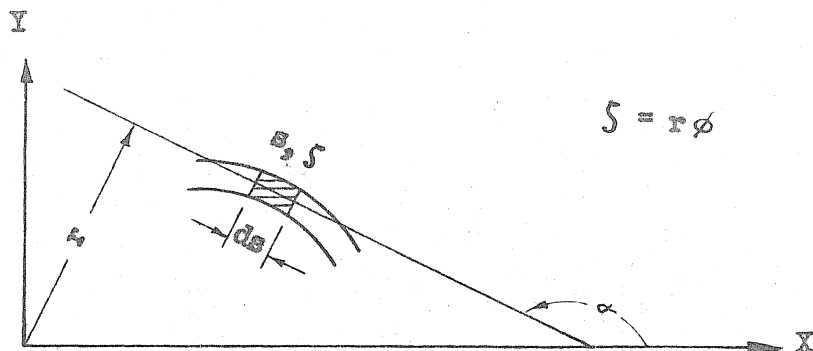


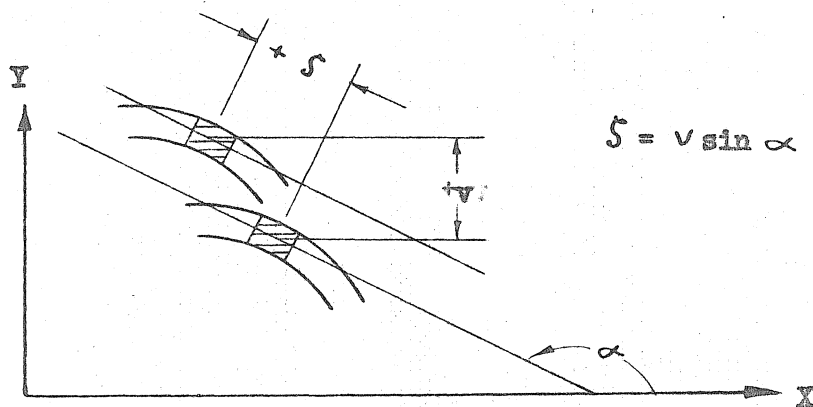
FIGURE 2

FORCES ACTING ON A WALL ELEMENT

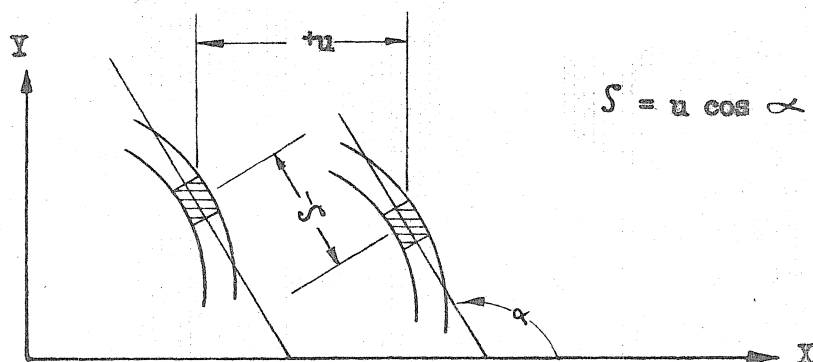




(a) Due to rotation



(b) Due to vertical translation



(c) Due to horizontal translation

Sign Convention

Positive  $\alpha$  is counterclockwise

FIGURE 3

TANGENTIAL DISPLACEMENTS

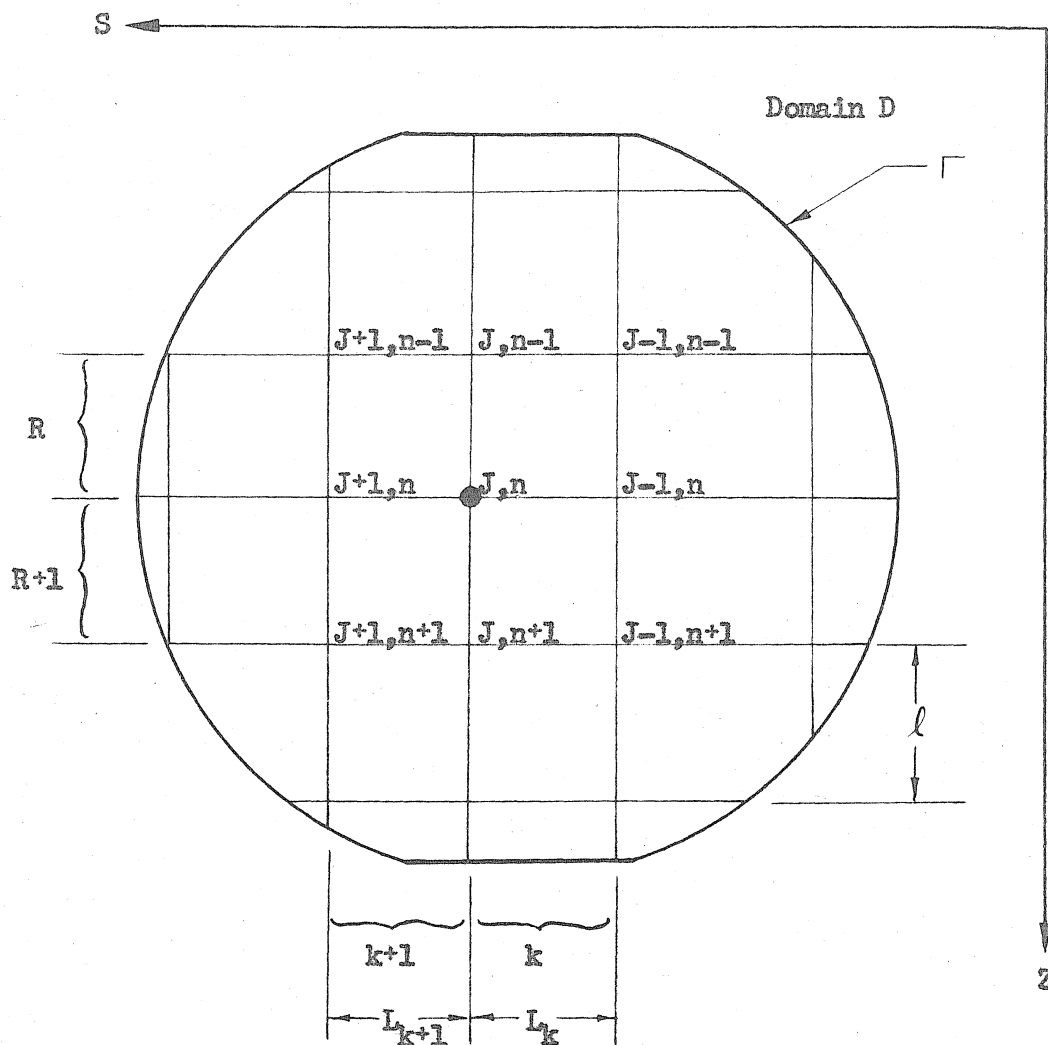
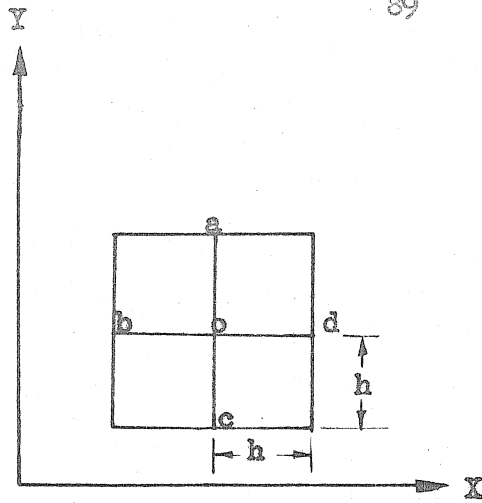
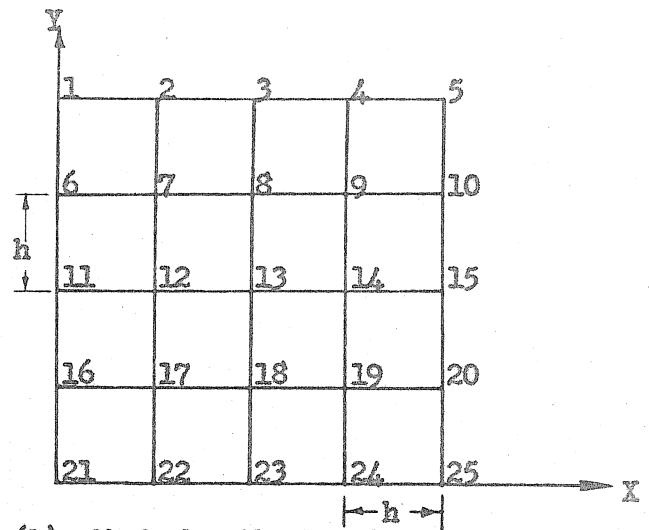


FIGURE 4

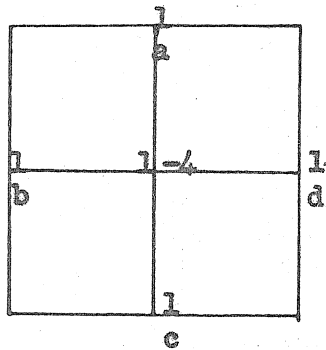
MESH FOR DIFFERENCE EQUATION



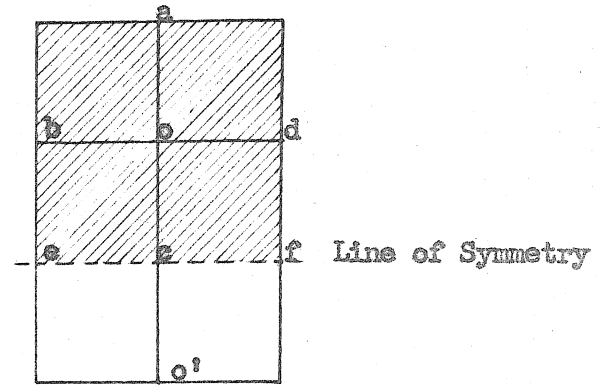
(a) Mesh for Difference Equation



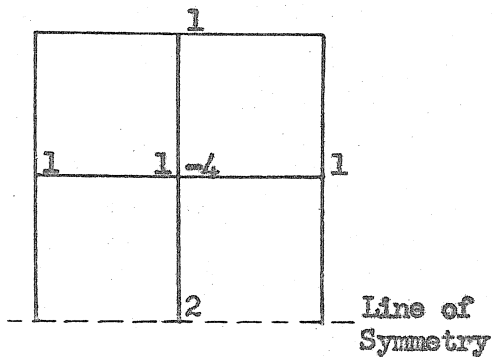
(b) Mesh for the Domain



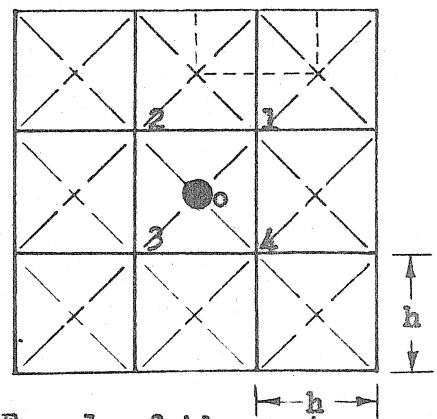
(c) Point Relaxation Operator for Laplace or Poisson Equation



(d) Mesh to Illustrate Line of Symmetry



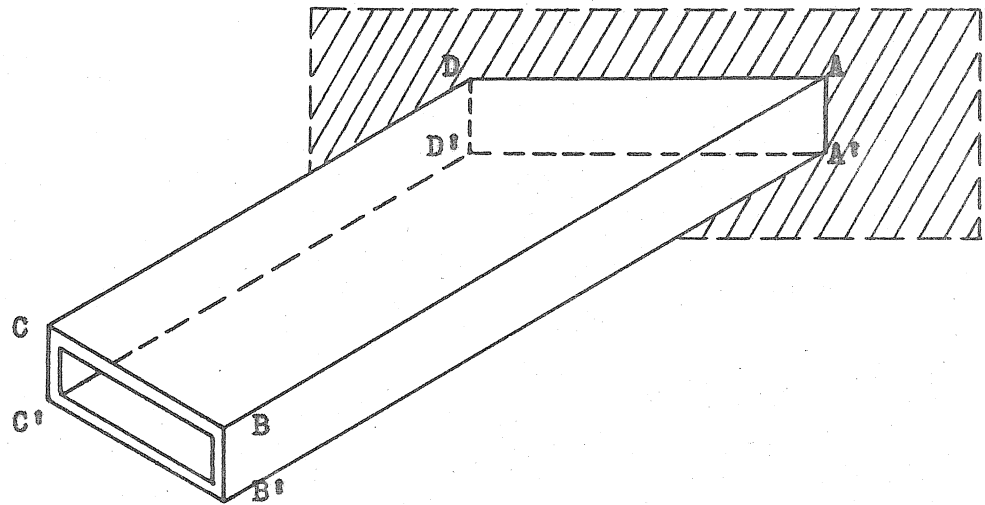
(e) Point Relaxation Operator for Laplace or Poisson Equation for Line Adjacent to Line of Symmetry



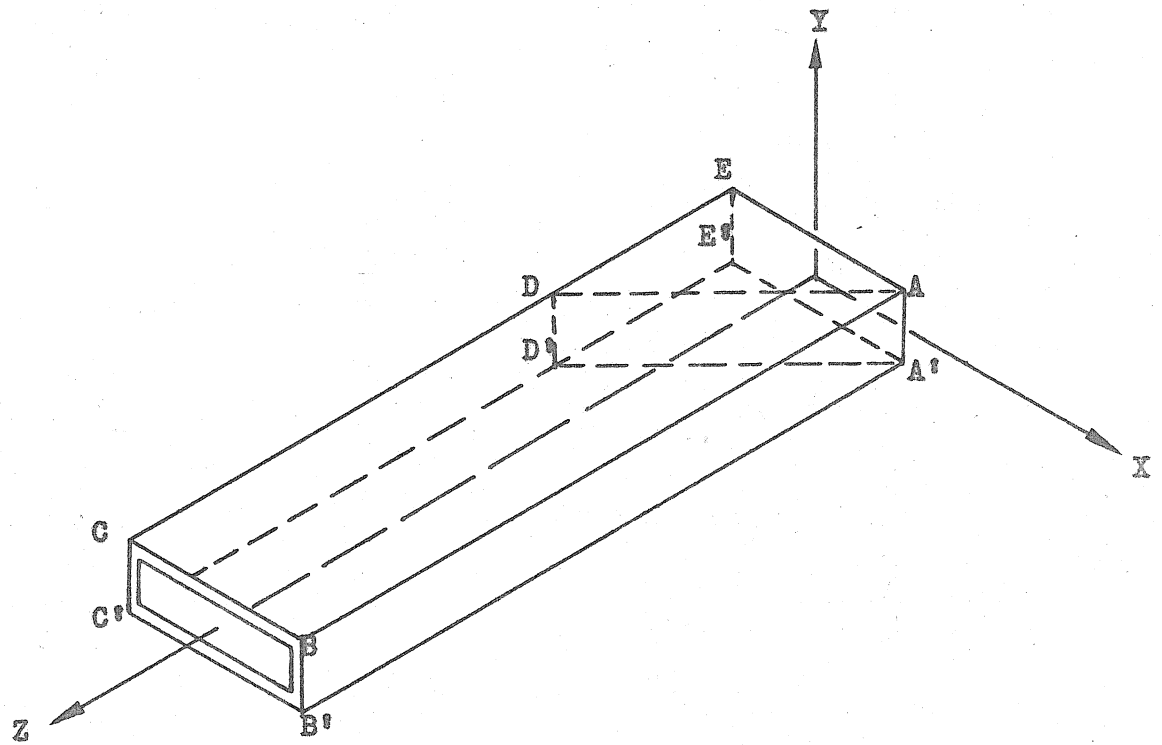
(f) Example of Advance to Finer Mesh

FIGURE 5

RELAXATION TECHNIQUE



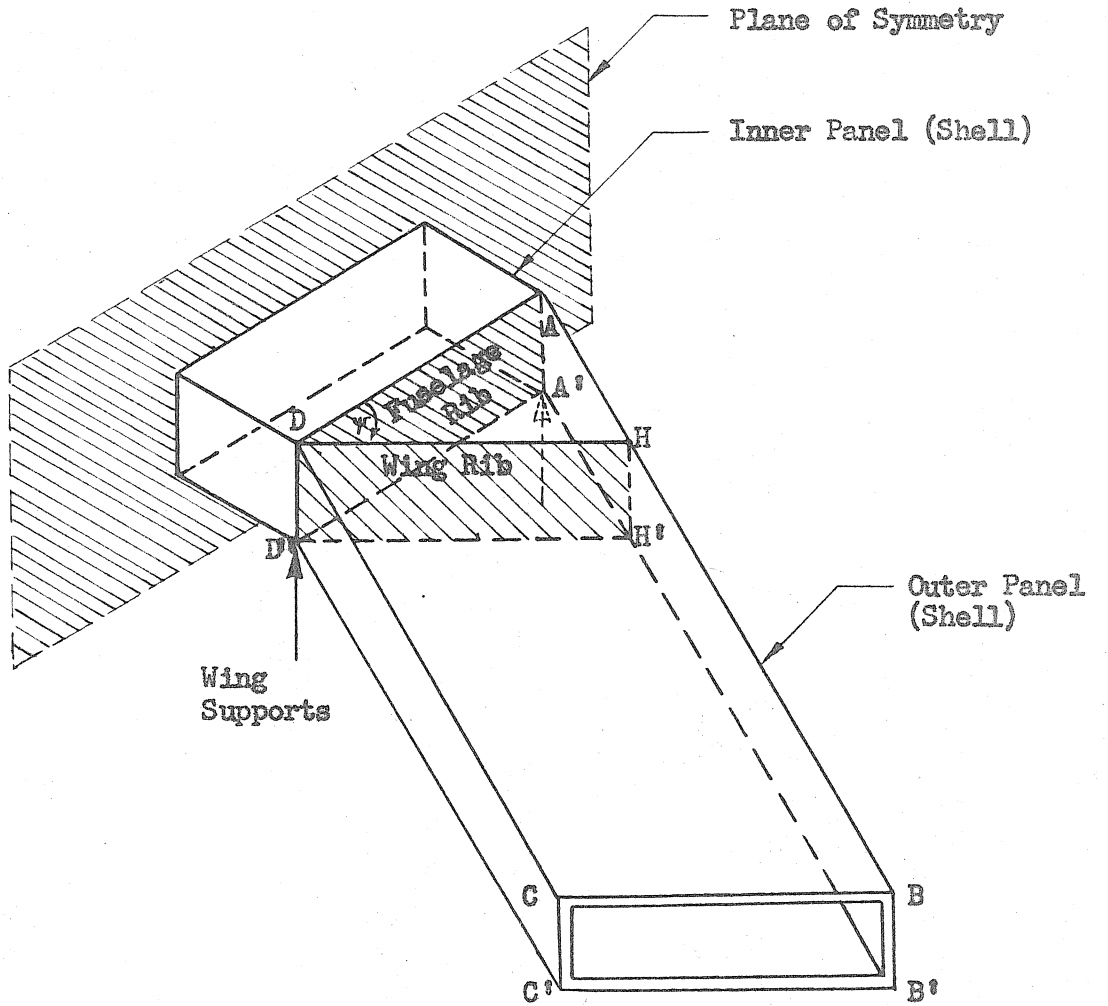
(a) Cantilever Beam on an Oblique Support



(b) Equivalent Cantilever Beam

FIGURE 6

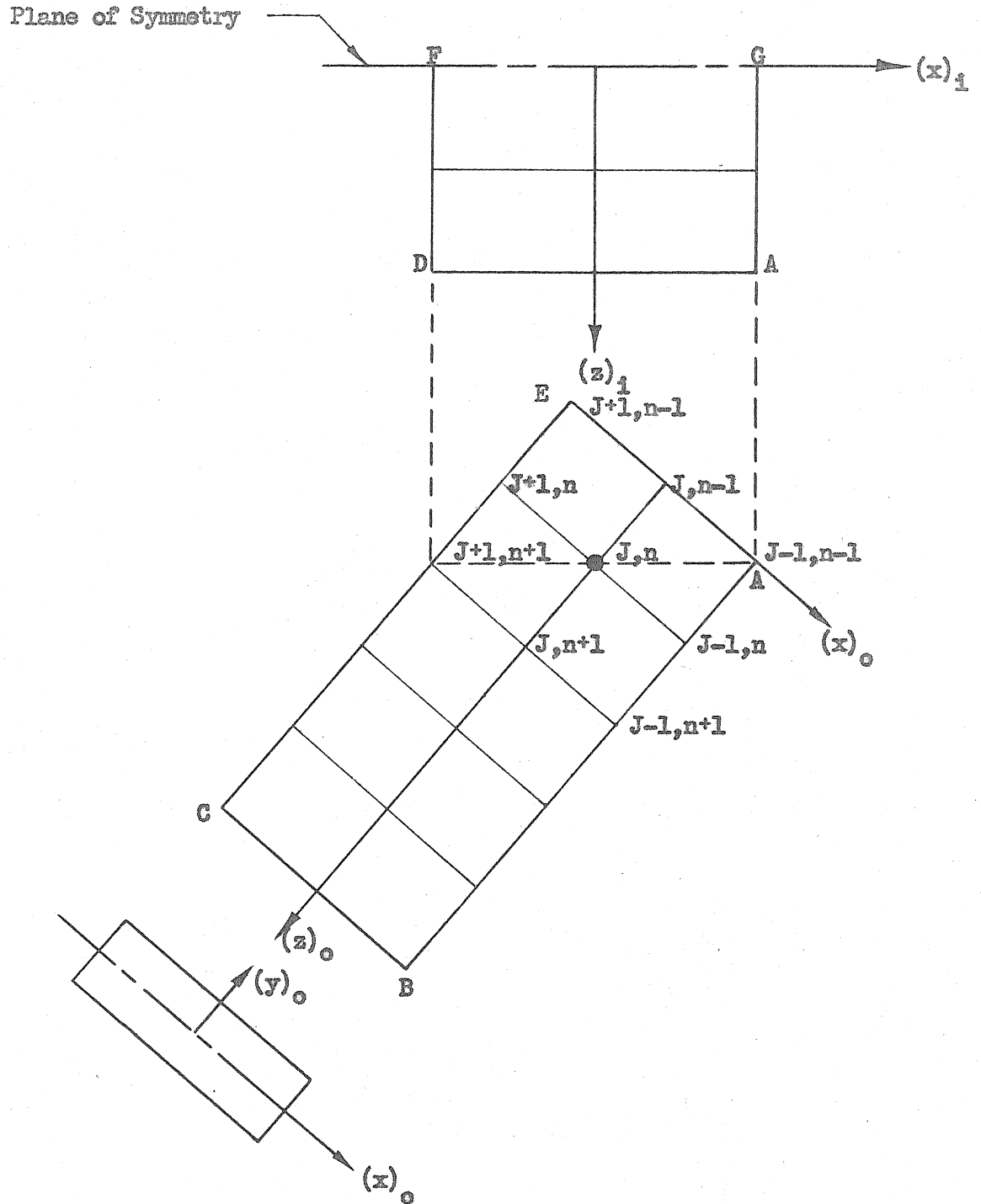
CANTILEVER BEAM ON AN OBLIQUE SUPPORT



(a) Swept Wing with a Carry Through Bay

FIGURE 7

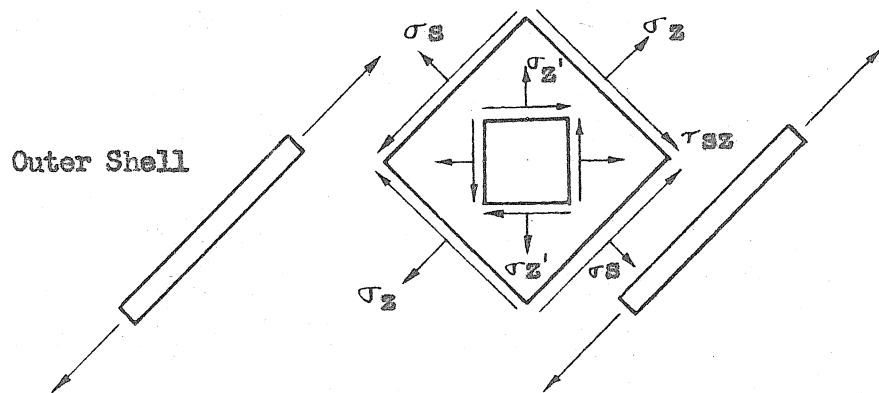
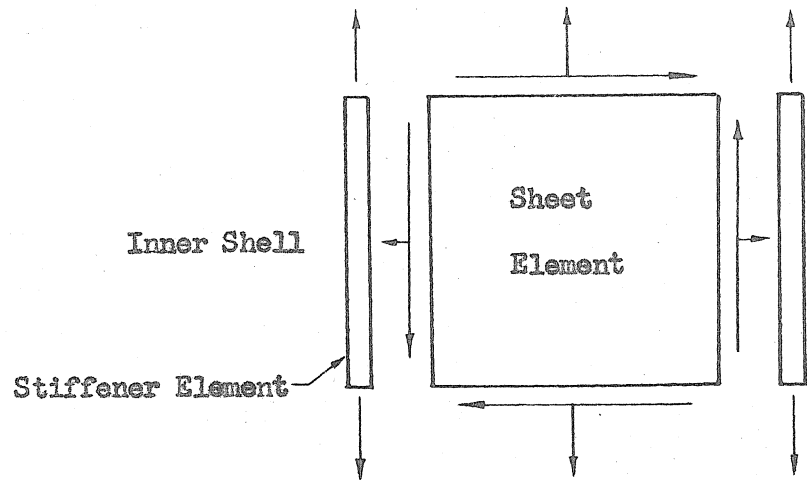
SWEPT WING WITH A CARRY THROUGH BAY



(b) Equivalent Wing and a Corresponding Relaxation Mesh

FIGURE 7 (CONTINUED)

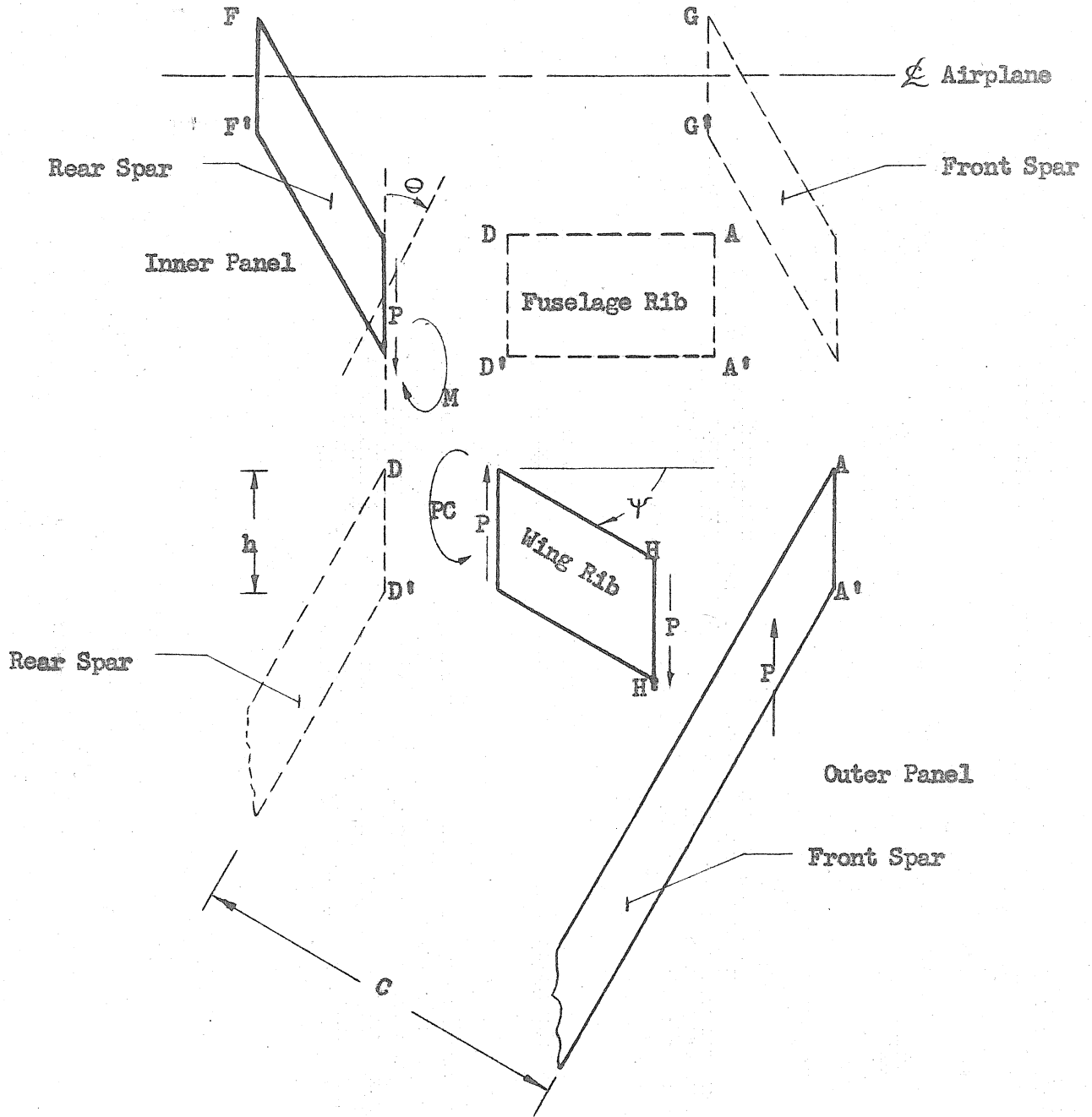
SWEPT WING WITH A CARRY THROUGH BAY



(c) Forces Acting at the Joints of the Stiffener and Sheet Elements

FIGURE 7 (CONTINUED)

SWEPT WING WITH A CARRY-THROUGH BAY

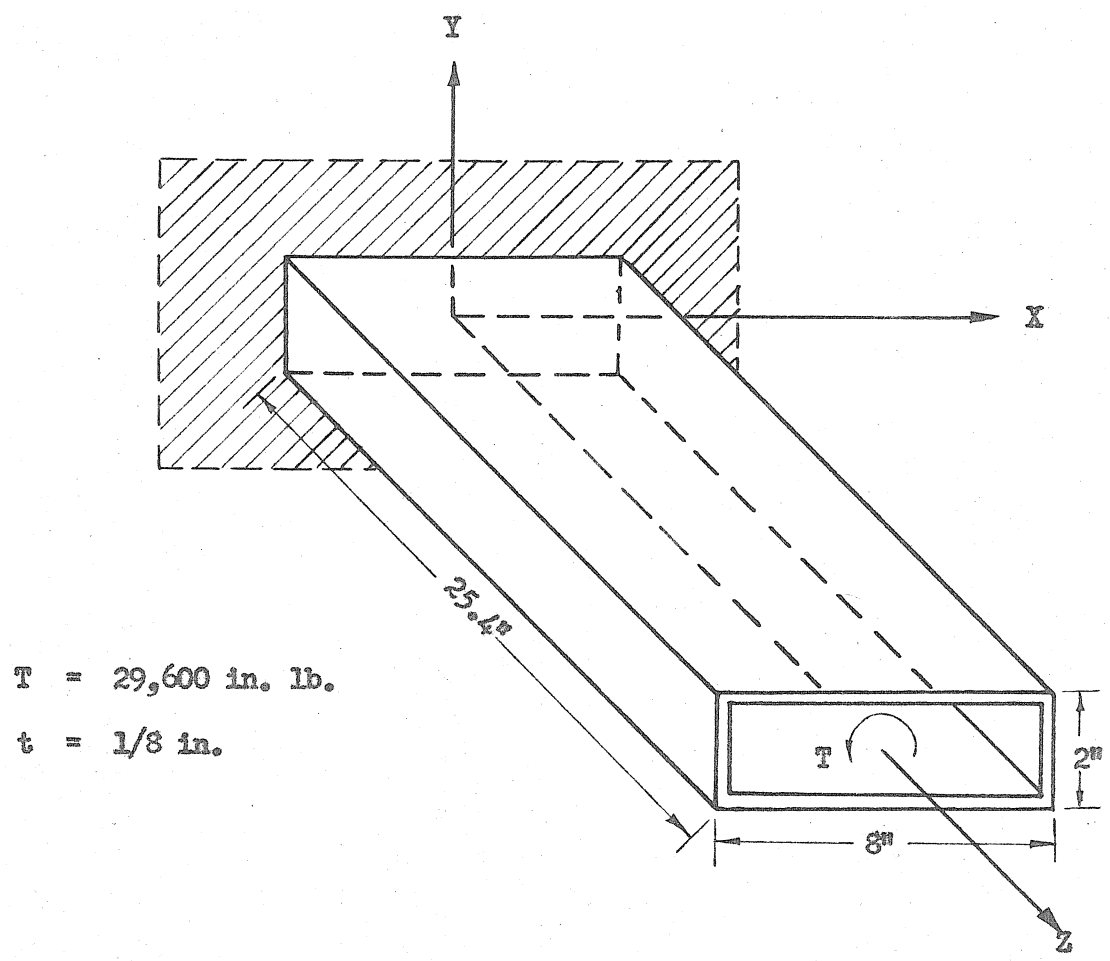


(d) Idealized Spars and Ribs of Swept Wing

FIGURE 7 (CONTINUED)

SWEPT WING WITH A CARRY THROUGH BAY

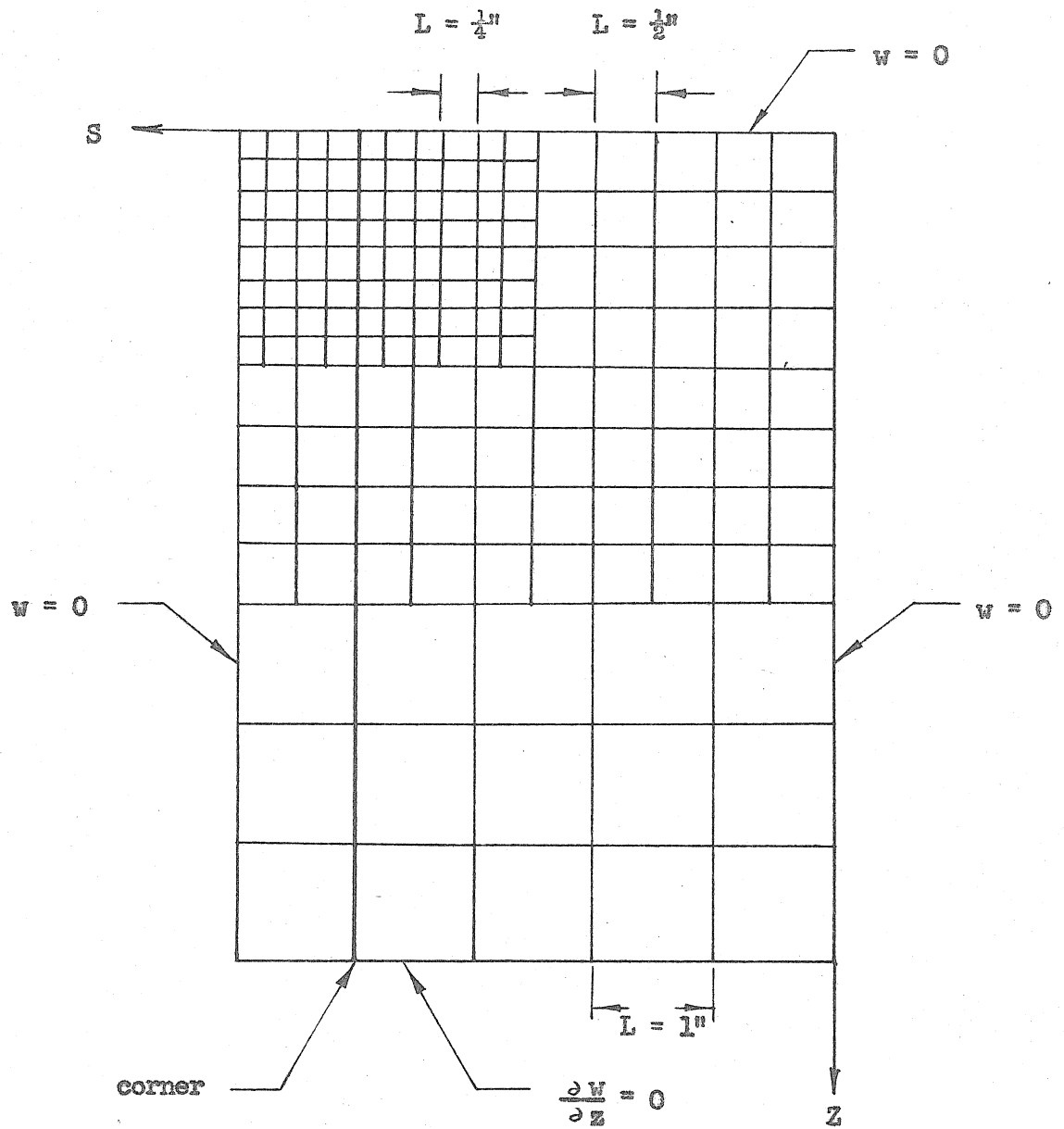




$T = 29,600$  in. lb.  
 $t = 1/8$  in.

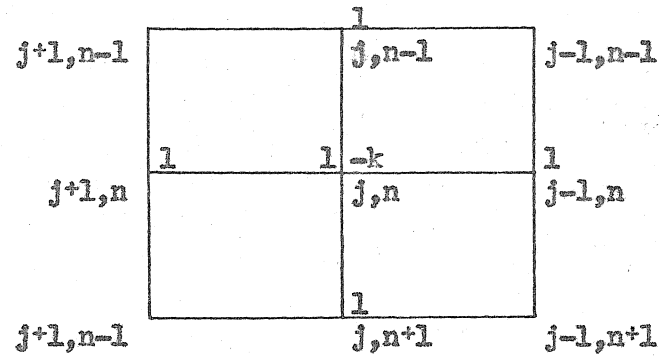
(a) Rectangular Tube

FIGURE 8  
RECTANGULAR TUBE UNDER TORSION



(b) Relaxation Mesh and Boundary Conditions

FIGURE 8 (CONTINUED)  
 RECTANGULAR TUBE UNDER TORSION

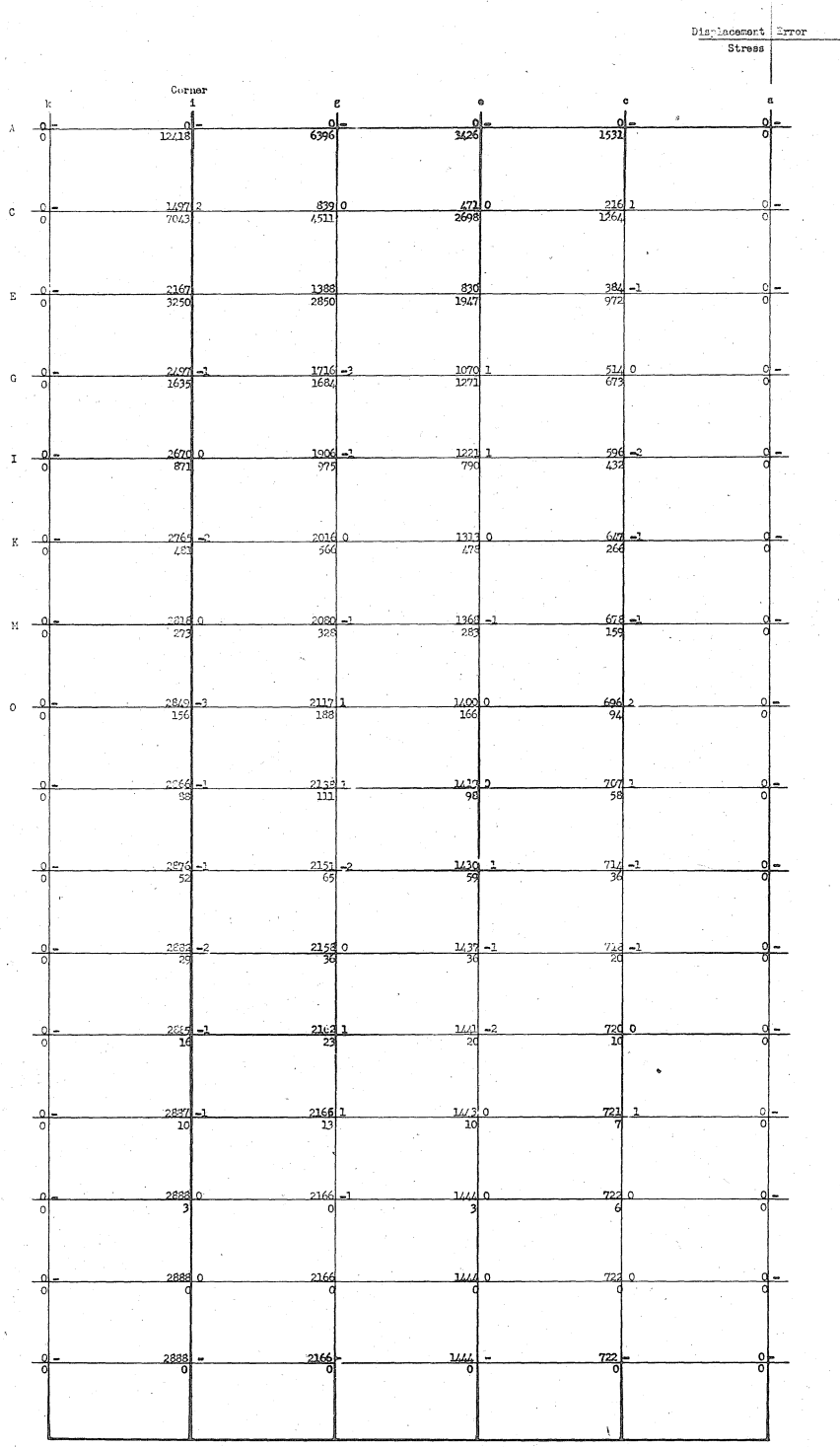


where

k	Region
4	Not Including Corner of Tube
3.55	Corner of Tube ( $L = 1$ in.)
3.775	Corner of Tube ( $L = \frac{1}{2}$ in.)
3.8875	Corner of Tube ( $L = \frac{1}{4}$ in.)

(c) Point Relaxation Operator

FIGURE 8 (CONTINUED)  
RECTANGULAR TUBE UNDER TORSION



The units of displacement and stress are in.  $\times 10^{-6}$  and psi, respectively

(a) Course Mesh (L = 1 in.)

FIGURE 9  
FINAL VALUES OF AXIAL DISPLACEMENTS AND STRESSES FOR RECTANGULAR TUBE UNDER TORSION

		Center										Displacement Error								
		Stress																		
		i	j	k	l	m	n	o	p	q	r	s	t	u	v					
A	0	0	6659	0	16213	0	9713	0	6539	0	4641	0	3348	0	2334	0	1482	0	722	0
D	0	1	445	1	1027	2	666	0	468	0	310	2	218	-1	174	0	111	0	54	0
C	0	1	754	1	1611	1	1162	1	866	0	666	2	477	-1	377	2	216	0	105	2
D	0	1	3243	1	6227	2	3629	1	4634	1	3660	2	2782	1	2008	1	1300	0	637	0
D	0	1	920	1	1881	2	1532	0	1181	1	903	1	676	2	483	-1	311	0	152	1
E	0	1	2223	1	4050	2	4056	0	3614	1	3016	2	2379	1	1755	1	1150	0	572	0
E	0	1	1865	1	2254	-1	1293	1	1222	2	1110	2	843	0	607	2	393	2	163	1
F	0	1	1509	1	2769	2	2932	1	2762	2	2412	2	1970	1	1482	1	988	2	494	0
F	0	1	1109	1	2411	1	1983	1	1606	0	1274	1	979	-1	711	6	463	1	228	2
G	0	1	2869	1	1956	2	2145	1	2100	1	1898	2	1586	1	1222	1	832	2	422	0
G	0	1	1259	0	2537	-1	2123	-1	1745	1	1402	-1	1087	0	795	1	521	-1	258	-2
H	0	1	760	0	1410	0	1580	0	1586	0	1469	0	1254	0	982	0	676	0	344	0
H	0	1	1308	-2	2658	1	2226	-1	1850	-1	1500	-2	1192	-2	862	0	571	-1	281	1
I	0	1	545	0	1027	0	1164	0	1190	0	1118	0	975	0	774	0	533	0	273	0
I	0	1	1373	0	2695	-1	2302	-1	1928	1	1574	-1	1237	-2	914	0	603	0	300	-2
J	0	1	396	0	754	0	858	0	890	0	845	0	741	0	598	0	416	0	214	0
J	0	1	1369	-1	2744	-2	2358	1	1987	-1	1630	-1	1286	0	954	-1	631	-1	314	0
K	0	1	286	0	546	0	637	0	670	0	637	0	599	0	455	0	318	0	162	0
K	0	1	1387	1	2779	0	2400	-2	2031	-2	1672	0	1323	2	984	0	652	0	325	0
L	0	1	208	0	396	0	468	0	484	0	421	0	429	0	344	0	240	0	124	0
L	0	1	1403	-1	2805	1	2430	0	2063	-1	1704	-2	1352	-1	1007	0	668	0	333	1
M	0	1	156	0	299	0	338	0	358	0	358	0	325	0	260	0	182	0	91	0
M	0	1	1111	0	2221	-2	2452	1	2086	1	1727	-2	1373	-1	1024	0	680	0	330	1
N	0	1	110	0	221	0	247	0	260	0	254	0	234	0	188	0	136	0	72	0
N	0	1	1418	-1	2839	-2	2468	-2	2109	2	1743	-3	1388	0	1026	0	689	0	344	-2
O	0	1	65	0	124	0	156	0	202	0	156	0	176	0	124	0	104	0	45	0
O	0	1	1421	-	2849	-	2476	-	2117	-	1751	-	1400	-	1043	-	696	-	346	-
P	0	1	13	0	104	0	52	0	162	0	52	0	136	0	58	0	78	0	6	0

The units of displacement and stress are  $\text{ins.} \times 10^{-6}$  and  $\text{psi}$ , respectively.

(b) Fine Mesh ( $L = \frac{1}{2}$  in.)

FIGURE 9  
FINAL VALUES OF AXIAL DISPLACEMENTS AND  
STRESSES FOR RECTANGULAR TUBE UNDER TORSION

		Corner													
		k							l						
		0	1	2	3	4	5	6	0	1	2	3	4	5	6
A	0	0	0	0	0	0	0	0	0	0	0	0	0	0	0
	0	3185	6773	11570	19695	13065	9737	7735	6396	5330	4522	3861	3276	2795	2311
	0	116	244	405	648	101	161	336	288	240	202	172	147	125	106
	0	2317	5915	9496	14001	10997	8775	7211	6084	5274	4628	4073	3594	3177	2782
B	0	219	454	730	1072	839	675	577	468	398	340	291	248	209	174
	0	2457	6979	7527	9711	8866	7709	6630	5707	4927	4251	3653	3133	2639	2210
	0	305	627	931	1376	1143	942	798	679	581	499	428	366	309	258
	0	2028	4930	5889	7345	7150	6798	5889	5200	4563	3978	3458	2977	2535	2119
C	0	375	765	1181	1642	1139	1181	1010	858	749	646	557	477	400	337
	0	1651	3237	4654	5772	5798	5538	5135	4641	4147	3666	3224	2782	2392	2002
	0	432	876	1342	1833	1489	1375	1193	1036	900	781	676	580	493	412
	0	1339	2613	3742	4652	4758	4567	4220	4095	3718	3313	2951	2597	2236	1898
D	0	478	956	1471	2000	1555	1540	1350	1189	1035	903	784	676	576	483
	0	1992	2119	3042	3809	3965	3952	3809	3715	3302	3003	2691	2392	2097	1768
	0	516	1032	1576	2132	1894	1679	1486	1311	1154	1012	883	764	652	548
	0	897	1712	2509	3159	3328	3354	3276	3120	2925	2691	2424	2171	1896	1612
E	0	440	1100	1654	2213	2011	1798	1602	1423	1260	1110	972	843	722	607
	0	743	1455	2093	2652	2808	2860	2821	2732	2597	2409	2197	1963	1729	1482
	0	573	1151	1737	2336	2110	1892	1703	1521	1353	1197	1052	915	785	662
	0	624	1209	1742	2223	2366	2431	2431	2379	2275	2132	1963	1768	1560	1352
F	0	498	1123	1728	2314	2103	1895	1709	1546	1435	1274	1123	970	842	711
	0	500	1014	1452	1872	2002	2080	2093	2070	2002	1885	1742	1573	1404	1209
	0	613	1229	1821	2480	2264	2069	1864	1682	1507	1342	1186	1036	891	756
	0	442	871	1261	1999	1716	1794	1833	1807	1755	1664	1534	1404	1261	1092
G	0	629	1260	1895	2577	2325	2123	1930	1742	1570	1409	1251	1092	939	785
	0	377	741	1066	1393	1282	1247	1286	1375	1521	1656	1782	1896	1995	2079
	0	642	1285	1931	2586	2378	2178	1986	1803	1624	1456	1290	1132	975	820
	0	312	624	923	1183	1287	1339	1352	1365	1326	1274	1196	1105	988	871
H	0	643	1308	1955	2628	2424	2226	2034	1850	1672	1500	1331	1172	1014	852
	0	260	520	793	1001	1105	1137	1146	1116	1100	1118	1140	1172	1214	1259

The units of displacement and stress are ins.  $\times 10^{-6}$  and psi, respectively.

(c) Finest Mesh ( $L = \frac{1}{4}$  in.)

FIGURE 9  
FINAL VALUES OF AXIAL DISPLACEMENTS AND  
STRESSES FOR RECTANGULAR TUBE UNDER TORSION

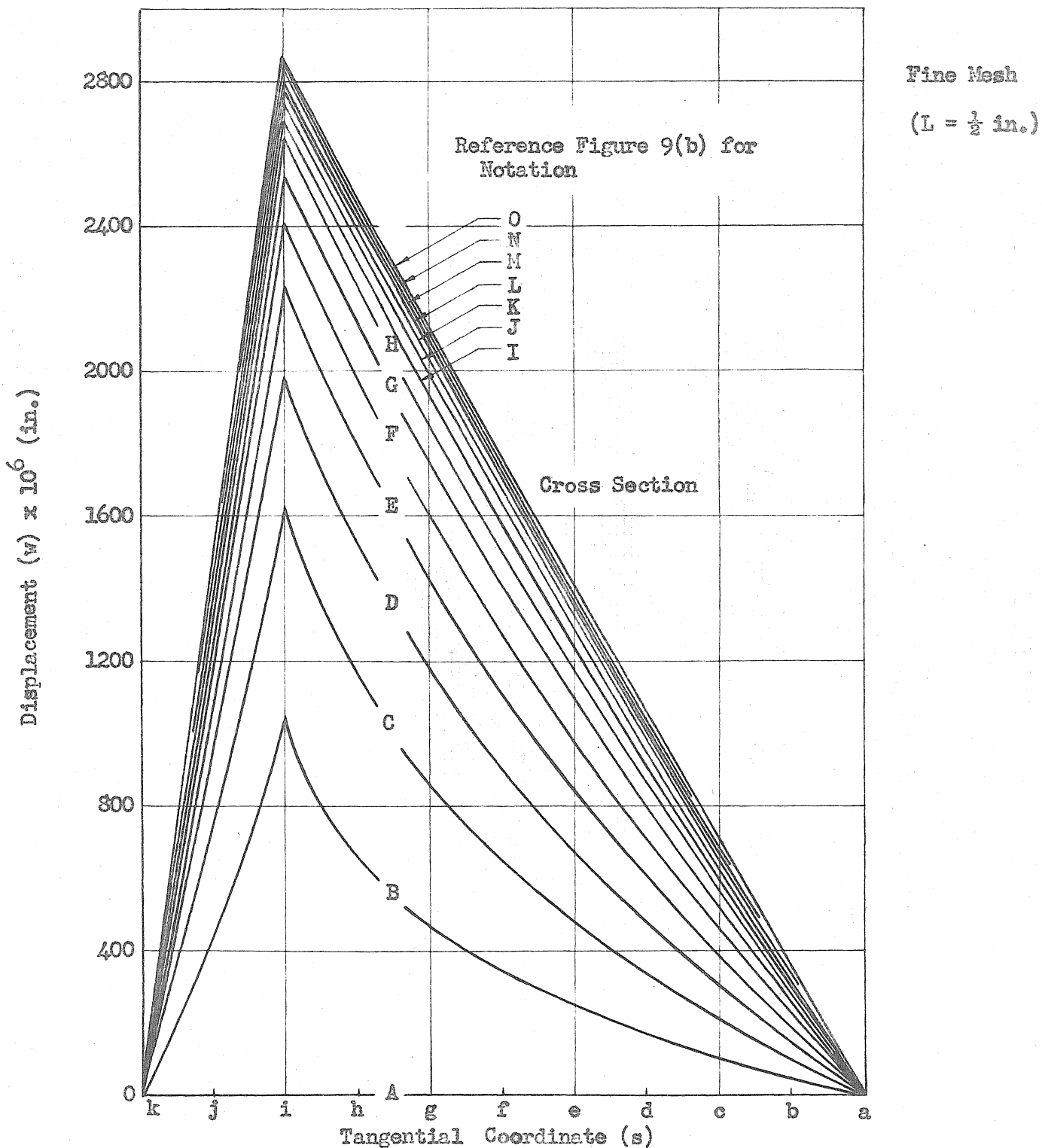


FIGURE 10

TANGENTIAL DISTRIBUTION OF AXIAL DISPLACEMENT FOR RECTANGULAR TUBE UNDER TORSION

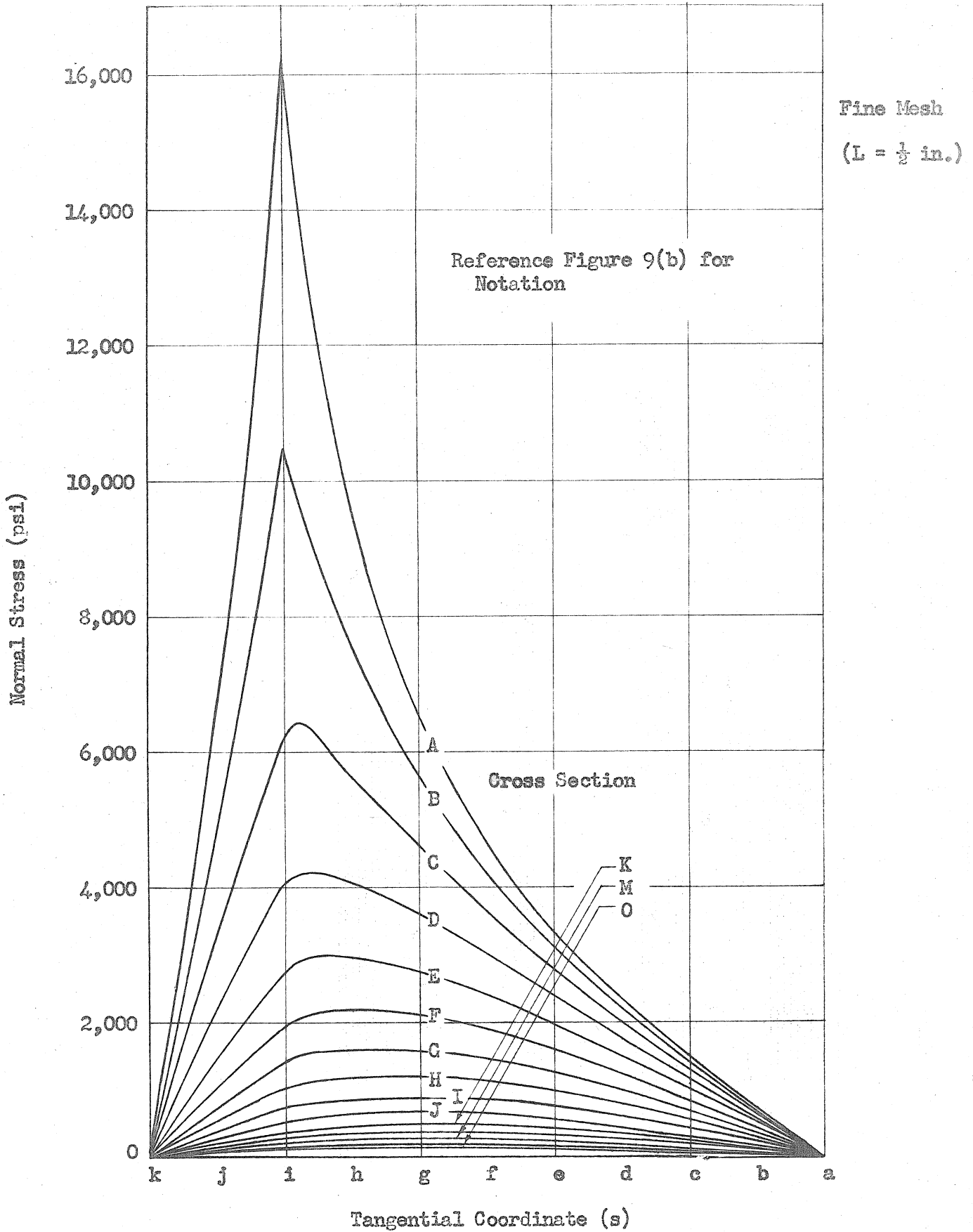


FIGURE 11

TANGENTIAL DISTRIBUTION OF NORMAL STRESS FOR RECTANGULAR TUBE UNDER TORSION



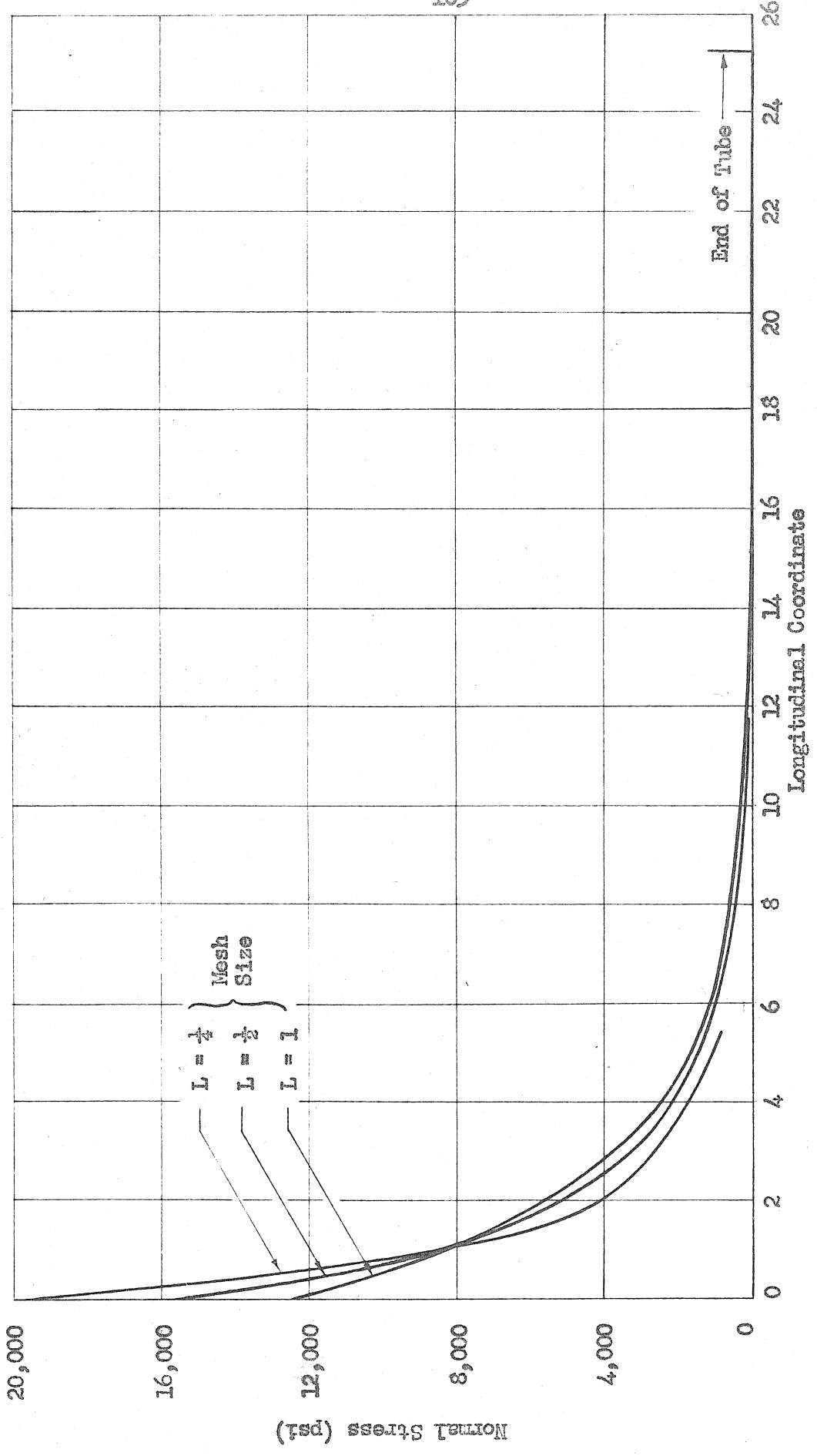


FIGURE 12  
AXIAL DISTRIBUTION OF NORMAL STRESS AT CORNER OF RECTANGULAR TUBE UNDER TORSION

Code

△ Analytical Solutions (Kármán-Chien)

○ Finite Difference Solutions

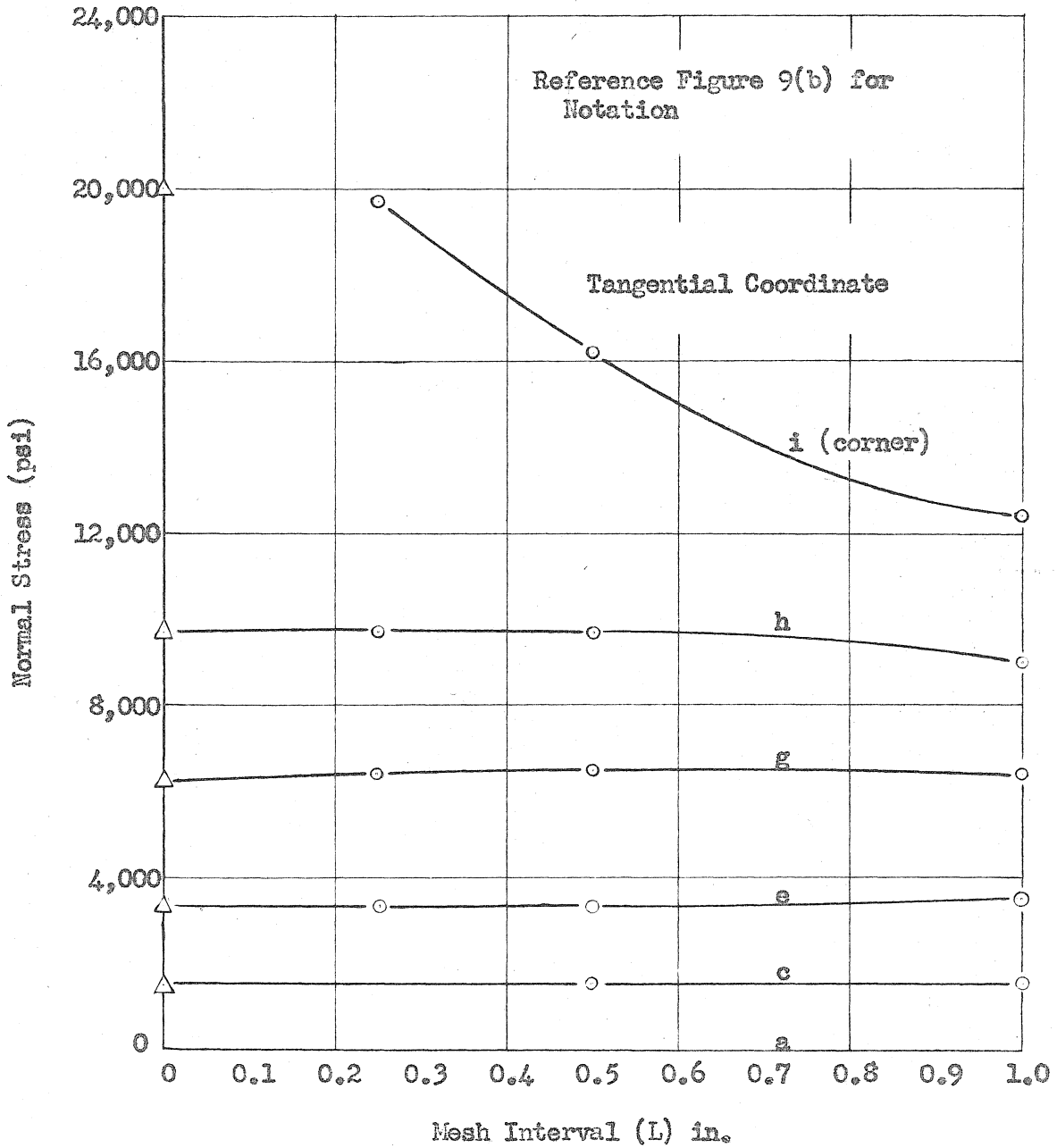
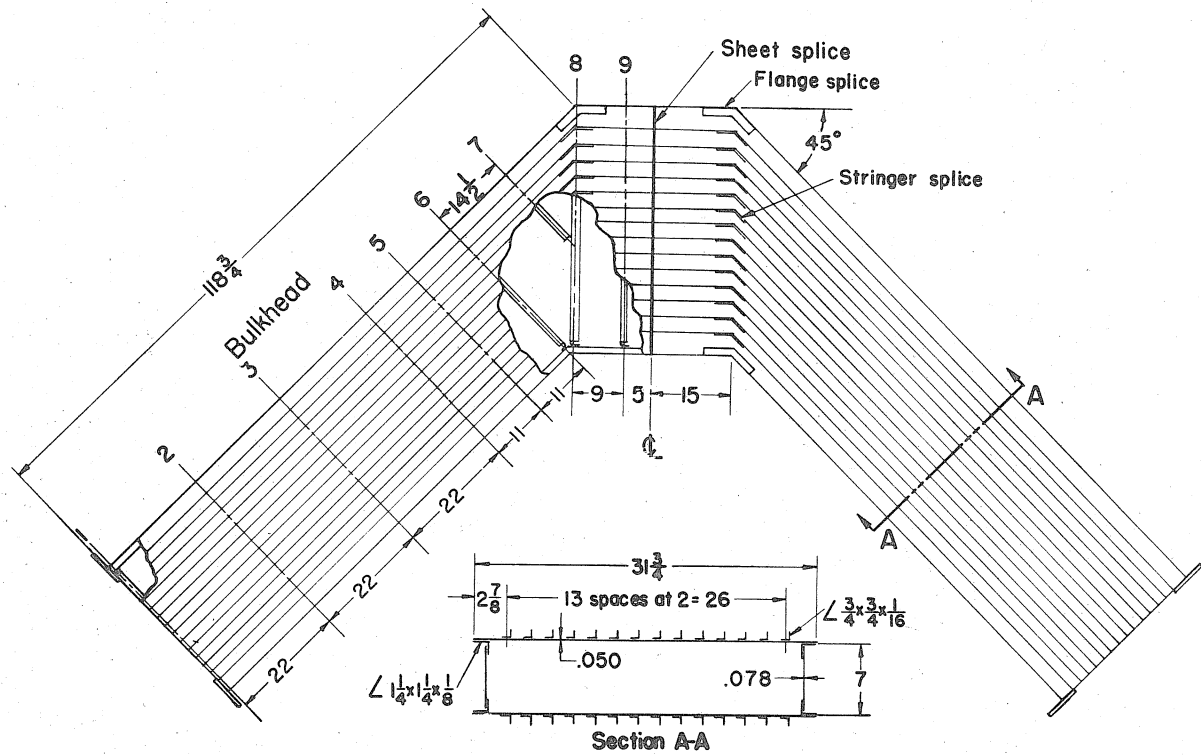


FIGURE 13

NORMAL STRESS AT SUPPORT FOR VARIOUS MESH SIZES

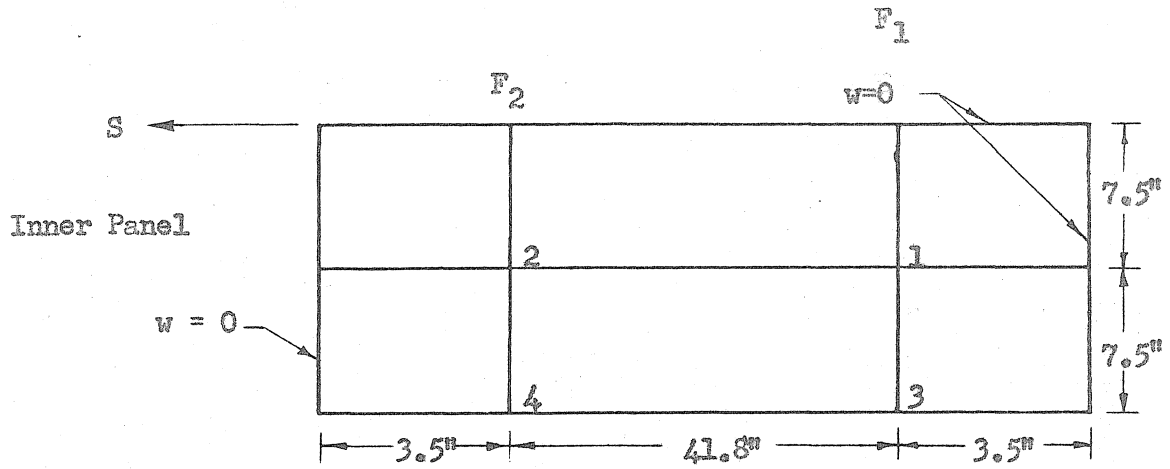
FOR RECTANGULAR TUBE UNDER TORSION



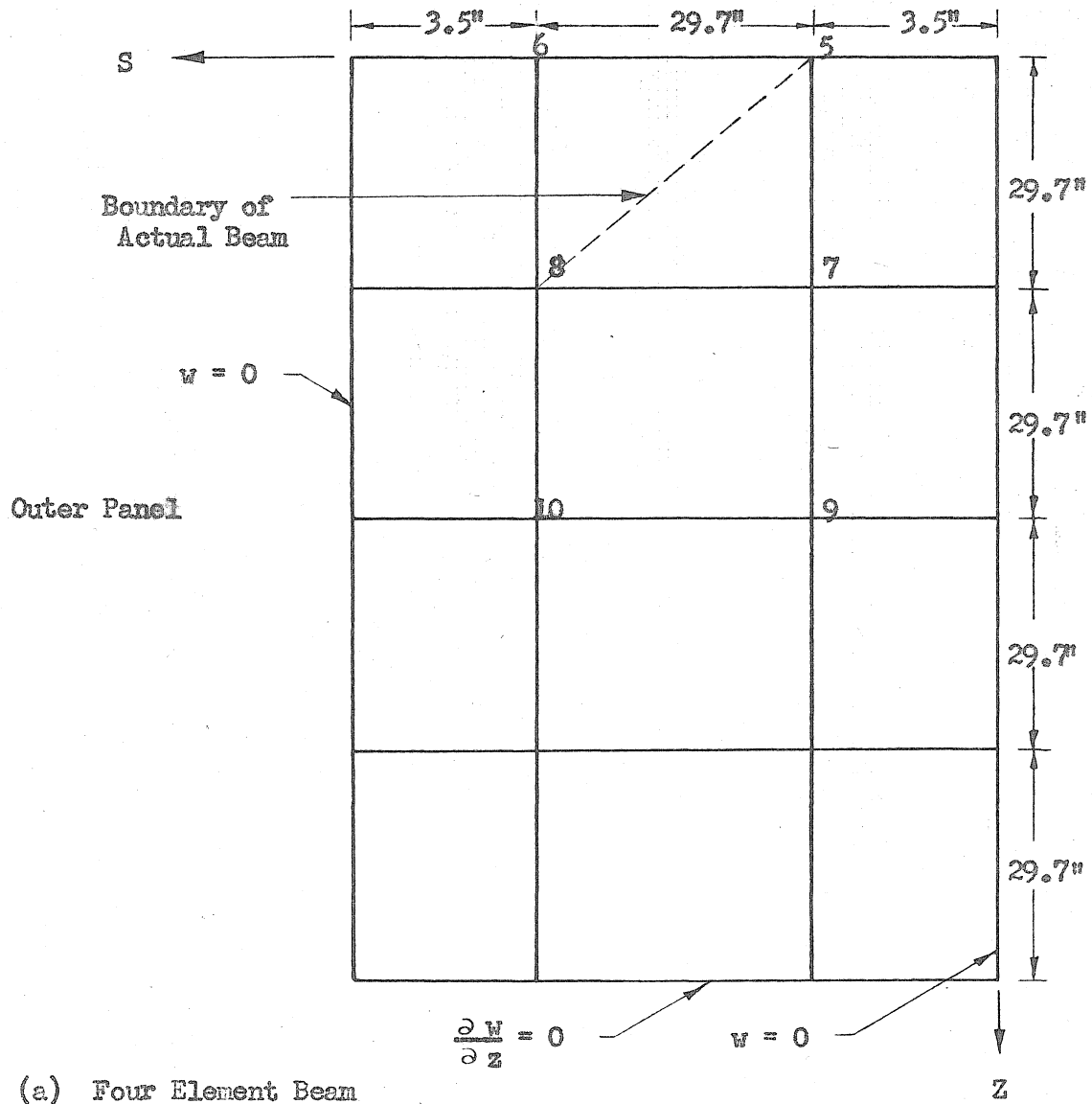
Dimensions in Inches

FIGURE 14

DETAILS OF NACA SWEEP BOX BEAM



Boundary Conditions at Joint Given in Section VII



(a) Four Element Beam

FIGURE 15

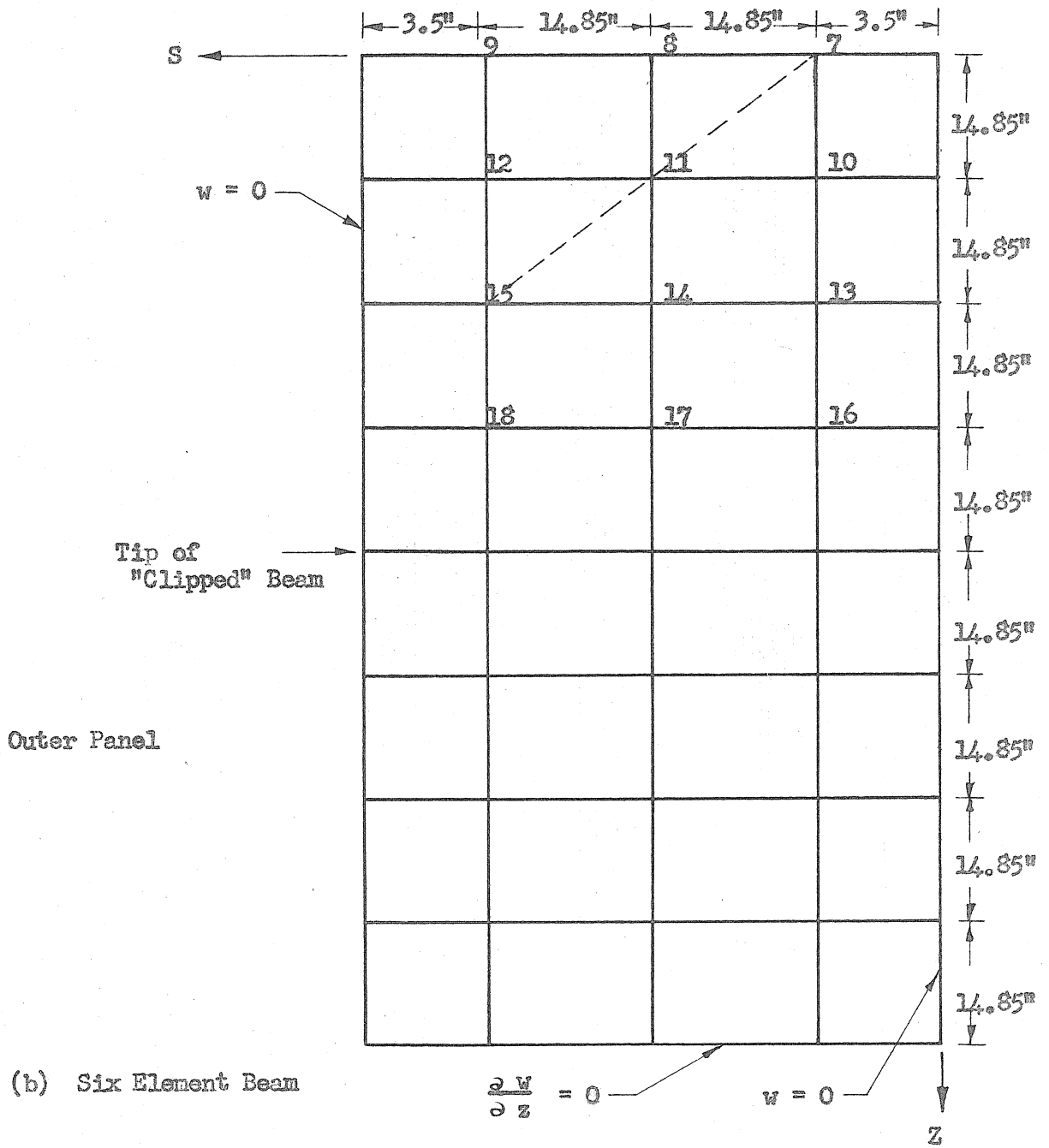
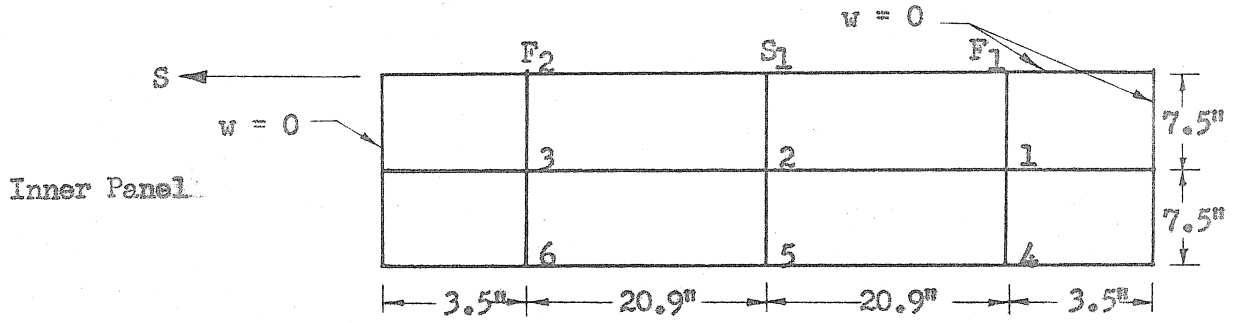
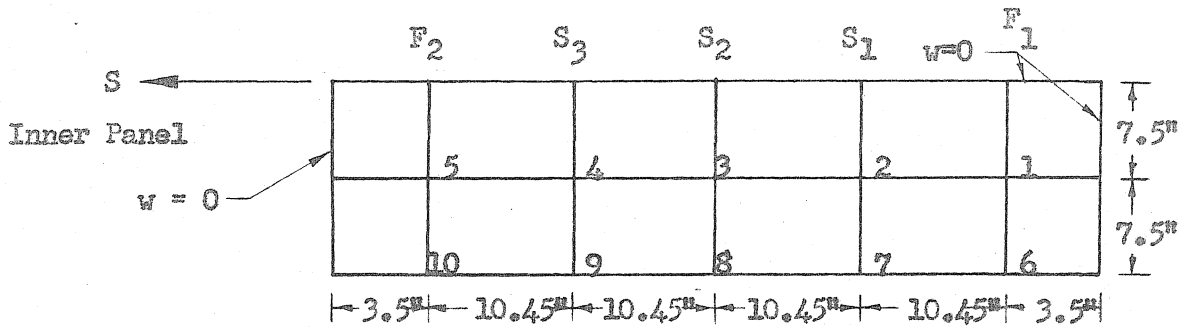


FIGURE 15



Boundary Conditions at Joint Given in Section VII

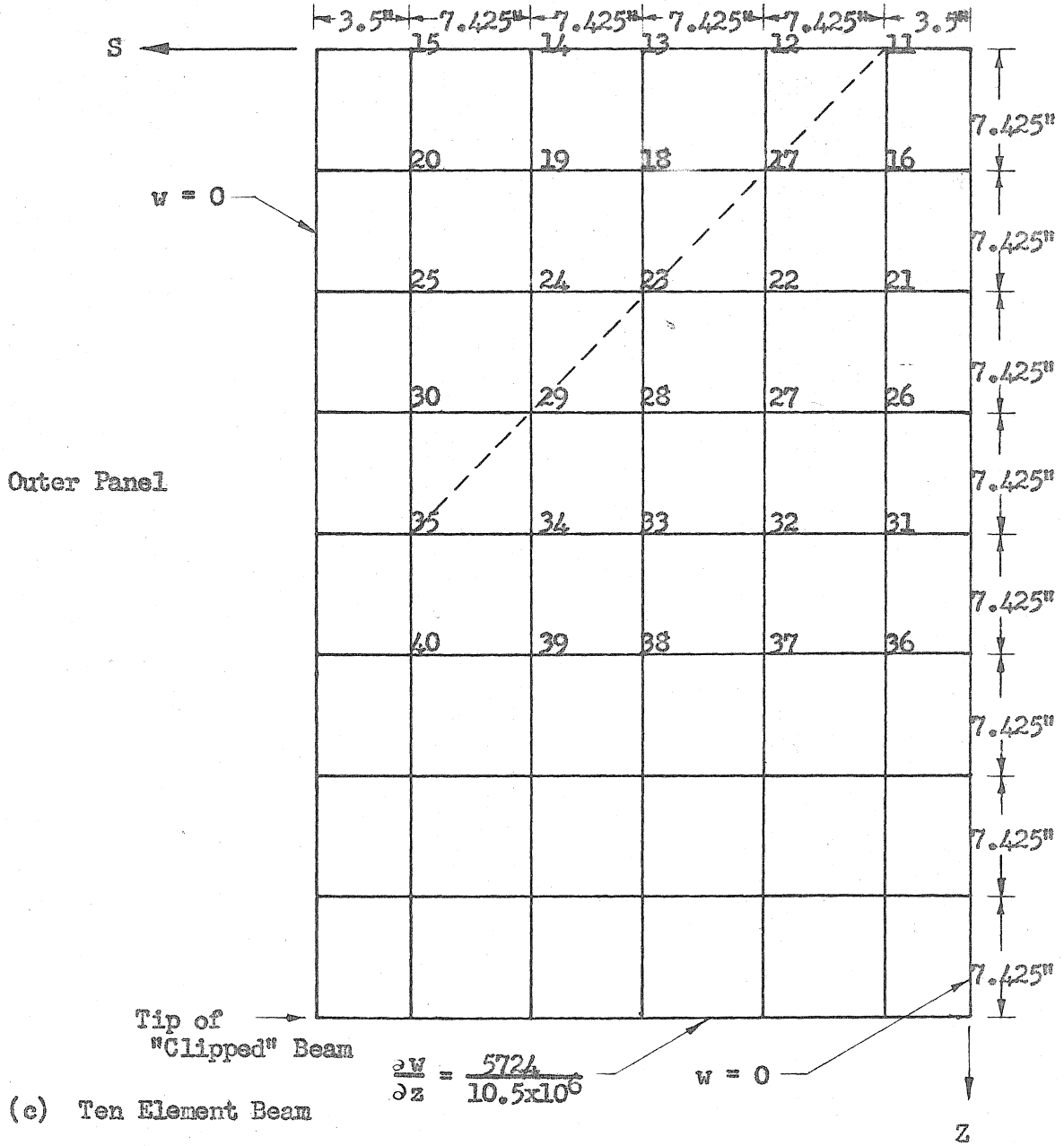
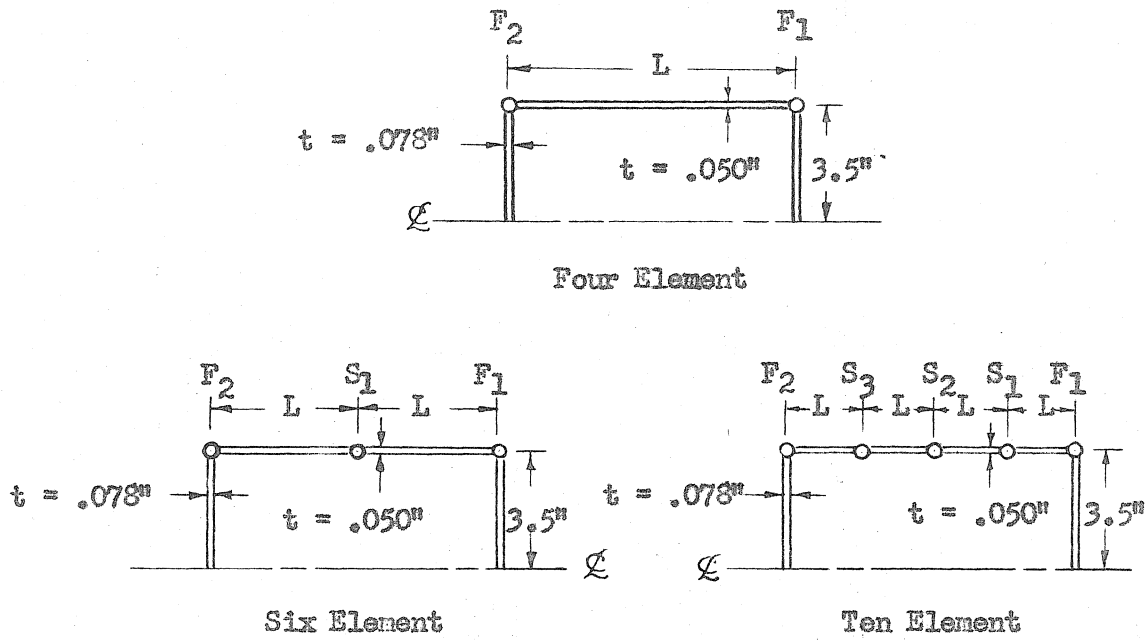


FIGURE 15

RELAXATION MESH AND BOUNDARY CONDITIONS FOR SWEEP BEAM



Element	Area (Sq. in.)	Inner Panel			Outer Panel		
		Flange	Stiffener	L(in.)	Flange	Stiffener	L(in.)
4	$a_{st}$	1.111	-	41.8	1.111	-	29.7
	$a_{sh}$	1.045	-		.742	-	
	$a_{st}$	2.156	-		1.853	-	
6	$a_{st}$	.783	.656	20.9	.783	.656	14.85
	$a_{sh}$	.522	1.045		.371	.742	
	$a_{st}$	1.305	1.701		1.154	1.398	
10	$a_{st}$	.619	.328	10.45	.619	.328	7.425
	$a_{sh}$	.261	.522		.186	.371	
	$a_{st}$	.880	.850		.805	.699	

FIGURE 16

IDEALIZED CROSS SECTIONS OF SWEEPED BEAM

Four Element Beam

	F <sub>2</sub>	F <sub>1</sub>	
	.021	1 -1	

			.326
	.346	1 -1	
			.326

Six Element Beam

Inner Panel

	F <sub>2</sub>	S <sub>1</sub>	F <sub>1</sub>	
	.0246	.0146	1 -1	

Outer Panel

				.0188
	.0188	1 -1		

Inner Panel

				.392
	.1192	.0842	1 -1	
				.392

.416

				.096
	.096	1 -1		
				.416

Outer Panel

Ten Element Beam

Inner Panel

	F <sub>2</sub>	S <sub>3</sub>	S <sub>2</sub>	S <sub>1</sub>	F <sub>1</sub>	
	.0348			.0538	1 -1	
			.0538	1 -1	.0532	
		.0538	1 -1	.0538		

Outer Panel

					.438
	.0477			.0842	1 -1
					.438
			.415	.0769	
		.0842	1 -1	.415	
				.415	
		.415	1 -1	.0842	
				.415	

Note: Reference Figure 5e, for line adjacent to tip, use number in parenthesis.

FIGURE 17

POINT RELAXATION OPERATORS FOR SWEEP BEAM



		F <sub>2</sub>	Inner Panel		F <sub>1</sub>	Displacement   Error	
						Stress	
0	-	0	-	0	-	0	-
0		8512		4557		0	
0	-	615	0	319	0	0	-
0		8708		4375		0	
0	-	1211	-	625	-	0	-
0		8904		4193		0	

Outer Panel

0	-	-3264	-	112	-	0	-
0		17878		4556		0	
0	-	880	0	1838	0	0	-
0		11428		5316		0	
0	-	3200	0	3119	0	0	-
0		6337		4763		0	
0	-	1164	1	1532	1	0	-
0		2958		2576		0	
0	-	4873	0	4906	0	0	-
0		0		0		0	

The data at each point of the grid is in accordance with the code shown in the upper right hand corner. The units of displacement and stress are ins. x 10<sup>-5</sup> and psi, respectively.

(a) Four Element Beam

FIGURE 18

FINAL VALUES OF AXIAL DISPLACEMENTS AND STRESSES FOR THE  
SWEEP WING WITH NO WING RIB UNDER SYMMETRICAL BENDING

		F <sub>2</sub>	S <sub>1</sub>		F <sub>1</sub>	Displacement	Error
			Inner Panel			Stress	
0	-	0	0	-	0	-	0
0		8813	5404		3577		0
0	-	645	384	0	243	0	0
0		9247	5348		3227		0
0	-	1321	764	-	161	-	0
0		9681	5292		2877		0

		Outer Panel					
0	-	-4798	-77	-	326	-	0
0		-	-		2439		0
0	-	-1232	540	0	870	3	0
0		-	5394		5253		0
0	-	934	1449	1	1812	0	0
0		12,765	6536		6780		0
0	-	2379	2389	1	2788	-1	0
0		8632	6370		6543		0
0	-	3376	3251	2	3663	-1	0
0		5724	5724		5724		0

The units of displacement and stress are ins.  $\times 10^{-5}$  and psi, respectively.

(b) Six Element (Clipped) Beam

FIGURE 18

FINAL VALUES OF AXIAL DISPLACEMENTS AND STRESSES FOR THE  
SWEPT WING WITH NO WING RIB UNDER SYMMETRICAL BENDING

		F <sub>2</sub>	S <sub>1</sub>		F <sub>1</sub>		Displacement	Error	
		Inner Panel						Stress	
0	-	0	-	0	-	0	-	0	-
0		8848		5327		3584		0	
0	-	648	0	378	0	213	0	0	-
0		9296		5257		3220		0	
0	-	1328	-	751	-	160	-	0	-
0		9744		5187		2856		0	
Outer Panel									
0	-	-4813	-	-70	-	325	-	0	-
0		30231		3206		3418		0	
0	-	-1237	0	531	0	864	0	0	-
0		20333		5292		5204		0	
0	-	939	0	1427	0	1797	0	0	-
0		12889		6412		6699		0	
0	-	2409	-1	2345	0	2759	0	0	-
0		8929		6140		6402		0	
0	-	3465	0	3164	0	3608	0	0	-
0		6441		5246		5412		0	
0	-	4231	0	3829	-1	4290	-1	0	-
0		4574		4062		4154		0	
0	-	4759	-1	4313	0	4783	-1	0	-
0		2966		2750		2793		0	
0	-	5070	-1	4607	-1	5080	0	0	-
0		1460		1386		1400		0	
0	-	5172	0	4705	0	5179	0	0	-
0		0		0		0		0	

The units of displacement and stress are ins. x 10<sup>-5</sup> and psi, respectively.

(c) Six Element Beam

FIGURE 18

FINAL VALUES OF AXIAL DISPLACEMENTS AND STRESSES FOR THE  
SWEPT WING WITH NO WING RIB UNDER SYMMETRICAL BENDING

		F <sub>2</sub>	S <sub>3</sub>	S <sub>2</sub>	S <sub>1</sub>	F <sub>1</sub>	Displacement	Error
		Inner Panel					Stress	
0	-	0	0	0	0	0	0	0
0	-	8274	6447	5453	4158	2177		0
0	-	619	455	391	303	127		0
0	0	9058	6293	5495	4326	1379		0
0	-	1294	899	785	618	167		0
0	0	9843	6139	5537	4494	581		0

		"Clipped" Outer Panel						
0	-	-7092	696	-190	212	139		0
0	0	55974	-14107	5621	2546	-445		0
0	-	-3742	75	195	437	249		0
0	0	38777	-3458	5268	3818	3557		0
0	-	-1608	207	555	752	642		0
0	0	25406	3967	5324	4914	6343		0
0	-	-149	636	948	1132	1146		0
0	0	17840	6753	5805	5643	7340		0
0	-	915	1162	1376	1550	1680		0
0	0	13343	7509	6159	6053	7481		0
0	-	1738	1698	1819	1988	2204		0
0	0	10493	7410	6279	6215	7227		0
0	-	2399	2210	2264	2429	2702		0
0	0	8528	6972	6215	6173	6795		0
0	-	2944	2684	2698	2861	3165		0
0	0	7000	6371	6003	5982	6258		0
0	-	3389	3111	3113	3275	3587		0
0	0	5724	5724	5724	5724	5724		0

The units of displacement and stress are ins.  $\times 10^{-5}$  and psi, respectively.

(d) Ten Element (Clipped) Beam

FIGURE 18

FINAL VALUES OF AXIAL DISPLACEMENTS AND STRESSES FOR THE  
SWEPT WING WITH NO WING RIB UNDER SYMMETRICAL BENDING

		F <sub>2</sub>	Inner Panel		F <sub>1</sub>	Displacement	Error
						Stress	
0	-	0	-	0	-	0	-
0		154		-994		0	
0	-	13	0	-73	0	0	-
0		210		-1050		0	
0	-	30	-	-150	-	0	-
0		266		-1106		0	
Outer Panel							
0	-	503	-	-106	-	0	-
0		-2380		-1001		0	
0	-	21	0	-259	-1	0	-
0		-1029		-81		0	
0	-	-79	0	-152	0	0	-
0		-217		240		0	
0	-	-102	-1	-123	0	0	-
0		-48		62		0	
0	-	-106	-1	-117	0	0	-
0		0		0		0	

The units of displacement and stress are ins. x 10<sup>-5</sup> and psi, respectively.

(a) Four Element Beam

FIGURE 19

FINAL VALUES OF AXIAL DISPLACEMENTS AND STRESSES FOR  
THE SWEEP WING UNDER THE LOADS IMPOSED BY THE WING RIB

		F <sub>2</sub>	S <sub>1</sub>		F <sub>1</sub>	Displacement	Error
			Inner Panel			Stress	
0	-	0	-	0	-	0	-
0	0	945		-343		-651	
0	-	73	0	-26	0	-50	-1
0	0	1099		-385		-749	
0	-	157	-	-55	-	-107	-
0	0	1253		-427		-847	

		Outer Panel					
0	-	842	-	-97	-	-76	-
0	0	-4525		604		-703	
0	-	339	0	-39	0	-151	0
0	0	-2587		216		-357	
0	-	110	0	-36	0	-177	0
0	0	-1071		21		187	
0	-	36	-1	-33	-1	-98	0
0	0	-332		11		350	
0	-	16	0	-33	0	-78	0
0	0	0		0		0	

The units of displacement and stress are ins. x 10<sup>-5</sup> and psi, respectively.

(b) Six Element (Clipped Beam)

FIGURE 19

FINAL VALUES OF AXIAL DISPLACEMENTS AND STRESSES FOR  
THE SWEEPED WING UNDER THE LOADS IMPOSED BY THE WING RIB

	$F_2$	$S_1$	$F_1$	Displacement	Error
				Stress	
Inner Panel					
0 -	0 -	0 -	0 -	0 -	0 -
	945	-301	-623		0
0 -	73 0	-23 0	-19 0		0 -
	1099	-343	-742		0
0 -	157 -	-49 -	-106 -		0 -
	1253	-385	-854		0
Outer Panel					
0 -	834 -	-94 -	-75 -		0 -
	4472	601	-686		0
0 -	337 0	-35 0	-146 0		0 -
	-2556	233	-318		0
0 -	111 0	-28 0	-165 0		0 -
	-1064	49	247		0
0 -	36 0	-21 0	-76 -1		0 -
	-361	46	452		0
0 -	9 -1	-15 0	-37 -1		0 -
	-131	35	201		0
0 -	-1 0	-11 0	-19 -1		0 -
	-42	25	92		0
0 -	-3 -1	-8 0	-11 0		0 -
	-11	18	42		0
0 -	-4 0	-6 0	-7 -1		0 -
	-4	11	18		0
0 -	-4 0	-5 0	-6 0		0 -
	0	0	0		0

The units of displacement and stress are ins.  $\times 10^{-5}$  and psi, respectively.

(c) Six Element Beam

FIGURE 19

FINAL VALUES OF AXIAL DISPLACEMENTS AND STRESSES FOR  
THE SWEEP WING UNDER THE LOADS IMPOSED BY THE WING RIB

	$F_2$	Inner Panel	$F_1$	
0	8538		4391	0
0	8743		4200	0
0	8948		4008	0

		Outer Panel		
0	17481		4389	0
0	11256		5302	0
0	6301		4803	0
0	2950		2586	0
0	0		0	0

The unit of stress is psi.

(a) Four Element Beam

FIGURE 20

FINAL VALUES OF NORMAL STRESS FOR THE SWEEP WING  
WITH A WING RIB UNDER SYMMETRICAL BENDING



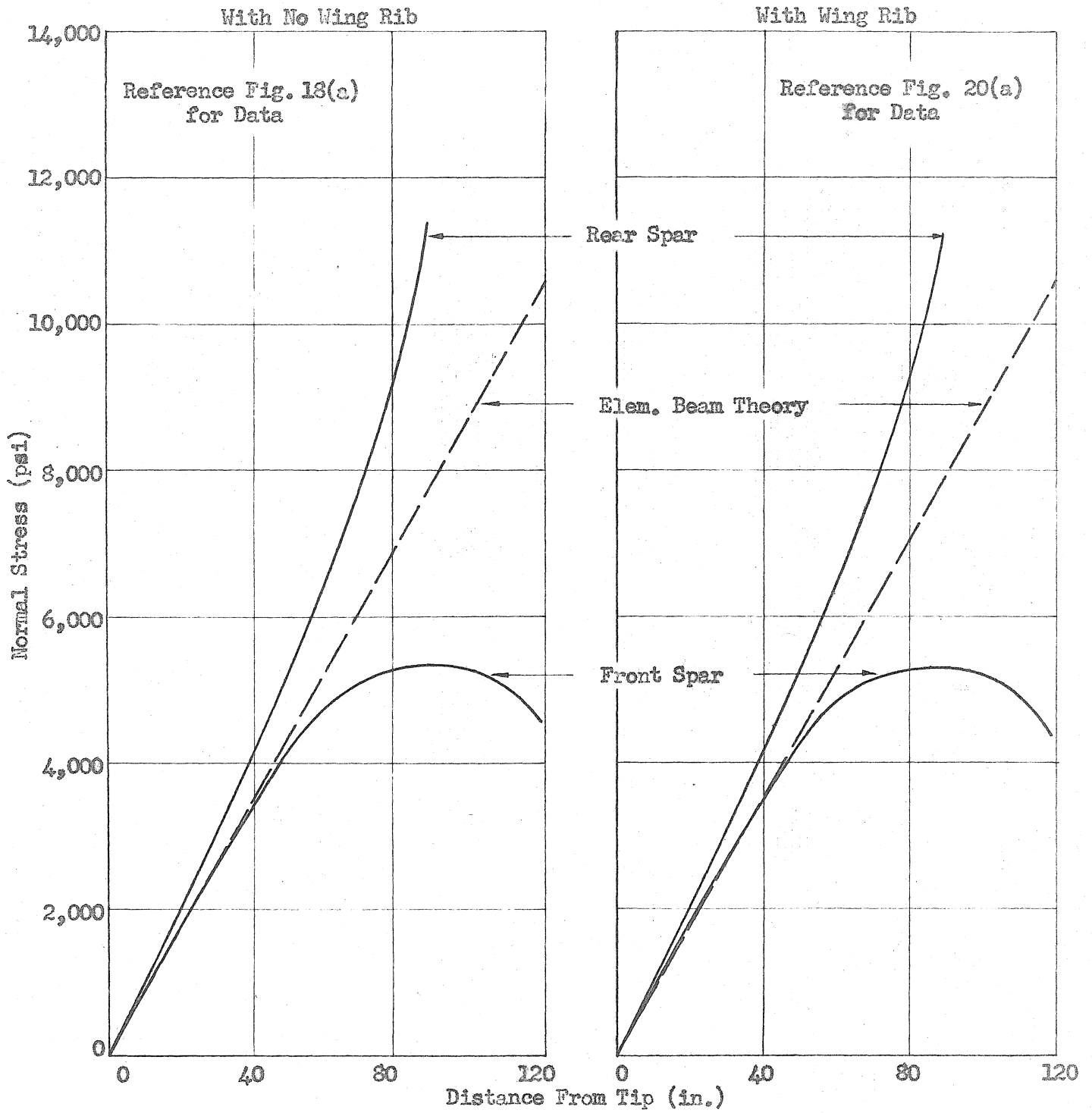
	$F_2$	$S_1$	$F_1$	
Inner Panel				
0	8720	5368	3668	0
0	9148	5303	3320	0
0	9515	5239	2971	0
Outer Panel				
0	29627	3125	2511	0
0	20678	5261	5247	0
0	13033	6405	6666	0
0	8978	6134	6341	0
0	6459	5241	5385	0
0	4580	4059	4142	0
0	2967	2748	2787	0
0	1461	1385	1398	0
0	0	0	0	0

The unit of stress is psi.

(b) Six Element Beam

FIGURE 20

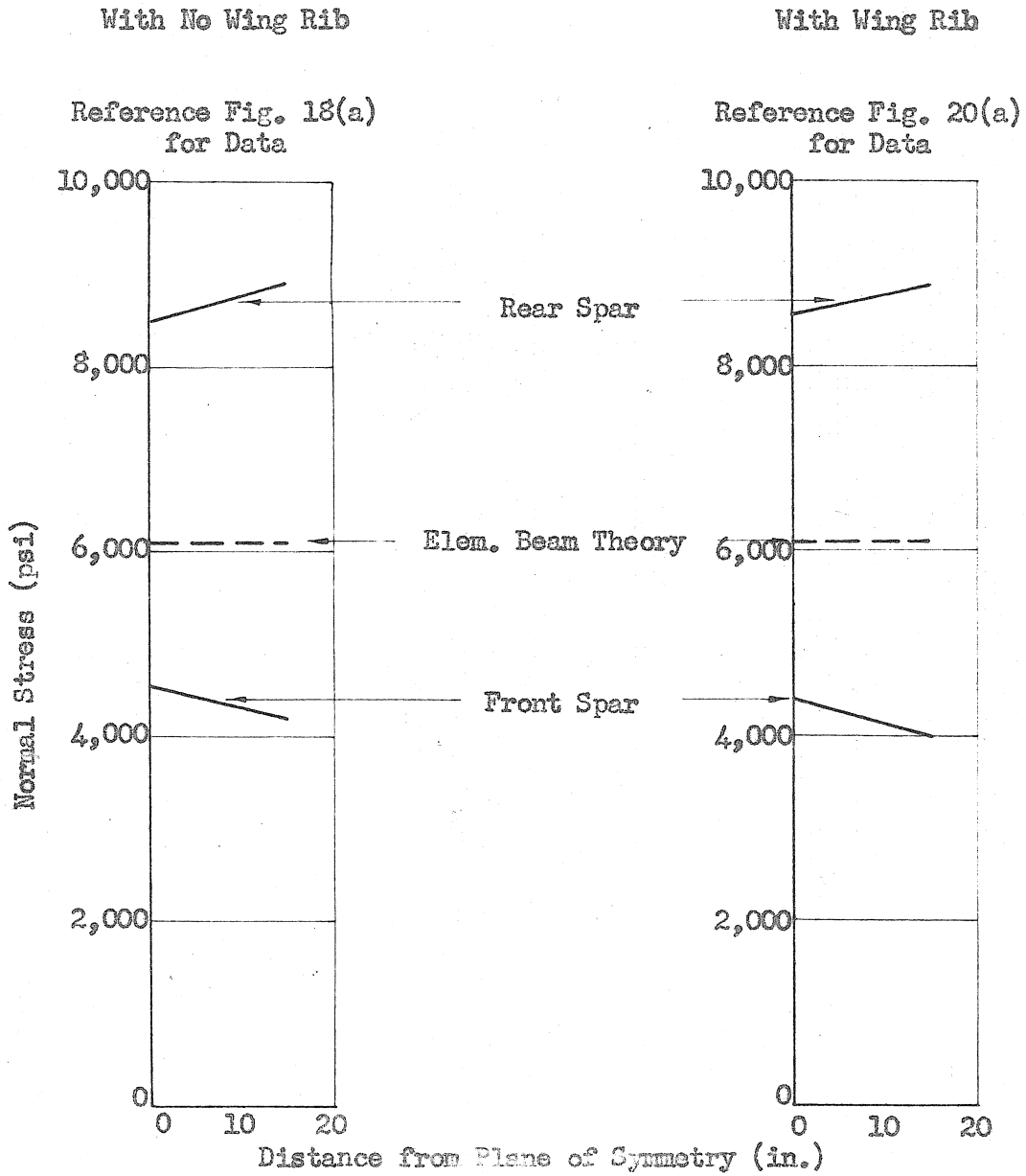
FINAL VALUES OF NORMAL STRESS FOR THE SWEEP WING  
WITH A WING RIB UNDER SYMMETRICAL BENDING



(a) Four Element Beam - Outer Panel

FIGURE 21

STRINGER AND FLANGE STRESSES OF SWEEPBACK BOX BEAM FOR TIP BENDING LOAD

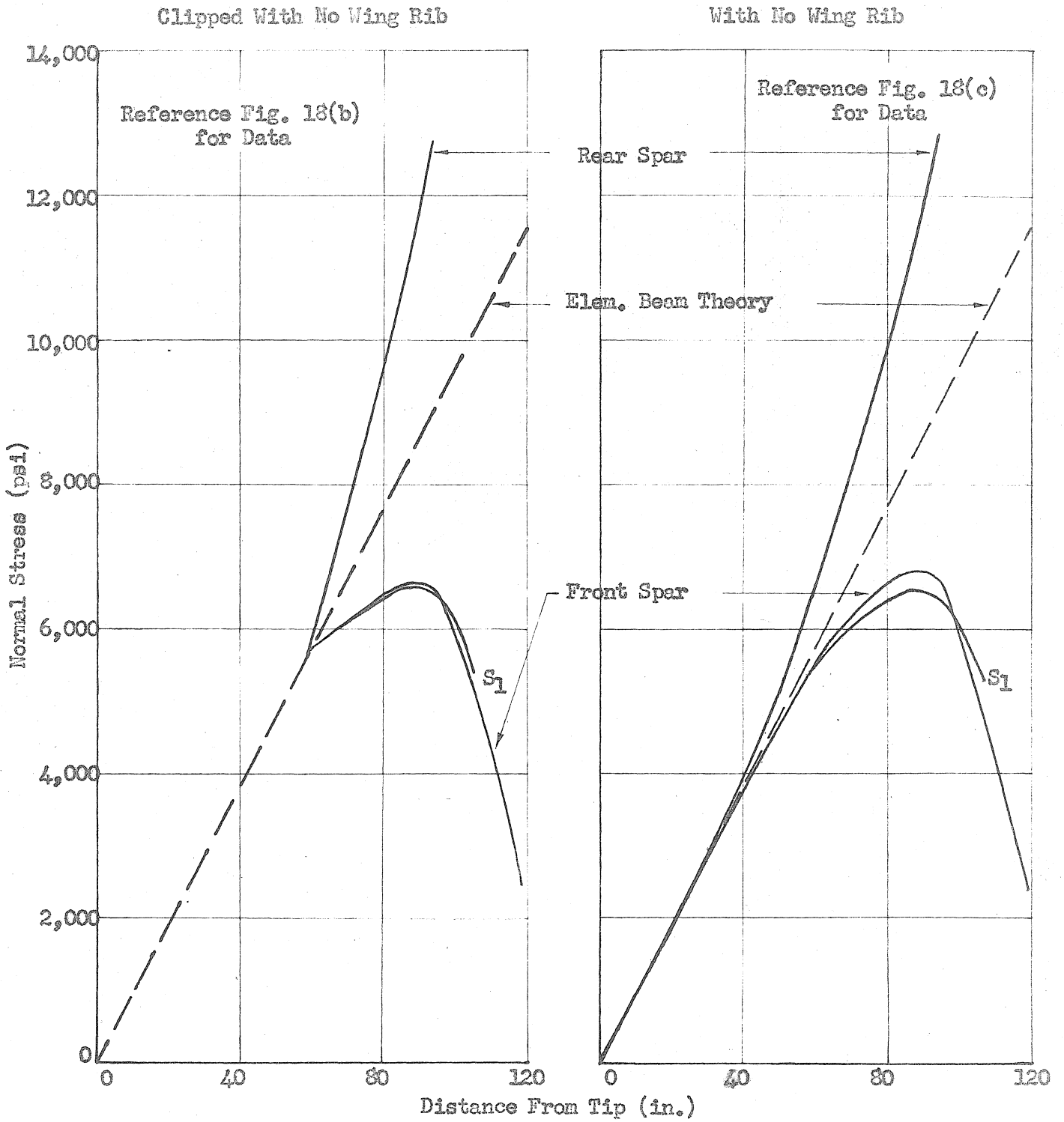


(b) Four Element Beam - Inner Panel

FIGURE 21

STRINGER AND FLANGE STRESSES OF SWEEPTRACK BOX BEAM FOR TIP BENDING LOAD

Reference Fig. 15(b) for Notation



(c) Six Element Beam - Outer Panel

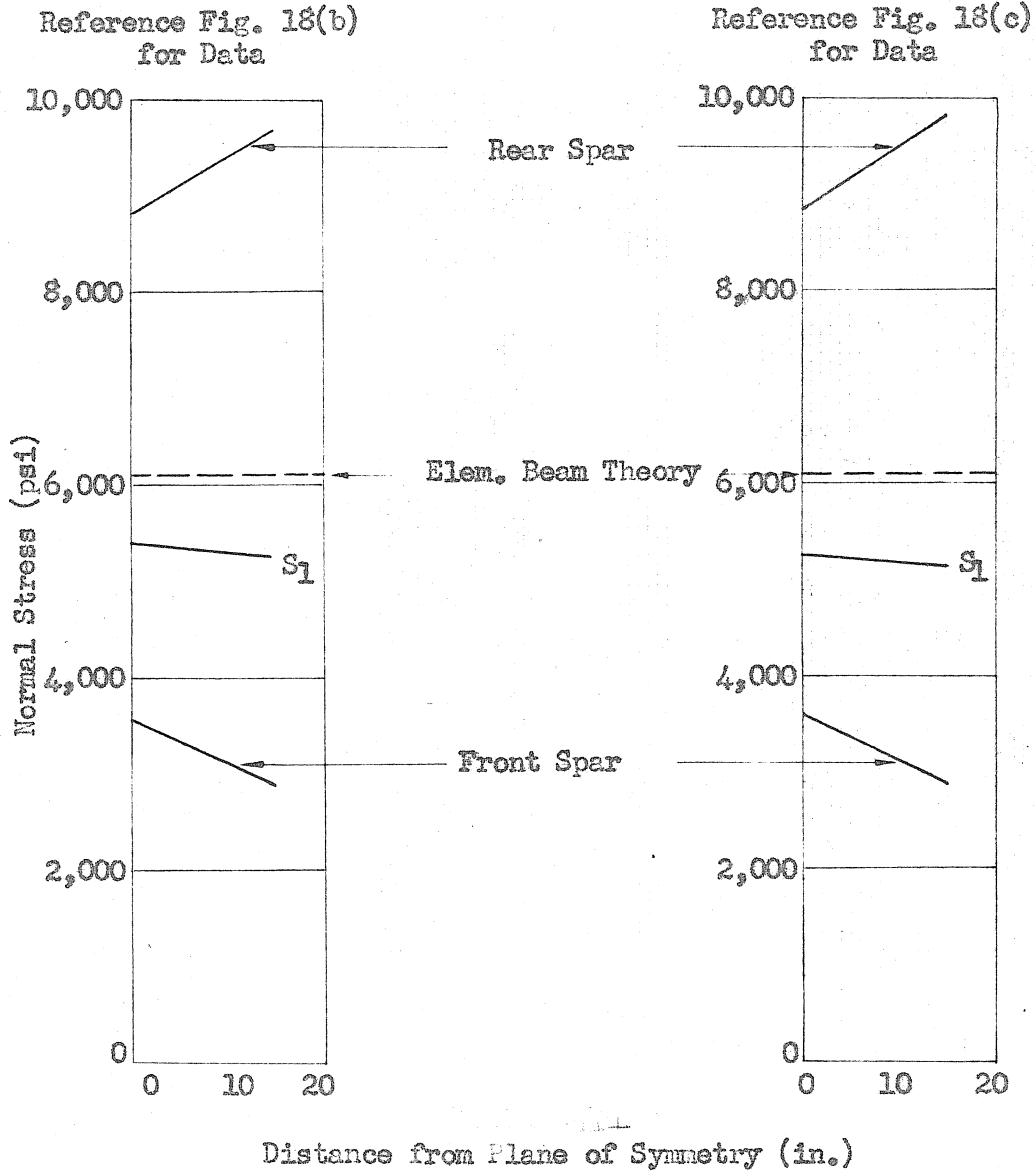
FIGURE 21

STRINGER AND FLANGE STRESSES OF SWEPTRACK BOX BEAM FOR TIP BENDING LOAD

Reference Fig. 15(b) for Notation

Clipped With No Wing Rib

With No Wing Rib

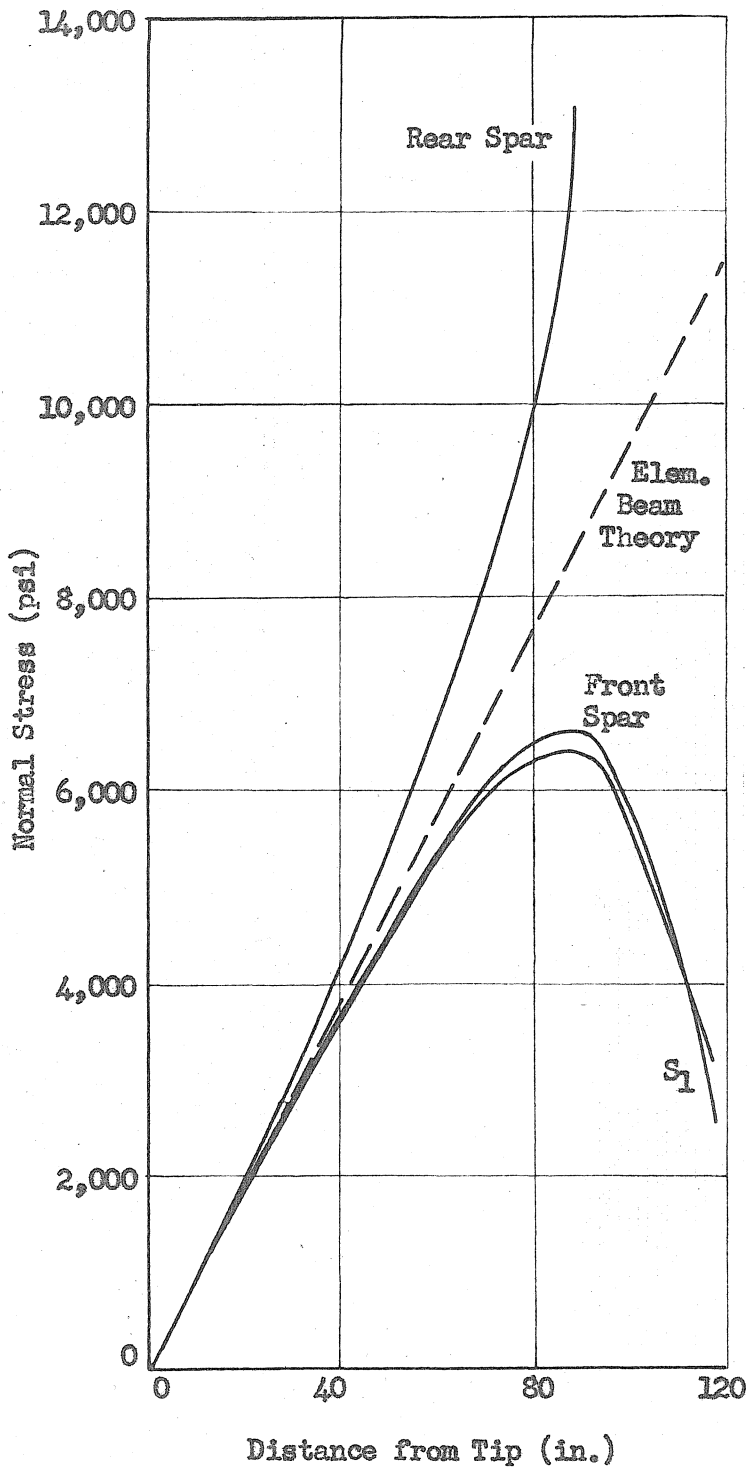


(d) Six Element Beam - Inner Panel

FIGURE 21

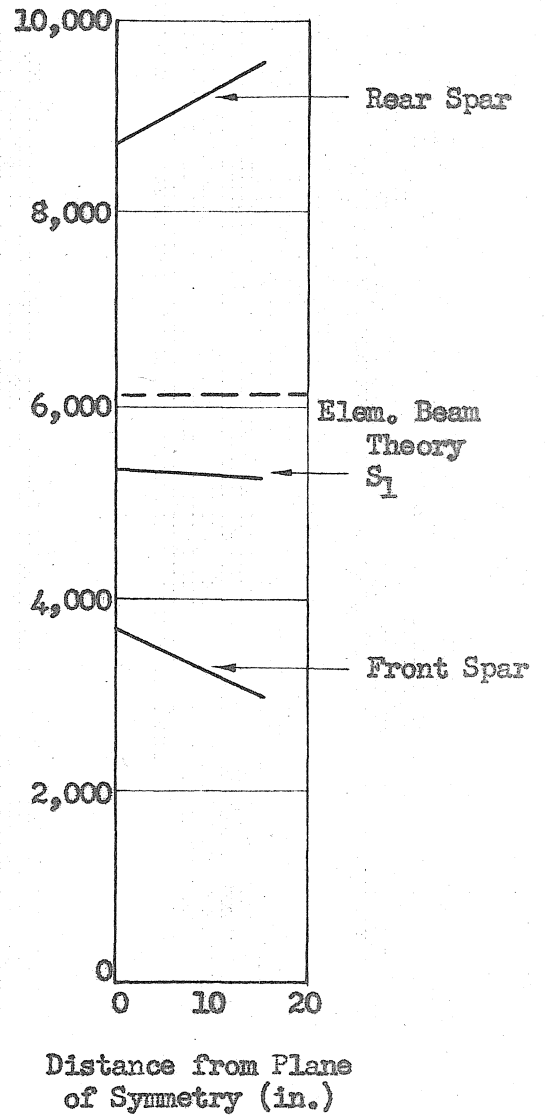
STRINGER AND FLANGE STRESSES OF SWEPTRACK BOX BEAM FOR TIP BENDING LOAD

Reference Fig. 20(b) for Data



Outer Panel

Reference Fig. 15(b)  
for Notation

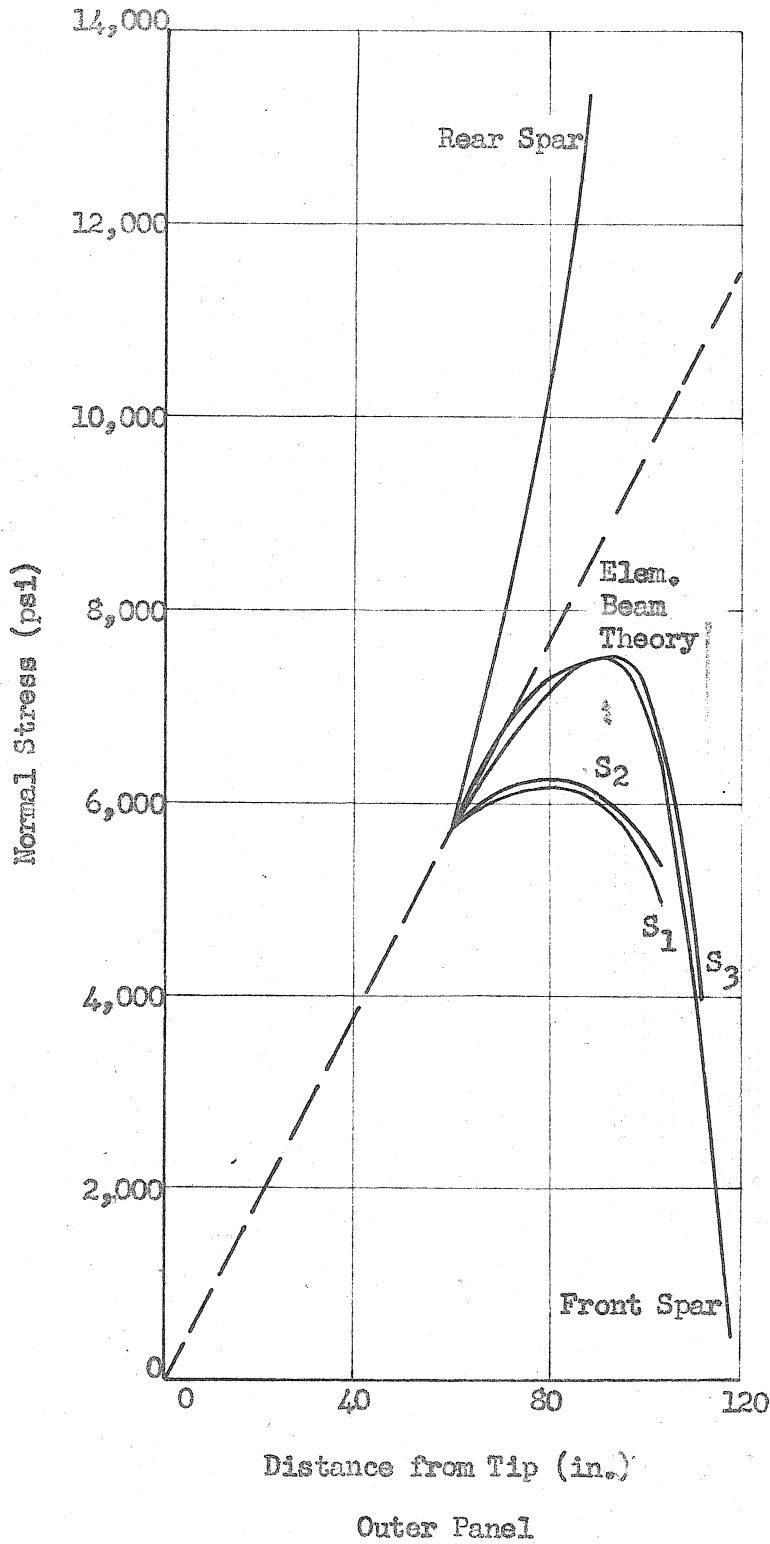


Inner Panel

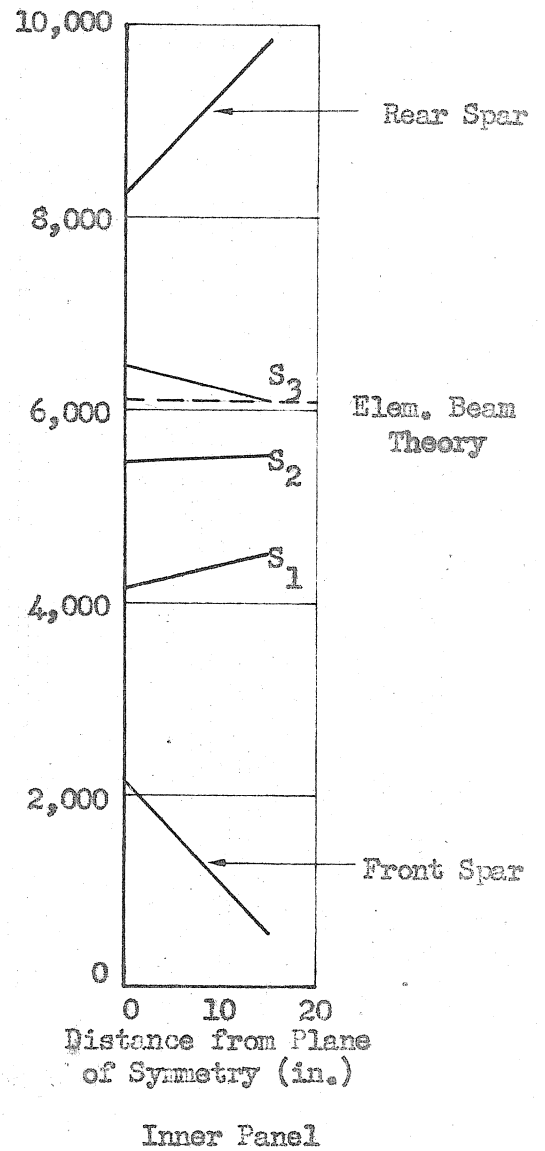
(e) Six Element Beam - With Wing Rib

FIGURE 21

STRINGER AND FLANGE STRESSES OF SWEEPBACK BOX BEAM FOR TIP BENDING LOAD



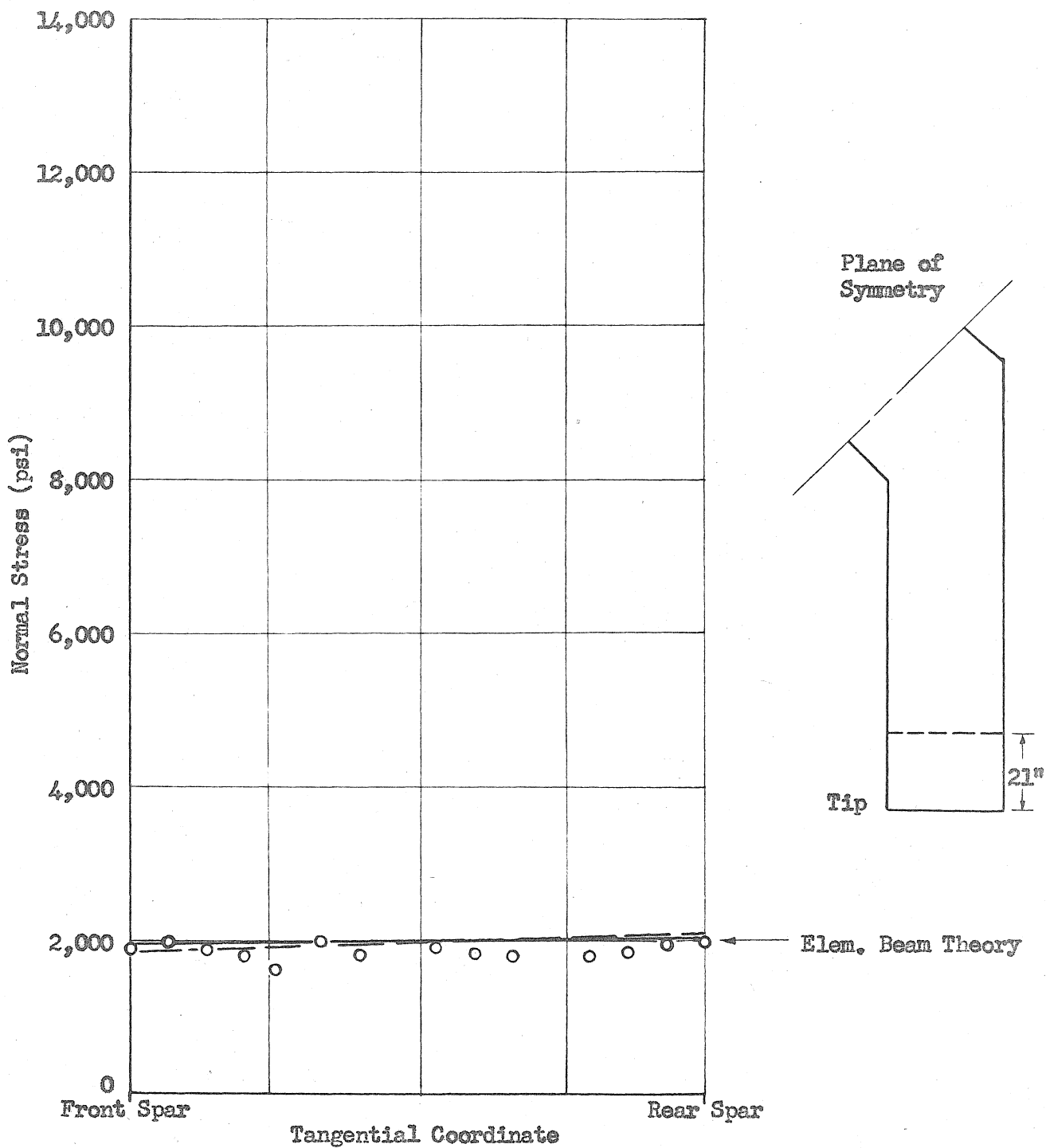
Reference Fig. 18(d)  
for Data  
Reference Fig. 15(c)  
for Notation



(f) Ten Element Beam - Clipped With No Wing Rib

FIGURE 21

STRINGER AND FLANGE STRESSES OF SWEEPBACK BOX BEAM FOR TIP BENDING LOAD



Notation

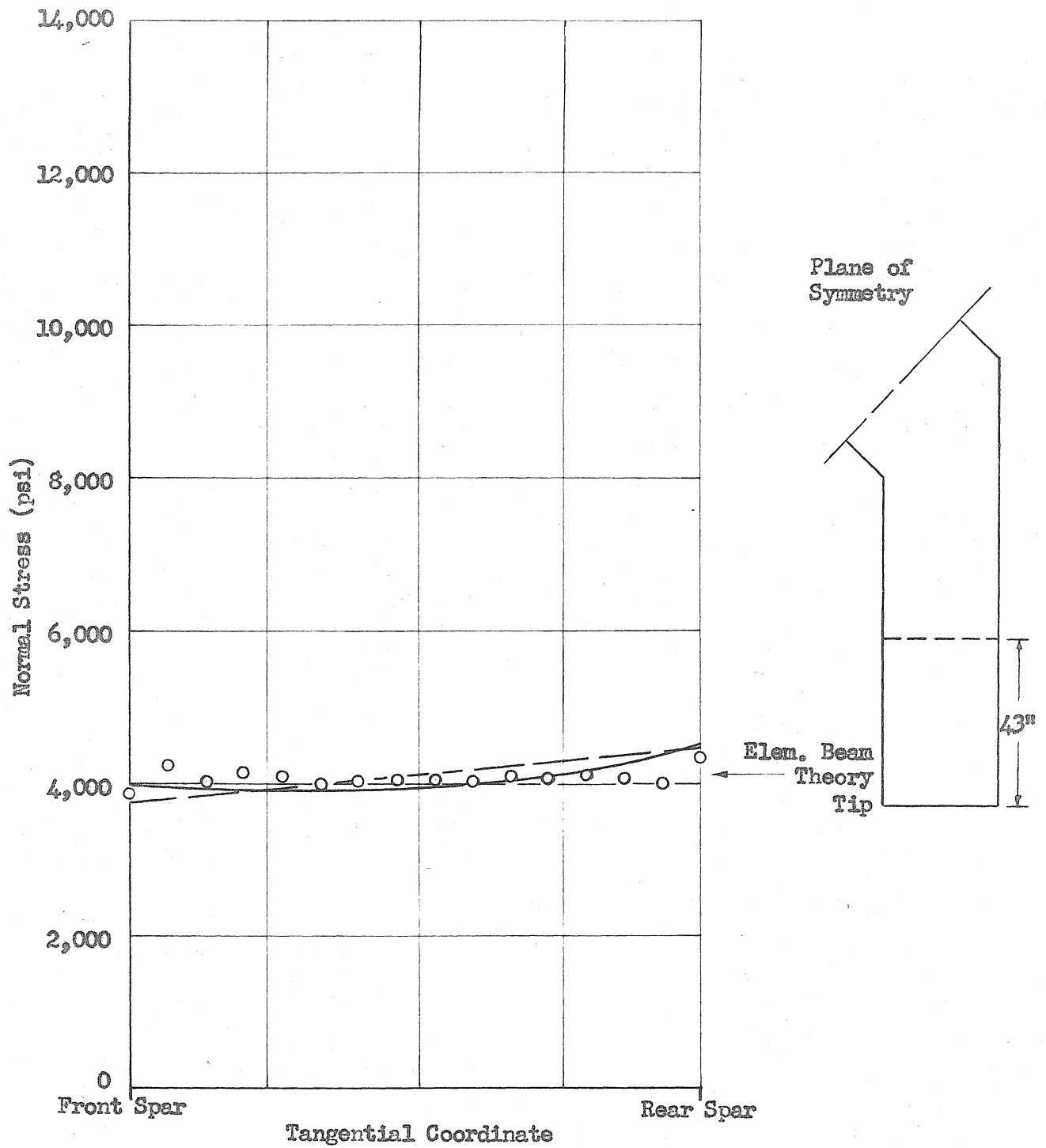
- Experimental Data (Reference N.A.C.A. T.N. 1525)
- Theoretical Curves (Reference Fig. 21)
- Four Element Beam (With Wing Rib)
- Six Element Beam (With Wing Rib)

(a) Cross Section 21 Inches from Tip of Wing

FIGURE 22

TANGENTIAL DISTRIBUTION OF NORMAL STRESS  
FOR THE SWEEPED WING UNDER SYMMETRICAL BENDING





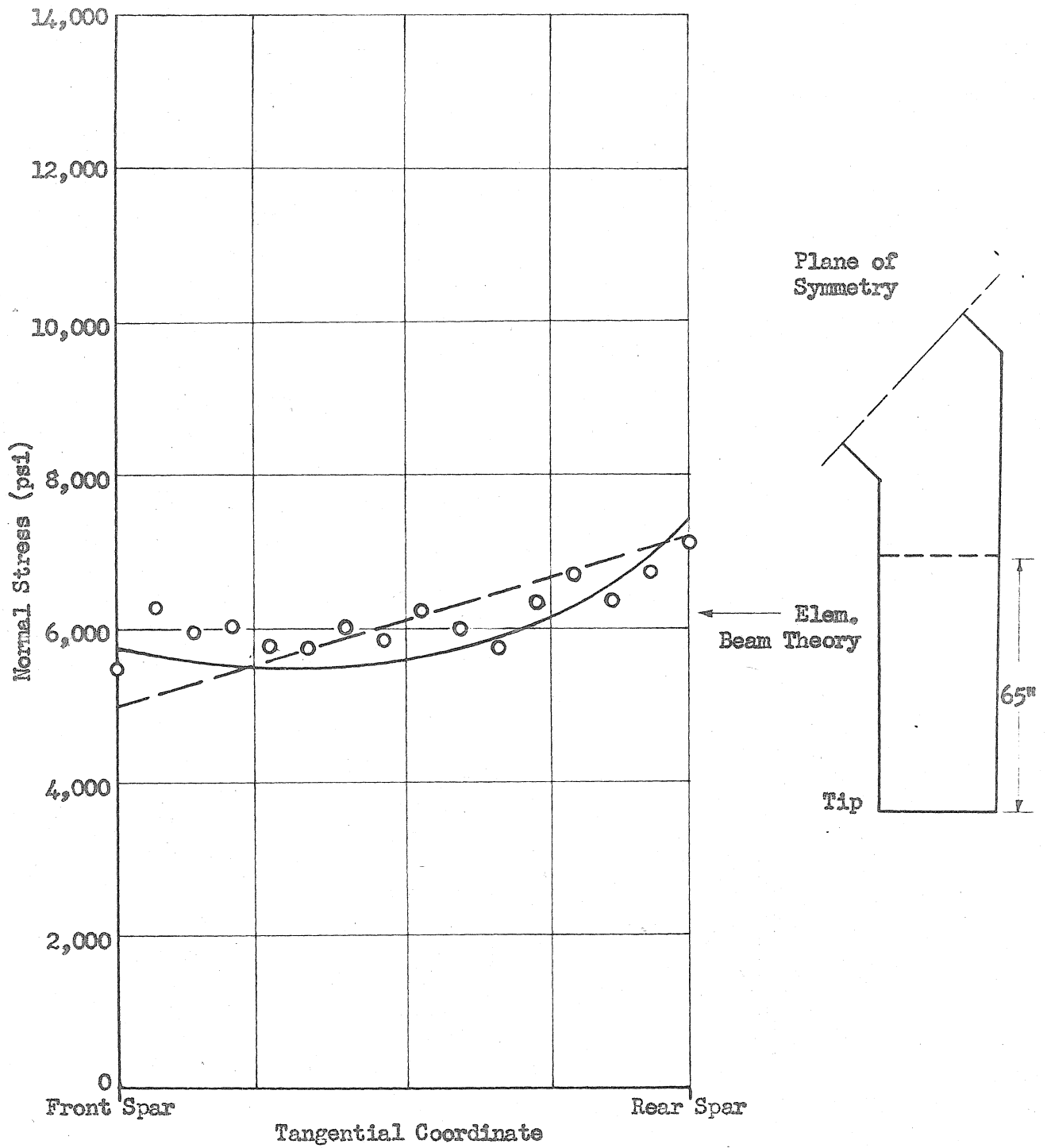
Notation

- Experimental Data (Reference N.A.C.A. T.N. 1525)
- Theoretical Curves (Reference Fig. 21)
- Four Element Beam (With Wing Rib)
- Six Element Beam (With Wing Rib)

(b) Cross Section 43 Inches from Tip of Wing

FIGURE 22

TANGENTIAL DISTRIBUTION OF NORMAL STRESS  
FOR THE SWEEP WING UNDER SYMMETRICAL BENDING



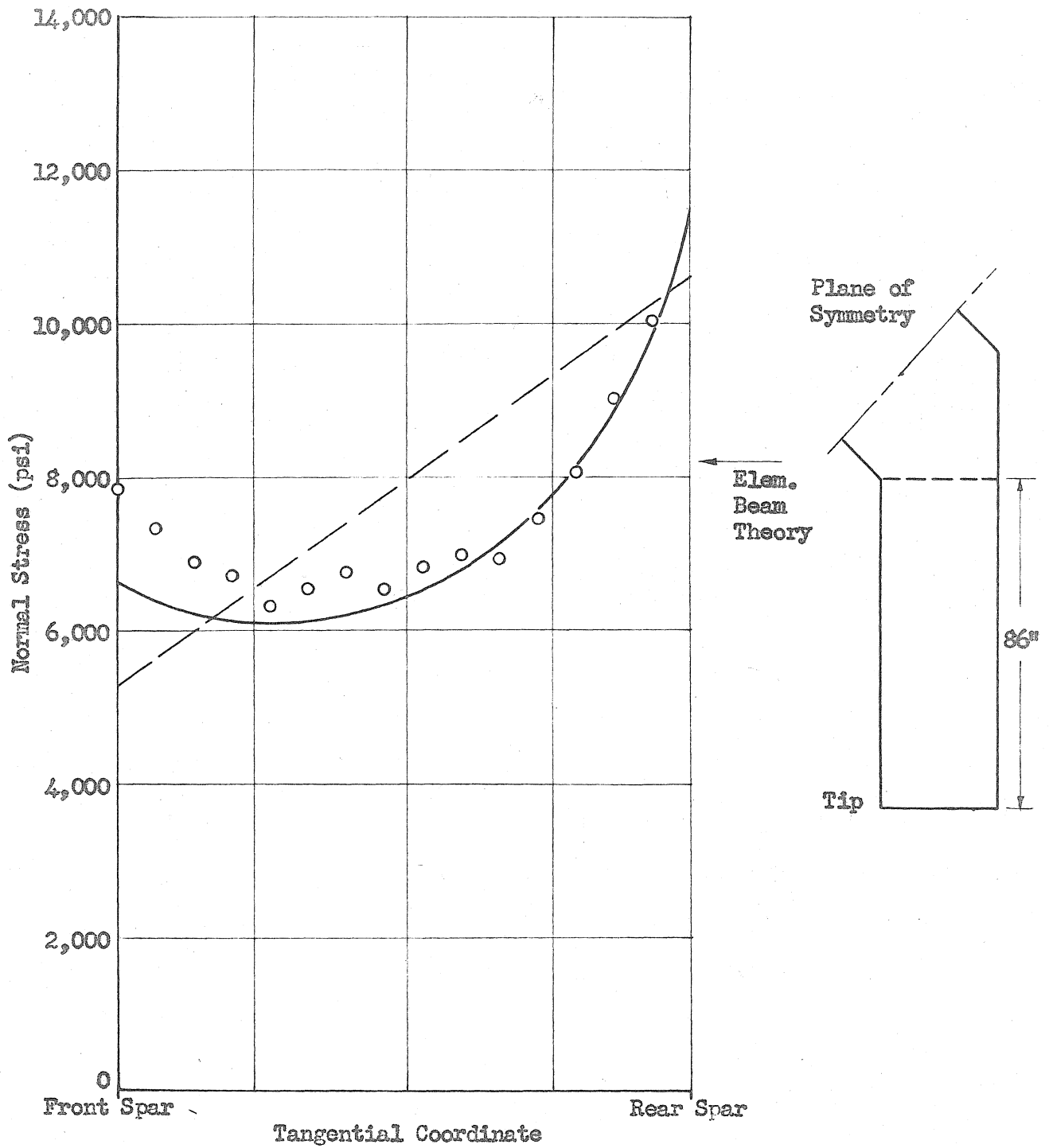
Notation

- Experimental Data (Reference N.A.C.A. T.N. 1525)
- — — Theoretical Curves (Reference Fig. 21)
- — — Four Element Beam (With Wing Rib)
- — — Six Element Beam (With Wing Rib)

(c) Cross Section 65 Inches from Tip of Wing

FIGURE 22

TANGENTIAL DISTRIBUTION OF NORMAL STRESS  
FOR THE SWEEP WING UNDER SYMMETRICAL BENDING



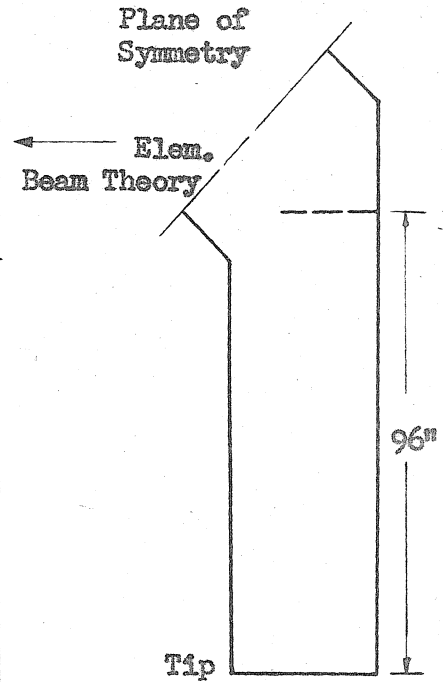
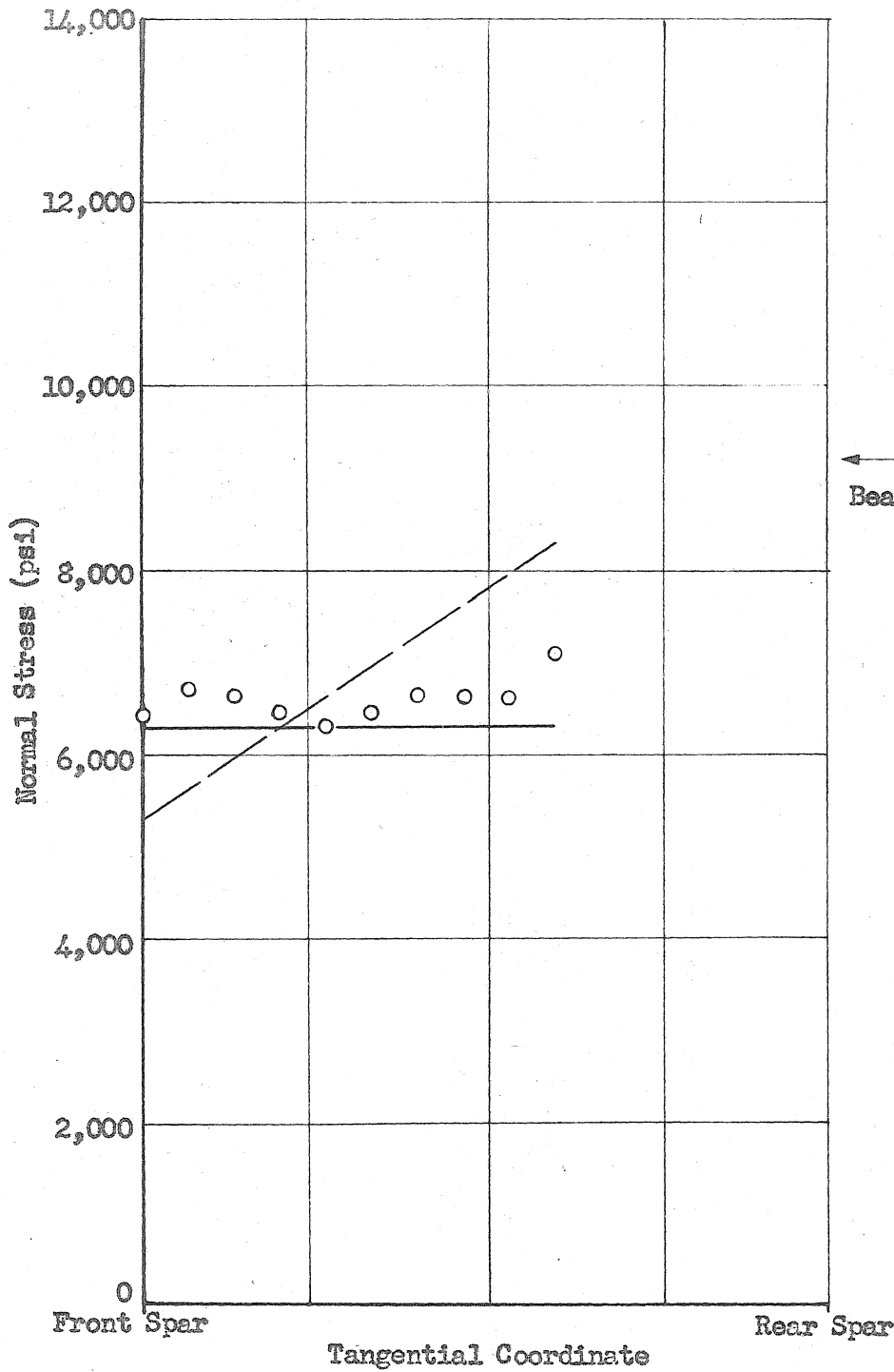
**Notation**

- Experimental Data (Reference N.A.C.A. T.N. 1525)
- Theoretical Curves (Reference Fig. 21)
- Four Element Beam (With Wing Rib)
- Six Element Beam (With Wing Rib)

(d) Cross Section 86 Inches from Tip of Wing

FIGURE 22

TANGENTIAL DISTRIBUTION OF NORMAL STRESS  
FOR THE SWEEP WING UNDER SYMMETRICAL BENDING



Note: Center Point of Theoretical Curve Obtained from Fig. 22(f)

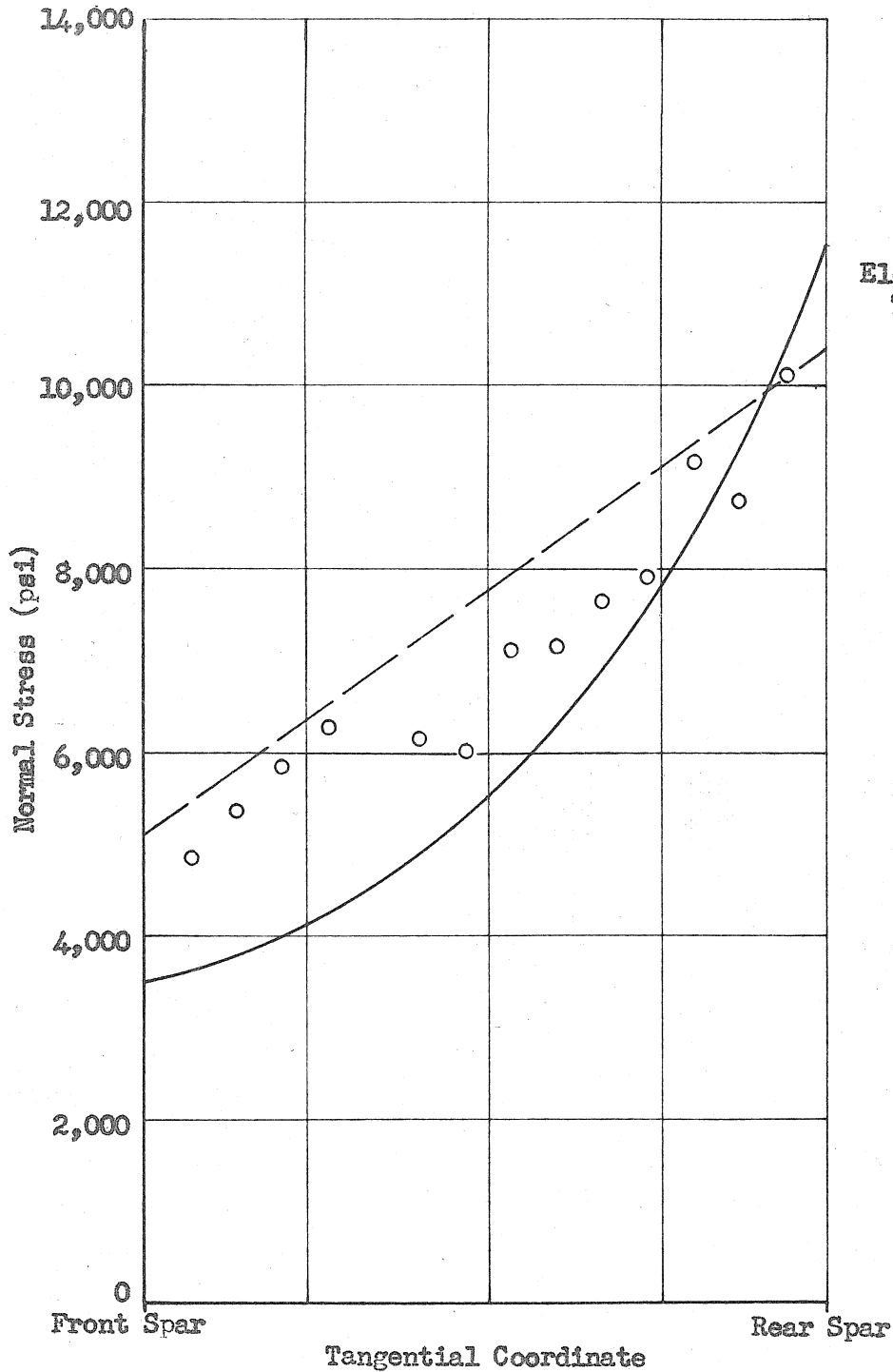
Notation

- Experimental Data (Reference N.A.C.A. T.N. 1525)
- Theoretical Curves (Reference Fig. 21)
- Four Element Beam (With Wing Rib)
- Six Element Beam (With Wing Rib)

(e) Cross Section 96 Inches from Tip of Wing

FIGURE 22

TANGENTIAL DISTRIBUTION OF NORMAL STRESS  
FOR THE SWEEP WING UNDER SYMMETRICAL BENDING



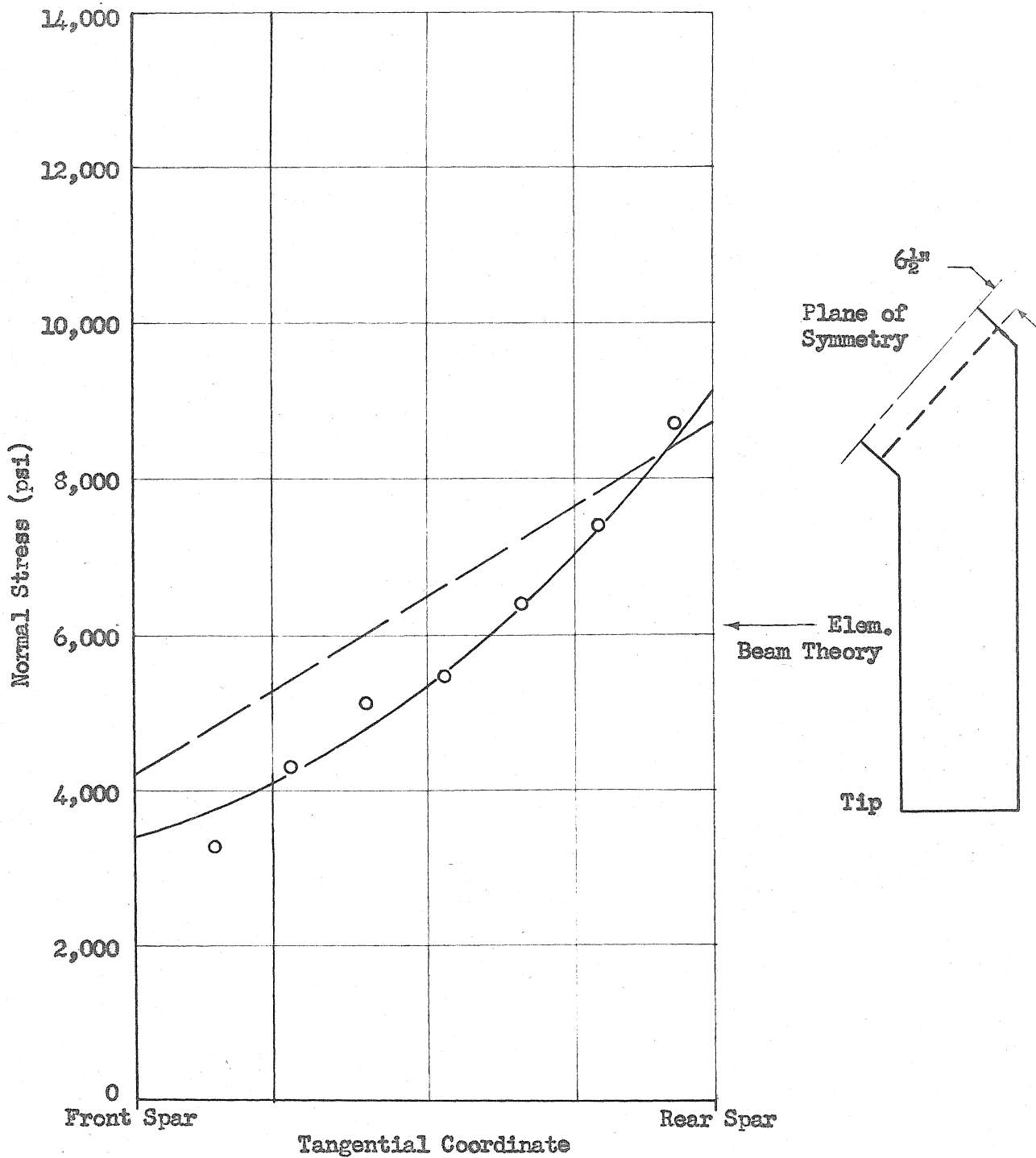
Notation

- Experimental Data (Reference N.A.C.A. T.N. 1525)
- Theoretical Curves (Reference Fig. 21)
- Four Element Beam (With Wing Rib)
- Six Element Beam (With Wing Rib)

(f) Cross Section 18 1/2 Inches from Plane of Symmetry

FIGURE 22

TANGENTIAL DISTRIBUTION OF NORMAL STRESS  
FOR THE SWEEP WING UNDER SYMMETRICAL BENDING



Notation

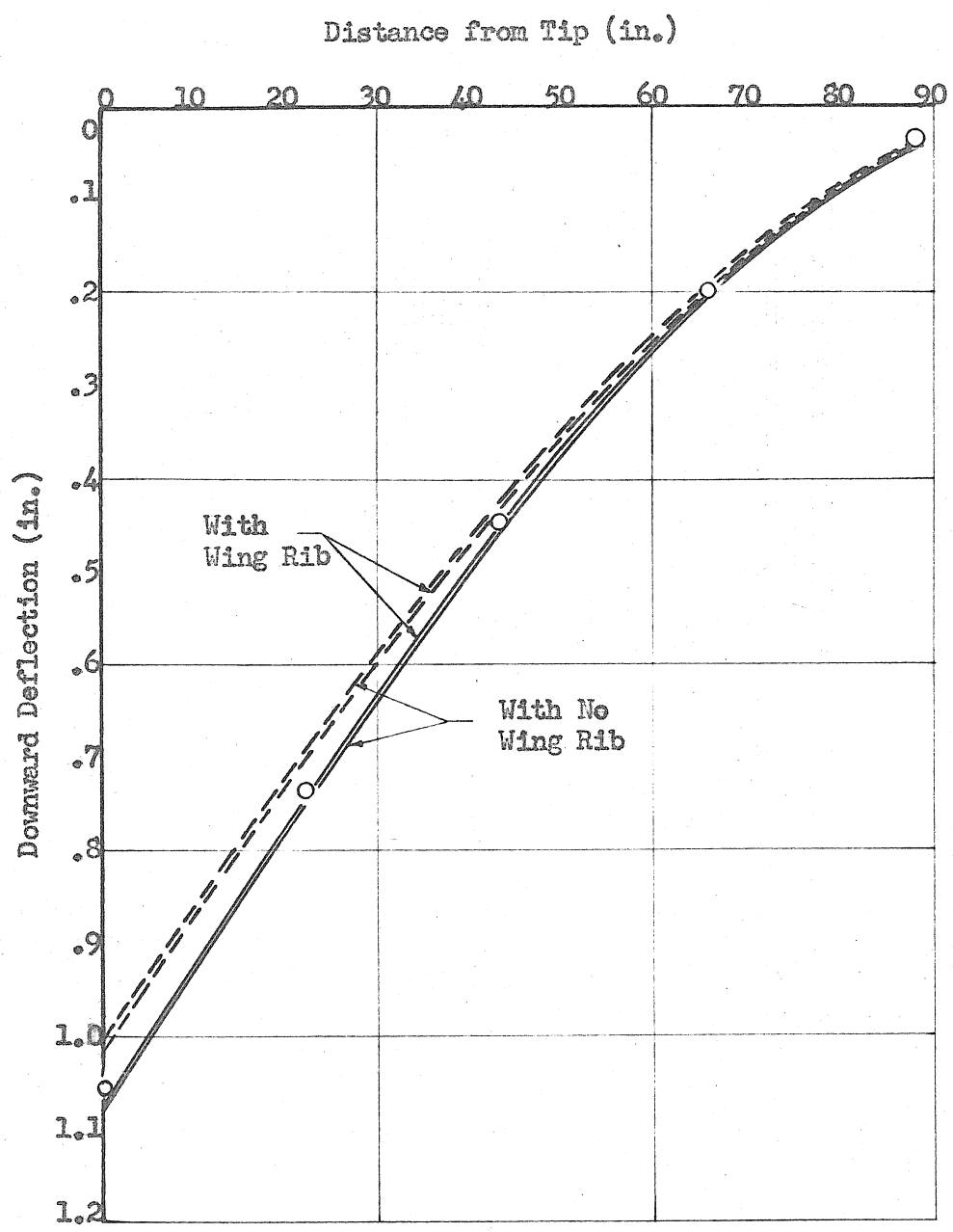
- Experimental Data (Reference N.A.C.A. T.N. 1525)
- Theoretical Curves (Reference Fig. 21)
- Four Element Beam (With Wing Rib)
- Six Element Beam (With Wing Rib)

(g) Cross Section  $6\frac{1}{2}$  Inches from Plane of Symmetry

FIGURE 22

TANGENTIAL DISTRIBUTION OF NORMAL STRESS  
FOR THE SWEEPED WING UNDER SYMMETRICAL BENDING

- Experimental Data (Reference N.A.C.A. T.N. 1525)
- Theoretical Curves (Reference Table 2)
- Four Element Beam
- Six Element Beam



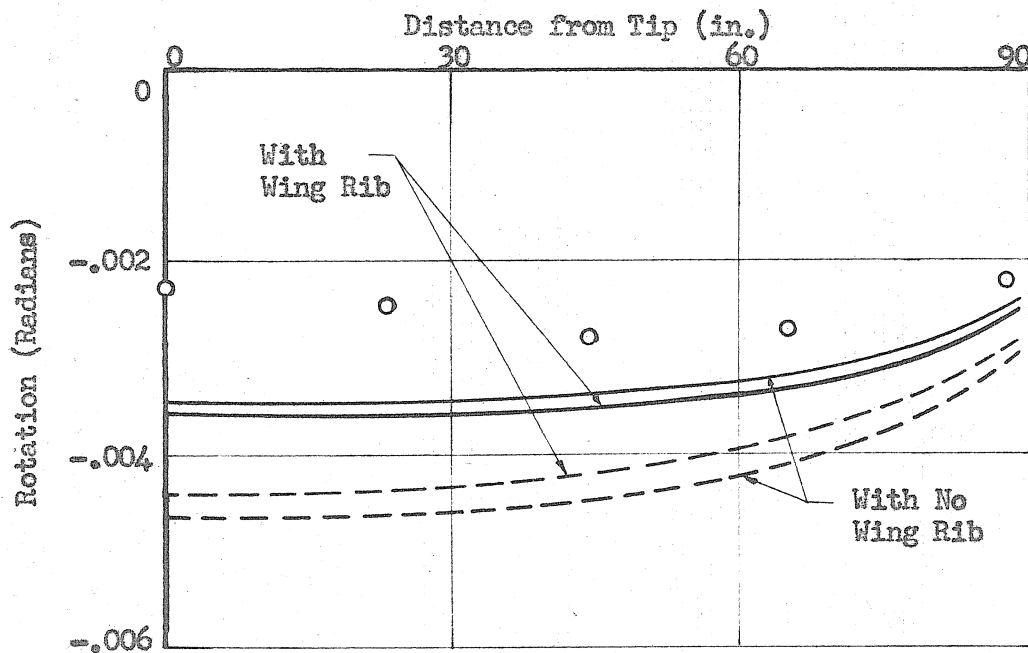
(a) Deflections of Centerline of Wing

FIGURE 23

DEFORMATIONS OF SWEEPED WING UNDER SYMMETRICAL BENDING

Notation

- Experimental Data (Reference N.A.C.A. T.N. 1525)
- Theoretical Curves (Reference Table 2)
- Four Element Beam
- Six Element Beam



Rotation Perpendicular to Spars

(b) Rotations of Wing

FIGURE 23

DEFORMATIONS OF SWEEP WING UNDER SYMMETRICAL BENDING